OCCUPANT INDUCED LATERAL AMPLIFICATIONS ON EXTERIOR DECKS

CONNECTION STIFFNESS AND DAMPING EFFECTS

By

JONATHON J. WALDRIP

A thesis submitted in partial fulfillment of
the requirements for the degree of

MASTER OF SCIENCE IN CIVIL ENGINEERING

WASHINGTON STATE UNIVERSITY
Department of Civil and Environmental Engineering

JULY 2016

To the Faculty of Washington State University:

The members of the Committee appointed to examine the thesis of

JONATHON J. WALDRIP find it satisfactory and recommend that it be accepted.

_____

Donald A. Bender, Ph.D., Chair

_____

William F. Cofer, Ph.D.

_____

James D. Dolan, Ph.D.

OCCUPANT INDUCED LATERAL AMPLIFICATIONS ON EXTERIOR DECKS

CONNECTION STIFFNESS AND DAMPING EFFECTS

Abstract

by Jonathon J. Waldrip, M.S.
Washington State University
July 2016

Chair: Donald A. Bender

Like many structures, the failure of an exterior deck could result in serious injury or even death.

Therefore, it is imperative that these and other like structures are designed for all applicable loads.

Physical testing and finite element (FEA) modeling have shown that lateral loads caused by

occupants can exceed the capacity of decks designed for wind and seismic events. Parameter

sensitivity analyses performed on the models presented in this thesis show that the deck board-to-

joist connection properties govern the response of the FEA model, warranting further

investigation. Monotonic physical testing carried out on deck board-to-joist connections

determined the softened cyclic stiffness and associated equivalent viscous damping (EVD) ratios

for 3 connection types. Hem-Fir joists and deck boards were tested with two fastening systems:

10d threaded nails and #10x3" deck screws. Additionally, Hem-Fir joists with Trex® composite

deck boards and #10x2¾" Trex® composite deck screws were tested.

Physical test results showed that for screwed connections, a rotational stiffness of 22000 lb.-in./rad

with an associated EVD of 7.3% critical damping is a good estimate of connection parameters.

Use of these values with FEA models provided lateral load amplifications that matched well with physical data from previous full-scale deck testing. Rotational stiffness values for the use of nailed deck board-to-joist connections were comparable to that of for screws, but higher EVD values resulted in lower overall simulated amplifications. Stiffness and damping values for the composite board set-up were both higher than that of screws resulting in lower initial amplifications, but the increased mass of the Trex® boards led to larger lateral load amplifications with higher substructure stiffness values.

A simplified 2D FEA model that produced similar results to the 3D full-scale FEA model was created to readily estimate lateral load amplifications for different deck layouts. An excel spreadsheet developed as a design aid calculates an estimated lateral load amplification for deck sizes and substructure stiffness values that are not within the scope of the full-scale 3D model. Finally, load amplifications for various deck sizes were compiled in an easy-to-use table for use in the lateral design of new or existing deck structures.

Table of Contents **Page**

List of Tables

List of Figures

xiv

1.0 - Introduction

The barbeque is going and burgers will be ready soon. The music is good and the guests are starting to dance out on the deck. Then without notice, the deck releases its grip on the house and the whole party falls 15ft, crashing to ground in a heap of debris. The guests might be injured and there is surely damage to both the deck itself and the envelope of the house that will result in costly repairs. This situation describes what could have happened to the high school Senior Skip-Day party in Nova Scotia on June 12, 2015 (Irish, 2015). Students gathered for a picture when the deck ledger broke at the connection to the main house sending the entire party to the ground. Luckily, in this incident, no one was killed, but 12 young partygoers were admitted to the local hospital with minor injuries.

Headlines such as *Nova Scotia Deck Collapse Leads to Injuries*, *Cookout Season Brings Rash of Deck Failures*, and *Another Deck Failure* (Professional Deck Builder Magazine, 2015) are appearing far too often. Structures that allow their occupants to interact with nature such as gazebos, and elaborate decks and porches are popular, but they are in constant contact with environmental hazards. As a result, they have a higher potential to cause risk to occupant safety. In fact, nearly 4,000 yearly injuries are caused by structural failures on decks alone (Shutt 2011; Legacy Services 2010). Such figures are unacceptable and investigation into mitigation methods is essential to reducing the number of such incidents.

Because of this increased publicity in outdoor deck structural failures, effective design of deck structures is becoming a significant issue in residential design. In addition to gravity, loads and the usual lateral loads such as wind and seismic, studies conducted at Washington State University

have explored occupants as a source for lateral loads. The studies indicated that occupant-induced lateral loads applied at various frequencies can amplify the static lateral load case and overcome existing design values established for wind and seismic events (Parsons, 2014 A: LaFave, 2014). The ASCE 7-10 load standard and the American Wood Council (AWC) design guide DCA6-12do not consider this occupant lateral load case. Therefore, it is imperative to characterize these loads, develop a model to explore their effect in various situations, and establish design aids to assist in eliminating the failure of new structures and to facilitate the retrofit of existing ones.

Physical testing of full-scale deck diaphragms indicated that the deck board-to-joist connection provided the majority of the lateral stiffness (Parsons, 2014b). A parameter sensitivity analyses, using finite element (FEA) software of the deck structure, with respect to the rotational stiffness and damping characteristics of the deck board-to-joist connection confirmed that this connection also greatly affects the dynamic amplification factors associated with occupant induced lateral loads. As a result, the objective of this study is to use physical testing to estimate the rotational stiffness and damping for the deck board-to-joist connection. Products of this investigation include a revised model that provides dynamic amplification factors from occupant induced lateral loads that have improved accuracy, a simplified FEA model based on the revised full model, and a design guide for the implementation of these loads in the design procedure for exterior deck structures.

2.0 -Literature Review

2.1 - Lateral Load Path in Exterior Deck Structures

Design engineers have a well-founded understanding of vertical load paths and designing for gravity loads is straightforward. However, the lateral design load path is less intuitive, leading to continued efforts to improve understanding of structural lateral behavior under lateral forces including wind, seismic, and occupancy. Regarding decks and patios specifically, multiple studies performed at Washington State University by P. Lyman (2013a, 2013b) characterized much of the lateral behavior of decks concerning the lateral resistance of wind and seismic loads as well as studies determining how these loads flow into the structure to which the deck is attached.

As illustrated in Figure 1 below, a deck can be idealized as a cantilevered deep-beam where shear characteristics govern its behavior. Lateral forces can be applied as a distributed force along an edge (wind), a body force (seismic), or a surface traction (occupant) to a wood framed diaphragm (the deck surface). Shear forces transferred through the diaphragm are resisted by unit shear along the ledger (Vu) and point loads representing posts or substructure support (Pr). Tension (T) and compressive (C) forces at each end of the deck resist the overturning moment, or the tendency for the deck to rotate off the main structure. Although the post/substructure resistance could participate in resisting overturning, typically the connection at the ledger is much stiffer than that of the substructure along that line of action, and it is reasonably conservative to assume that overturning forces are resisted by the hold-downs and ledger connections alone.
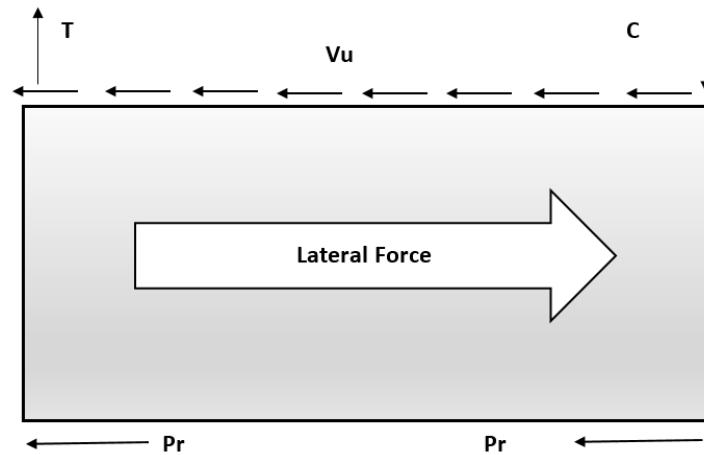
Figure 1: Illustration of lateral load path through a deck structure.

This research defining the lateral load path in exterior deck structures led to several publications regarding lateral load consideration in the design of deck structures that ultimately may influence the AWC design guide for deck structures, DCA6-12 (2012). International Building Code (2012) states "decks shall be positively anchored to the primary structure" (R507.1). DCA6-12 is also vague, mentioning the use of hold-downs sufficient to withstand a force of 1500 lb. each. This is a conservative load estimate based on the research performed by P. Lyman et al. (2013a, 2013b). Lyman's research provides an example that result in 650 lb. hold-down requirements for wind forces and 250 lb. hold-down requirement for seismic forces. These values were based on a 12 ft. x 12 ft. deck connected via lag bolts to a 2nd story ledger and assuming a substructure interactions were minimal. Lyman (2013b) also proposed that a conservative design with a 1.5:1 aspect ratio would attract about 1250 lb. of seismic force resulting in 625 lb. of hold-down forces, well below the required value of 1500 lb. Current proprietary mechanical connectors such as the Simpson Strong-Tie DTT2Z provide up to 2105 lb. of resistance. This is well beyond code requirements, but for specific cases hold-down requirements could exceed these values and additional design should be completed in order to sufficiently trace all loads back to the primary structure.

In order to accurately trace loads from exterior decks to the primary structure, the full load path must be determined. Parsons et al. (2014b) conducted a study that explored the lateral load path from the deck surface to the primary structure. The test consisted of a 12 ft. x 12 ft. deck structure made with 2x10 nominal joists and 1x6 nominal Trex® composite deck boards attached to a simulated house diaphragm. Several tests were performed: one without deck boards attached and one with; one fully constructed deck with compression and tension hold-downs. The first two tests indicated that the stiffness of the deck without the deck boards attached was 97 lb./in and 2,600 lb./in with the deck boards attached. This suggests that the deck board-to-joist connection provided greater than 95% of the lateral stiffness of the diaphragm (Parsons et al., 2014b). The results of the second set of tests were not intuitive. The hold-downs proved to have a minimal effect on the way that the deck performed during short term testing. This was determined to be due to the joist hangers chosen, and the location of the hold-downs.

Parsons' (2014b) tests consisted of joists connected to the ledger via screws. Preliminary experiments showed that hangers utilizing nails or a toe-nailed pattern performed poorly when the joist was loaded in tension (Parsons et al. 2014b). Joist hangers are primarily designed for vertical load resistance. As a result, many joist manufactures allow the use of nails in the joist hangers despite the requirements stated in Section 1604.8.3 of the IBC (2012) stating that "Such attachments shall not be accomplished by the use of toenails or nails subject to withdrawal." It could be interpreted that this requirement applies mainly to the connection of the deck ledger to the primary structure. However, if the load cannot reach the ledger because of nails loaded in withdrawal, the usefulness of ledger screws diminishes.

Calculations performed by Parsons (2014b) on the 10d common nails vs. Simpson Strong-Tie #9 screws showed that screws have a 5x larger withdrawal capacity of 750 lb. for screws vs. 150 lb. for nails. The high withdrawal strength of the screw-fastened joists led to an unexpected result for the forces in the tension hold-downs. Per Figure 2 below, when the decks were loaded laterally, they experienced large shear deformations relative to the simulated house diaphragm. As a result, the joists rotated as the deck deformed into a parallelogram shape. This type of deflection caused the hold-down on the tension side to be pushed towards the ledger resulting in compression while the compression hold-down experienced tensile forces upwards of 3800 lb., more than what was calculated for the tension hold-down using the static idealization for the deck structure (Figure 4, Parsons et al., 2014b).
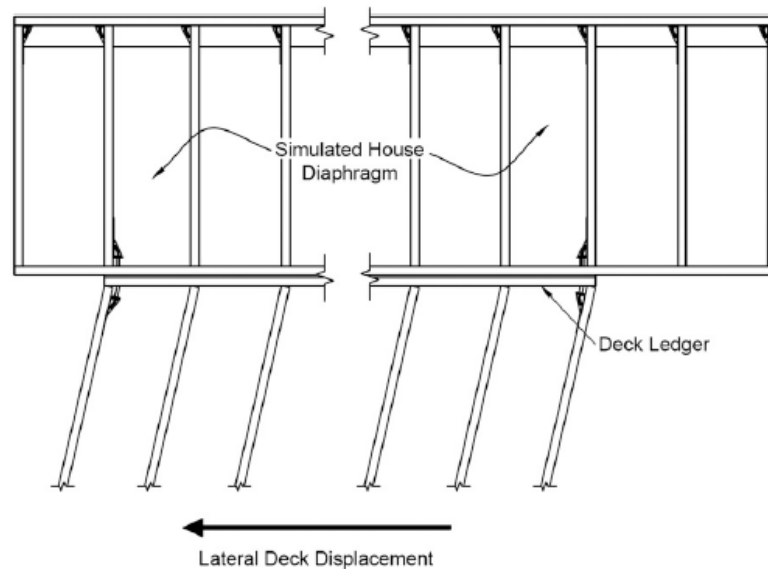
Figure 2: Illustration of deck deformation in relation to the primary structure.

Figure 4 illustrates that the compression hold-down tensile force development, in Parsons' (2014b) test, as it is pulled away from the ledger and the deck bears on the ledger. In contrast, the tension hold-down force diminishes to zero with more deflection as it is rotated towards the ledger.
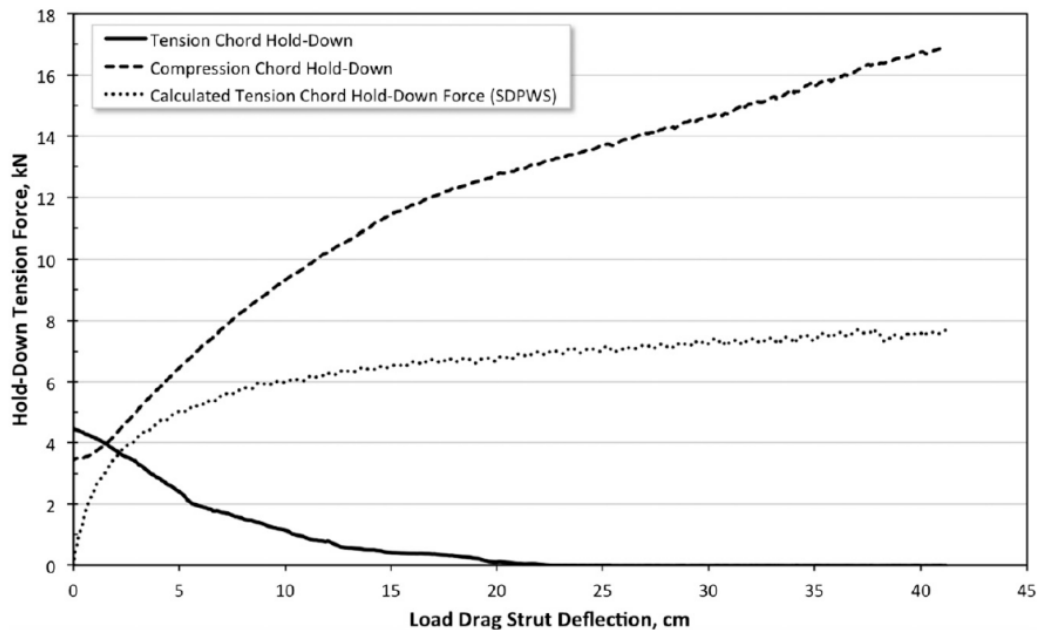
Figure 3: Hold Down reactions vs. displacement, (Parsons et al., 2014b)

It is possible that this reaction was due to the stiffness in the diaphragm (provided by the deck board-to-joist connection) being small compared to the overall stiffness of the joist hangers loaded in withdrawal from the ledger. This would cause shear deformation before rigid body rotation of the deck. The conclusion that tensile forces might have developed in the tension hold-down if nails were used in the attachment of the joists is illustrated in Figure 4. When screws are used, overturning forces are resisted by the joist hangers and ledger bolts rather than the hold-downs. Although the structural redundancy of the system would be decreased, if nails were used in place

7

of screws in the joist hangers, the hold-downs might perform according the load-path assumptions made during the design of the structure (Parsons et al. 2014b).

A – Proposed Tension/Compression force transfer when joists are attached with screws

B – Proposed Tension/Compression force transfer when joists are attached with nails.
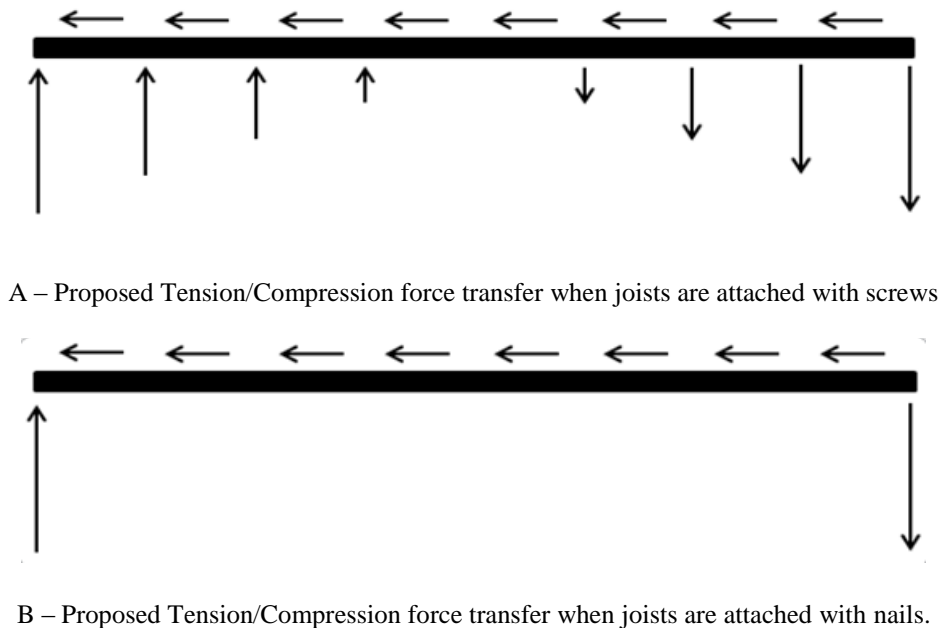
Figure 4 : Force transfer into deck ledger utilizing screws (Case A above) vs. nails (Case B above) to connect joist hangers to the deck ledger

2.2 - Occupancy Induced Lateral Loads in Deck Structures

A study performed by Parsons et al. (2014a) explored the effect of dynamic lateral loads on decks. Parsons notes that, "model building codes and consensus standards in the United States are silent on the subject of dynamic *lateral* loads from occupancy on decks". However, other structures constructed for the use in entertainment venues are required to take into account amplified lateral loads. For example, as per ASCE 7-10 Table 4-1, Footnote k, stadiums and grandstands are required to be designed for a minimum of 24 plf along the seats based on work done by Homan et

al. (1932). Homan et al. (1932) found that occupants are capable of synchronizing their movements with that of the structure and impart a cyclic load at the same frequency as the natural period of the structure. The Duhamel integral with a sinusoidal forcing function can be utilized to show that for a single degree of freedom (SDOF) system, displacements and loads become greatly amplified when the frequency of the forcing function approaches the natural frequency of the structure (Filiatrault, et al. 2013). The same idea can be applied to an entire structure.

For decks, vertical dynamic load effects are already accounted for. ASCE 7-10, Table 4 states that the gravity live load on a deck must be "1.5 times the live load for the occupancy served." However, as stated above, no such requirement exists for lateral loads on deck structures. It is unreasonable to imply that structures intended for social uses such as exterior decks be excluded from a similar requirement, given the evidence that such loads can be generated.

Because lateral dynamic loads area not accounted for in deck design, Parsons et al. (2014a) performed a study that explored the effect of occupant-induced lateral loads on an exterior deck structure. A 12 ft. x 12 ft. deck was constructed and test subjects applied lateral loading via a swaying motion, attempting to match the natural period of the structure and cause large deflections. The subjects first attempted to apply a cyclic load perpendicular to the deck ledger. The results showed that for a group representing a 40 psf vertical live load, the vertical-to-lateral load amplification of about 0.10. Because the structure was very stiff in that direction, the imparted load caused relatively small deflections, resulting in reaction forces at the ledger that did not account for the inertial effect of the deck moving. In conclusion, Parsons et al. (2014a) surmised that a group of humans representing a 40psf gravity live load has the ability to apply a static traction

of approximately 4psf to the deck surface when to the load is oriented parallel to the joists (see

Table 1).

Occupant load level, kPa (psf)	Deck-board orientation to ledger	Total force, kN (lb)	Uniform lateral load, kPa (psf)	Dynamic load factor
0.48 (10)	Parallel	1.00 (224)	0.08 (1.6)	0.16
0.48 (10)	45°	1.00 (226)	0.08 (1.6)	0.16
0.96 (20)	Parallel	1.77 (398)	0.13 (2.8)	0.14
0.96 (20)	45°	2.42 (543)	0.18 (3.8)	0.19
1.44 (30)	Parallel	1.83 (411)	0.14 (2.9)	0.10
1.44 (30)	45°	2.14 (482)	0.16 (3.3)	0.11
1.92 (40)	Parallel	2.90 (651)	0.22 (4.5)	0.11
1.92 (40)	45°	2.23 (502)	0.17 (3.5)	0.09

Table 1: Forces occupants generated from cyclic loading: perpendicular to the ledger

Once the static surface traction was determined, the test subjects then applied a cyclic force by swaying back and forth parallel to the deck ledger. Similar to the results of Homan's research, the participants exhibited the natural tendency to synchronize with one another and the structure with which they interacted. The participants could only produce the observed surface traction in a cyclical manner with a maximum frequency of about 1Hz (Parsons et al., 2014a). Because spring-mass-damper systems exhibit amplified oscillation magnitudes when excited at their resonant frequency, the deck system showed severe support reaction increases when the occupants excited the structure at its fundamental frequency. For this scenario, a group representing a 40psf vertical load produced an amplification of 0.30 times the vertical force. When combined with the observation from Table 1, a 4psf lateral surface traction applied in a cyclic manner should result in amplified support reactions of 3 times the static case (Parsons et al. 2014a).

Occupant load level, kPa (psf)	Deck-board orientation to ledger	Total force, kN (lb)	Uniform lateral load, kPa (psf)	Dynamic load factor
0.48 (10)	Parallel	1.42 (320)	0.11 (2.2)	0.22
0.48 (10)	45°	2.52 (567)	0.19 (3.9)	0.39
0.96 (20)	Parallel	4.37 (983)	0.33 (6.8)	0.34
0.96 (20)	45°	3.84 (862)	0.29 (6.0)	0.30
1.44 (30)	Parallel	6.36 (1,431)	0.47 (9.9)	0.33
1.44 (30)	45°	4.42 (9,945)	0.33 (6.9)	0.23
1.92 (40)	Parallel	7.77 (1,747)	0.58 (12.1)	0.30
1.92 (40)	45°	4.54 (1,020)	0.34 (7.1)	0.18

Table 2: Forces occupants generated from cyclic loading: parallel to ledger

During the test, the occupants exhibited a tendency to sway in a skiing-type motion with little movement at the waist, concluding that the amplifications observed were primarily due to the inertial effects of the moving deck mass. Structural dynamic theory and the general equation of motion display that as the deck reaches peak displacement (an observed +/- 7in at the end of the deck), the velocity may be zero, but the acceleration is at its peak, and thus so is the load.

$$F(x) = m\ddot{x} + c\dot{x} + kx$$

As the natural frequency is approached and the deflection increases, so do the resulting reactions. The Duhamel integral method for damped sinusoidal forcing functions results in a dynamic amplification is a function of the only damping ratio when an SDOF system is excited at the natural frequency (Filiatrault, et al. 2013). By assuming 10% critical damping, the load amplification should be about 5 times the static load. In order to get the amplifications observed, damping would have to be 16% of critical damping. This is of course assuming that the deck acts as a SDOF system and the load application was perfectly sinusoidal. Both of these assumptions are not necessarily true and could be what leads to this discrepancy.

2.3 - FEM Modeling

Following the study performed by Parsons et al. (2014a) an exploration of the effect of deck geometry and substructure stiffness on the forces generated by occupancy was undertaken. To accomplish this, LaFave (2015) created FEA models to augment the experimental testing performed by Parsons (2014a). A series of several models was created including variables such as deck board orientation (parallel or perpendicular to the ledger), aspect ratio of the deck geometry (ranging from 12 ft. x 24 ft. to 24 ft. x 12 ft.), and the substructure stiffness.

Each FEA model was constructed to reflect the actual construction and subjected to similar load conditions as that of the full-scale testing. Each model underwent three analyses. First a static analysis was performed to provide a benchmark for comparison with other analyses. Second, a frequency analyses extracted the natural frequencies, and associated mode shapes of the structure for use in the third analysis. The third analysis was a dynamic modal analysis that would apply a surface traction in a sinusoidal manner with forcing frequencies ranging from 0-1.0 Hz. The full scale testing showed that a group of humans could only produce input frequencies up to about 1.0 Hz, thus the limit in the frequency range (Parsons et al., 2014a). During each analysis, lateral joist forces and post reactions were monitored at various points within the frequency range. From this output, the load amplification at each frequency point could be determined by normalizing the observed loads with respect to the static analysis providing a set of data similar to that pictured in Figure 5, which displays the results from a 12 ft. x 24 ft. deck model. When the forcing function has a frequency of 0 Hz, the load is analogous to a static case and the load amplification is 1.0. However, as the forcing function reaches a frequency close to the natural frequency of the deck, the load becomes amplified. In this case a maximum 4.28 times the static case is observed. Due

the asymptotic nature of resonant frequency responses, a phase shift occurs in the data at the resonant frequency of 0.485 Hz.
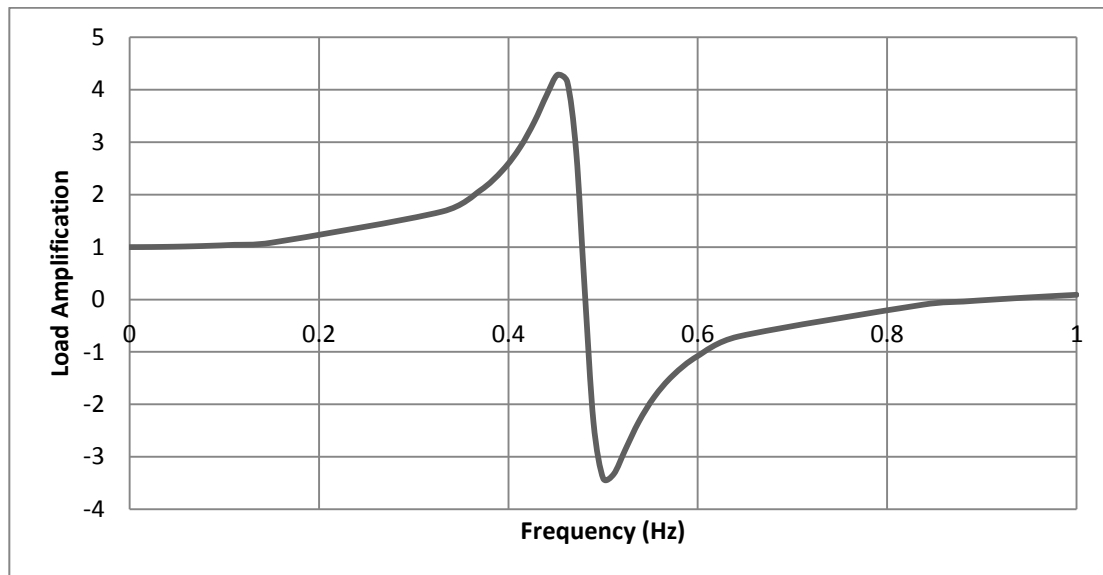
Figure 5: Example of Deck Analysis Results for a 12ft x24ft deck

In addition to individual model results as depicted in Figure 5, comparisons of the load amplifications to the substructure stiffness were quantified. The substructure could be defined as embedded posts, a braced frame, or various configurations that could result in a variety of lateral stiffness. Figure 6 depicts the maximum response of the same 12 ft. x 24 ft. deck, but it instead displays the peak amplification from a given frequency sweep with respect to a range of substructure stiffness. As the substructure stiffens increases, the natural frequency of the system increases. Consequently, the load amplification increases as well from the higher accelerations present in maintaining higher frequency cyclic motion. However, there is a steep drop in load amplification once the resonant substructure reaches a certain stiffness value due to the assumption that humans can only produce cyclic load frequencies up to 1 Hz.
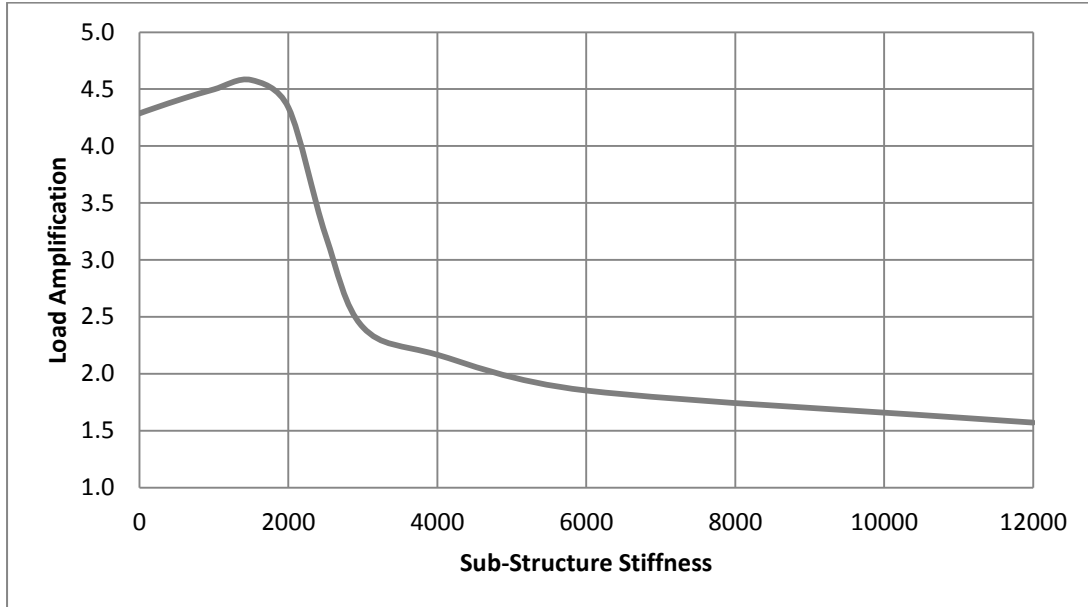
Figure 6: Load Amplification vs. Substructure Stiffness for a 12'x24' deck.

The sudden drop in load amplification observed in Figure 6 is attributed to the natural frequency of the deck structure rising above 1.0 Hz as the substructure stiffness increases (See figure 7). Although there still is an amplified load associated with that natural frequency, the disparity between the natural frequency and the frequencies obtainable by occupants grows, causing the observed load amplification to decrease. As a consequence, if the system stiffness of flexible deck structures can be increased enough to bring the resonant frequency above 1.0 Hz, the amplified load (and consequently support requirements) are greatly reduced.
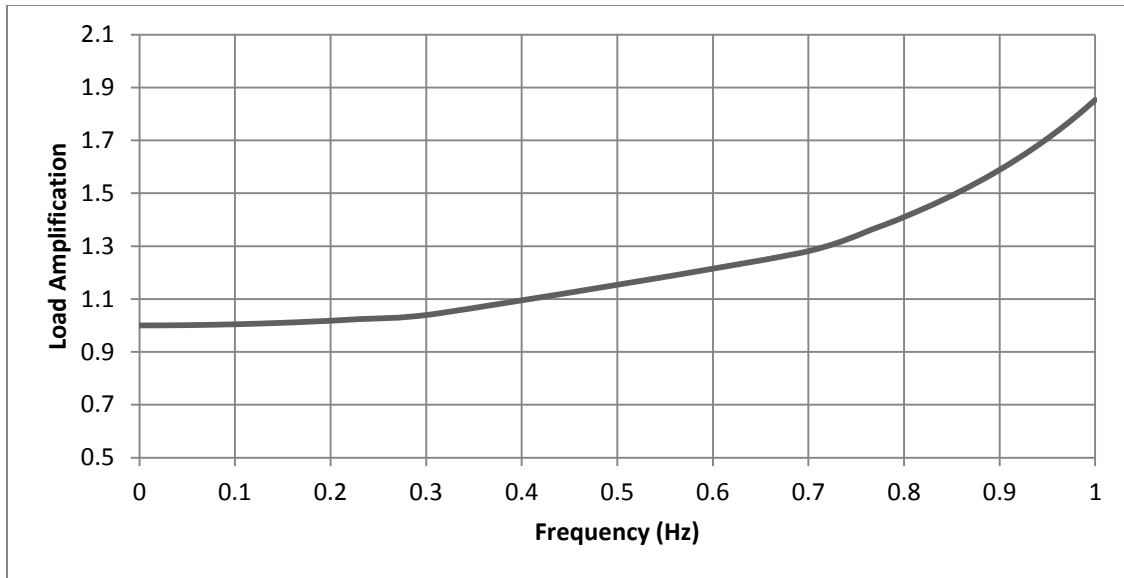
Figure 7: Example of deck response where the natural frequency is beyond 1Hz

Results from the FEM analyses performed by LaFave (2015) showed load amplifications ranging from 1.3 to 4.5 times the original total shear produced by the static load case. In many cases, these amplified loads open up the possibility that the unit shear within the deck (as well as connection demands along the ledger, anchor points and posts) from occupant loads could become larger than the wind or seismic loads for which decks are currently designed.

3.0 – Effects of Deck Board-to-Joist Rotational Stiffness and Damping

In the previous full-scale FEA model for the occupant induced lateral load amplification of deck structures, the rotational stiffness for the deck-board to joist was set to 36611 lb.-in./rad for use in the FEA model for predicting occupant induced lateral load amplifications on exterior decks (LaFave, 2015). Although this value seemed to give reasonable results, it is approximately 45% of the required rotational stiffness based on the load slip equations for the group action factor outlined in Section 10.3.6 of the NDS (AWC, 2012). The disparity of this value and the estimated value (combined with the influence of this connection suggested by Parsons et al. (2014a)) points to a possible flaw in the results of the models. In conclusion, several parameter sensitivity analyses were performed on the FEA model regarding the rotational stiffness and damping of this connection to determine their effect on the model outputs and the need for further exploration/testing. This chapter will focus on a description of the model, the parameter sensitivity analyses for the effects of the deck board-to-joist connection, and results from physical testing performed on three types of simulated deck board-to-joist connections. Additionally, the quantification of values for rotational stiffness and damping, and how these new values affect the full-scale model are discussed.

3.1 - FEA Model

This section serves to describe, in detail, the construction of the model by LaFave (2015). It includes general layout, material properties, member connectivity, boundary conditions and loading, analysis procedures, and how the results were interpreted.

3.1.1 - General

LaFave (2015) developed a model using the FEA program ABAQUS that was calibrated to the tests performed by Parsons et al. (2014a). The FEA model was intended to predict similar load applications for a range of deck sizes from 12 ft. x 24 ft. to 24 ft. x 12 ft. The model was designed to easily incorporate a user defined substructure stiffness to view the effects of different support systems on the load cases. The model is set in 3-dimensional space and runs both static and dynamic analyses. Results from these analyses provide load reactions that are summed into total shear within the deck system. Comparing the results to the static case allows for the calculation of load amplification for use in the design of lateral force resisting systems. An example of the full scale model is displayed in Figure 8.
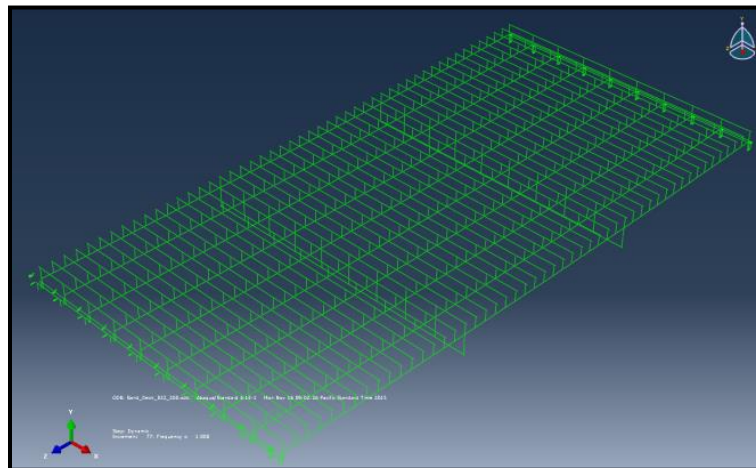
Figure 8: Example of 12 ft. x 24 ft. ABAQUS model

3.1.2 - Member Properties

Members are Euler-Bernoulli beam elements, idealized as 3-dimensional line elements with the associated properties described in the following sections. The conceptual construction of the deck model consists of nominal 2x6 deck boards, spaced at 5.75 in. on center. This allows for a 0.25 in.

clear space between each deck board. Deck boards connect to nominal 2x10 joists spaced at 16 in. on center. Joists hang from double nominal 2x12 ledgers on either end of the deck. The inner ledger is secured to the primary structure, modeled as a rigid connection to ground. This assumes that stiffness of the primary structure diaphragm (2nd story floor diaphragm for example) is much stiffer than the deck diaphragm, supported by the results of Parsons et al (204b). The outer portion of the deck is assumed to be either free (no substructure), or connected to ground via springs of varying stiffness depending on the desired substructure contribution. Each board is modeled with the specific gravity, modulus of elasticity, shear modulus, and profiles similar to that of a Hem-Fir specimen graded as No. 2 of that size (for some cases, this was altered to reflect the properties of Trex Select® deck boards). Members are assumed to be continuous. However, this allows for more direct load transfer through the diaphragm and might cause the diaphragm to be stiffer than segmented sections, but the effect is assumed negligible.

3.1.3 - Member Connectivity

Rigid links connect the 3D line element to its boundary coordinates. The rigidity of the links is achieved via assumed properties of stout steel bars. The steel bars are assigned no mass so they connect members together only via a stiff element. Member interaction is defined by springs connecting one edge of a rigid link to its counterpart on a separate member. Springs have a defined stiffness in each of the six degrees of freedom (DOF's) that correspond with the connectors used in that location. As displayed in Figure 9, translational DOF's 1 and 3 are equal to two fasteners loaded laterally as defined by NDS group action factor equation for load-slip. Translational DOF 2 relates to the withdrawal capacity of the two fasteners. Rotational DOF 5 is equal to the couple moment/radian stiffness provided from the coupe moment from the offset fasteners.

18
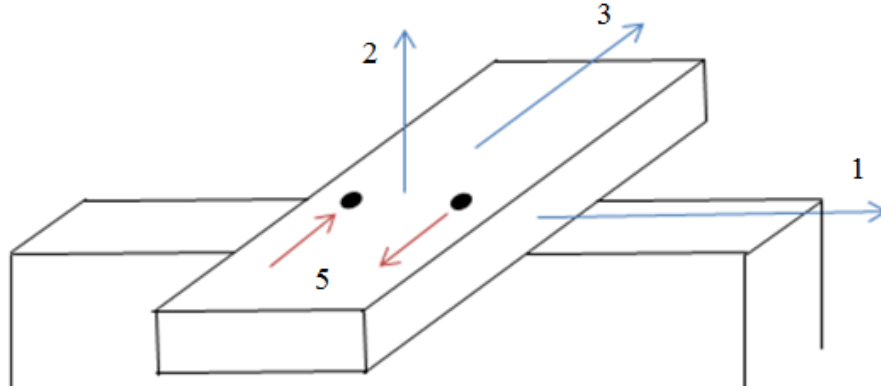
Figure 9: Stiffness degrees of freedom of a deck board-to-joist connection

3.1.4 - Boundary Conditions and Loading

Because the main result of interest is lateral load amplifications, boundary conditions of the model adequately restrict vertical displacement. Joist end rotations are restricted to prohibit rollover from lateral loading. Rollers provided at post support points restrict movement to the horizontal plane and support the deck from excessive vertical deflections. Omission of either of these restraints causes the stiffness matrix of the model to become singular. Singular stiffness matrices cannot be inverted and used to solve the system equation $P = K\Delta$. Consequently, such restraints are necessary to maintain a positive-definite system stiffness matrix, allowing the solution to be attainable. Loading to the model is achieved via line-loads placed along the deck boards' longitudinal axes. The line load is 0.1667 lb./in. along each board, equating to a surface traction of approximately 4psf. This value was selected as the static surface traction as per research performed by Parsons et al. (2014a) that demonstrated that 4 psf was the maximum cyclic load occupants can provide when inertial effects of a moving deck mass were removed.

3.1.5 - Analysis Procedure

Three steps of analysis were performed with the FEA deck model: static, modal, and dynamic analyses. In the static case, the load was applied monotonically, and the lateral base reactions at the posts and ledger attachment points were observed. The total resistance is equal to the total shear applied to the deck surface (i.e. 600 lb. for a 12 ft. x 12 ft. deck). The results from this step are used to calibrate and confirm the results from the modal and dynamic analyses.

The modal analysis is used to determine the mode shapes and Eigenvalues, and associated natural frequencies of the structure using a Lanzcos Eigen-solver normalized by displacement. Eigen-solvers solve the following Eigenvalue equation based off the dynamic equation of motion for each mode shape:

$$(\omega^2 M + K)\phi = 0$$

Omega (ω) is the frequency, M is the mass matrix, K is the stiffness matrix, and phi (ϕ) is the Eigenvector. Although ABAQUS has other Eigen-solvers that may be faster and more efficient, the Lanczos solver is the most applicable to a general case. For the use in ABAQUS, it is also the only one that produces viewable results, as well as being able to be incorporated into coupled dynamic effects.

For this model, in order to accurately capture mass distribution, the number of mode shapes considered equals a value approximately 20-30% of the total number of DOF's (LaFave, 2015). The process was fairly calculation-intensive. Other solving techniques are more appropriate to deal

with large amount of DOFs, but dynamic coupling is necessary to take into account the interaction of board stiffness and connection properties across the model. Although faster, the other methods failed to account for this. Additionally, the extraction of the first Eigen frequency is desired due the association with the first dynamic mode (the natural frequency that relates to the largest load amplification). When other methods were used in order to speed up analysis, the results of the dynamic case did not agree with the static analysis results, and natural frequencies cannot be collected.

The dynamic analysis is a mode-based steady-state type of analysis specifically designed to determine the steady state response of a system to harmonic excitation. In other words, it performs a sinewave sweep analysis and directly applies to the occupant induced load type desired for the study. When humans match the natural frequency of the deck, they impart forces in a cyclic manner that is very close to, if not exact, harmonic motion. This analysis technique relies on mode shapes (Eigenvalues determined in the frequency analysis), takes into account structural damping and has the ability to perform frequency sweeps. As per this study, direct modal damping of between 5 and 10% is reasonable. The model is very sensitive to changes in this value and the derivation of the appropriate value is a major discussion point of this study. Because research performed by Parsons et al. (2014a) concluded that humans can produce loads up to a frequency of about 1.0 Hz, a frequency sweep was performed from 0-1.0 Hz. Recorded data points were concentrated close to the natural frequency of the system so as to more accurately capture the peak amplification.

3.1.6 - Analyzing Model Results

The results of the dynamic analysis were collected for the reactions at post supports and locations along the ledger. These values and their corresponding frequencies were extracted from the data file and exported to Excel. Using Excel, the reactions were summed to determine the total shear in the system. For a frequency of 0 Hz (approx. $1.5*10^{-11}$ in the model) the total shear should be close to that found in the static analysis or checked by hand using general statics. If it is not, most likely not enough modes were determined during the analysis. In this case, the number of modes desired should be increased and the analysis re-run. For different excitation frequencies, the total shear is normalized by the static case, providing load amplifications. These amplifications are then tabulated and graphed for comparison with other models. Finally, along with the load amplifications, the natural frequency for each model is obtained from the Eigenvalue output. The first value corresponds to the lowest frequency which is associated with the first dynamic mode. In the case of this model, this value corresponds to the dominant mode shape for the amplification of interest.

3.2–Parameter Sensitivity Analysis | Deck Board-To-Joist Rotational Stiffness

3.2.1–Methods

Parsons' (2014b) findings on the importance of deck board-to-joist connection effects were explored through a parameter sensitivity analysis performed on the FEA model for lateral deck load amplifications. Three deck models (constructed to be 12 ft. x 24 ft., 12 ft. x 12 ft., and 24 ft. x 12 ft.) were subjected to varying degrees of deck board-to-joist rotational stiffness and substructure stiffness. The stiffness of the connection ranged from 9152.75 lb.-in./rad to a value of 73222 lb.-in./rad. The lower value represents a system that is 25% as stiff as the original value of

36611 lb.-in./rad and the upper value is twice that of the original value. The lower value is viewed as the effects of a softened rotational stiffness from prolonged cyclic loading, or perhaps simply a system that would provide little rotational stiffness such as one with hidden deck fasteners. The higher value represents a value closer to that of the actual value that should be used if the current procedure was followed with corrected values. In addition to the three deck board-to-joist rotational stiffness values tested, the substructure stiffness was varied from 0 lb./in. as a conservative value to 12,000 lb./in. where it was observed that any additional increase had marginal effects. The results collected were the individual response of the deck for select substructure stiffness values to see the effect on natural frequency as well as the peak load amplification for the entire range of substructure stiffness in order to observe the total effect of the deck board-to-joist rotational stiffness given many substructure set-ups.

3.2.1 – Results and Discussion

The responses of total shear amplification and reaction forces were observed at each point in the test. The results for the 24 ft. x 12 ft. model are summarized in Table 3 below. In concurrence with the results from Parsons et al. (2014b), the results from the parameter study illustrated that as the rotational stiffness of the deck board-to-joist connection increased, the stiffness of the diaphragm was greatly affected. As expected, with an increase in diaphragm stiffness, an increase in natural frequency was also observed. Figures 10-12 display the results from the analysis on the 24 ft. x 12 ft. deck with substructure stiffness of 0 lb./in. and 1500 lb./in., as well as the maximum load amplifications for the entire range of substructure stiffness.

Table 3: Total Shear Amplification with varying deck board-to-joist connection stiffness and substructure stiffness

Connection Stiffness	25%	100%	200%
Substructure Stiffness	9152.75	36611	73222
0	4.251	4.287	4.308
200	4.378	4.333	4.337
600	4.558	4.420	4.396
1000	4.657	4.498	4.451
1500	4.709	4.580	3.959
2000	4.719	4.338	2.836
2500	4.759	3.216	2.341
3000	4.646	2.409	2.081
4000	3.344	2.167	1.813
6000	2.422	1.853	1.592
12000	1.868	1.571	1.409
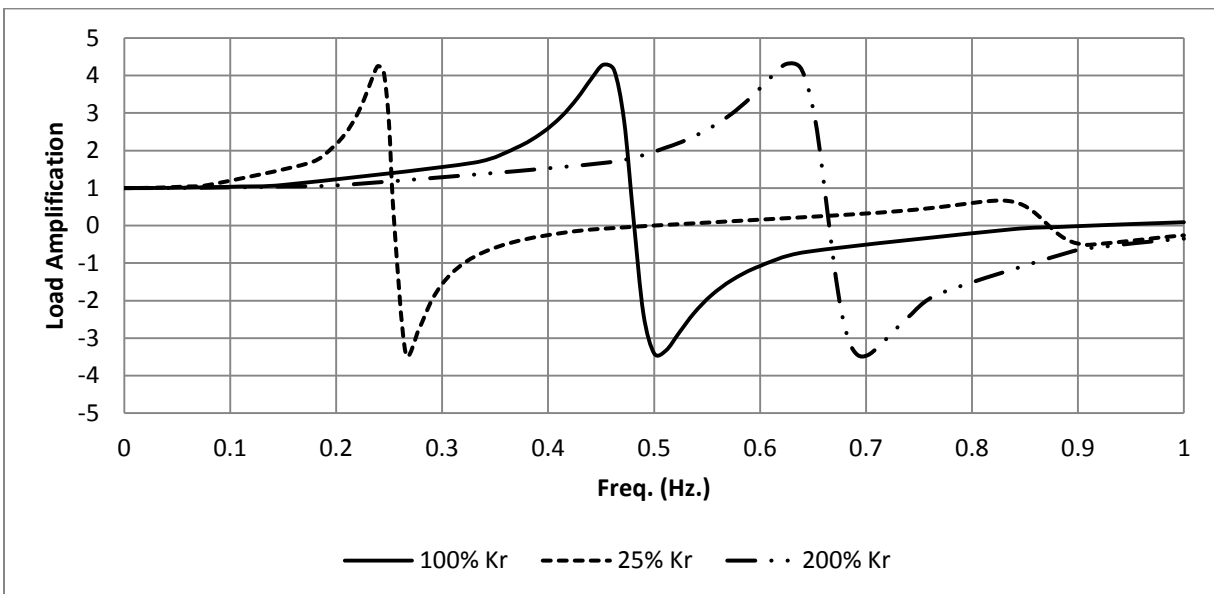
Figure 10: Total Shear Amplification of 24ft x12ft deck structure under lateral load with zero substructure stiffness.
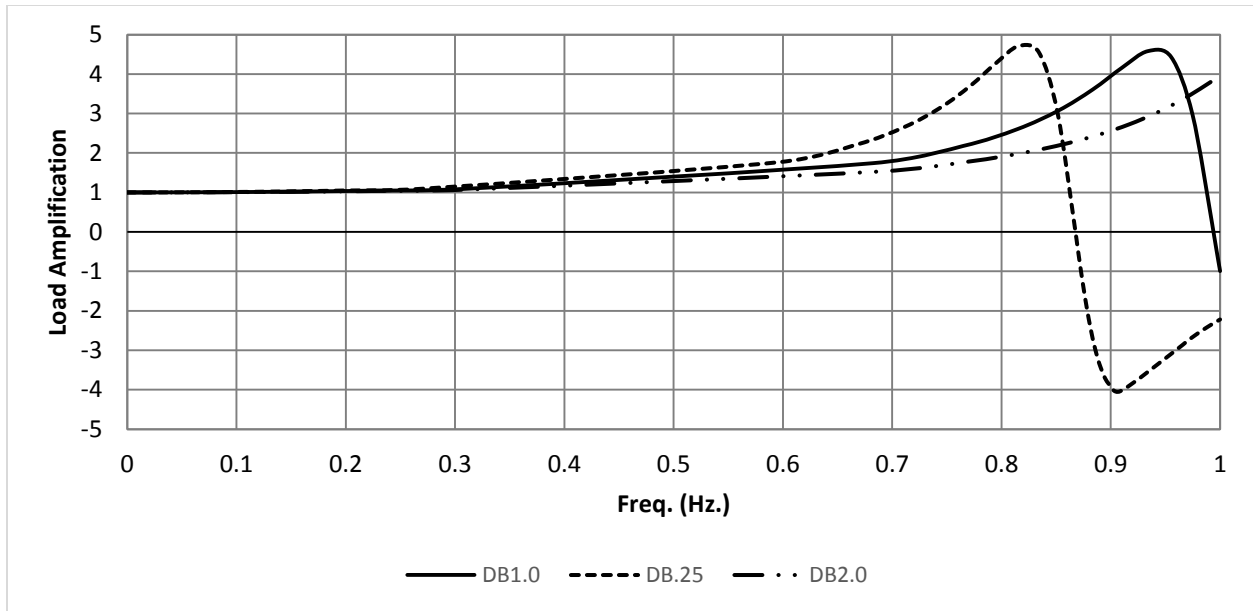
Figure 11: Total Shear Amplification of 24 ft. x 12 ft. deck structure with 1500 lb./in. substructure.
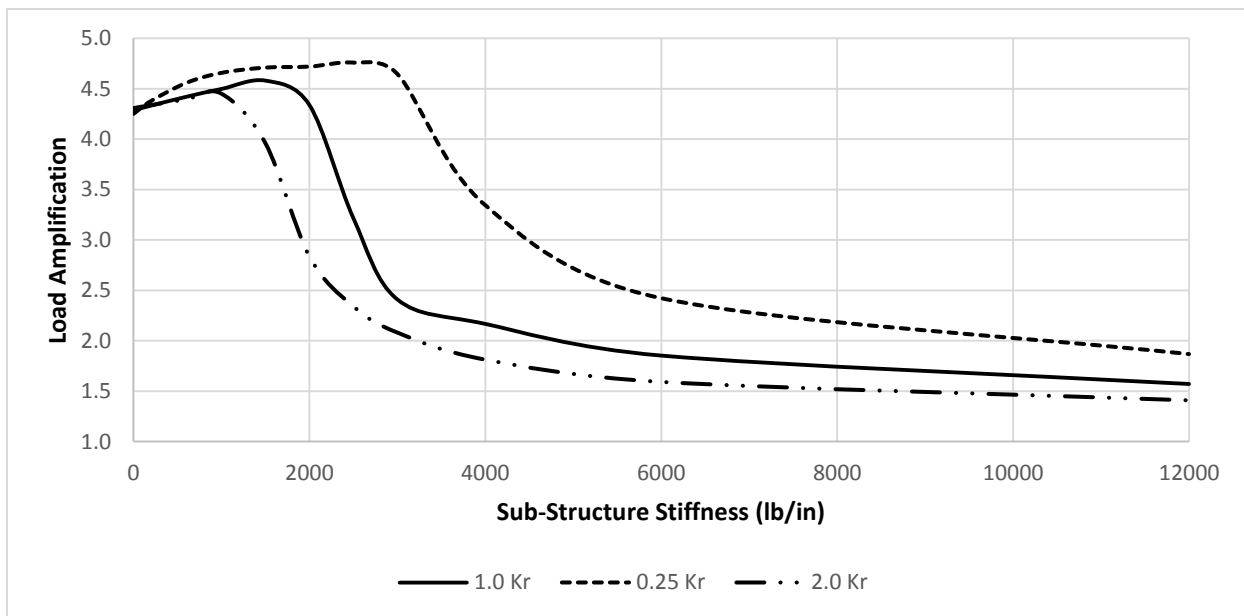
Figure 12: Maximum Total Shear Amplification of 24 ft. x 12 ft. Deck with varying substructure stiffness.

By considering Figures 10 and 11, it is observed that the natural frequency of the structure increases dramatically with the differences in deck board-to-joist rotational stiffness. Because the modal analysis used in the testing of the deck model considered a limited range from 0 to 1.0 Hz, the higher initial frequency pushed the response of the structure with the increased rotational stiffness out of the considered frequency range sooner while the structure with the lower rotational stiffness remained in the frequency range of 0 to 1.0 Hz for longer. Considering Figure 12, this resulted in a lower peak amplification (considering all substructure stiffness values) was observed when the deck was stiffened because the deck system did not stay in the frequency range of interest for as large of a range of substructure stiffness. As well, the peak amplification for the structure increased with decreased rotational stiffness due to its lower initial natural frequency. As demonstrated by Figure 12, the amplification of the structure can greatly vary, depending on the deck board-to-joist stiffness, between substructure stiffness of 1000 lb./in. and 6000 lb./in.

Depending on the true variation in deck board-to-joist rotational stiffness compared to that of the current model, the actual amplification for a given substructure frequency could be as much as 50% higher or 25% lower than what is depicted by the current model for a 24 ft. x 12 ft. deck. The results were confirmed with analyses from the models for deck sizes 12 ft. x 12 ft. and 12 ft. x 24 ft. See Figures30 through 32 in Appendix A for the results of these analyses. Although the trends are similar, differences in the results include the natural frequency at zero substructure stiffness and its effect on the response of the system. Because as the aspect ratio decreased in the 12 ft. x 24 ft. model, the diaphragm becomes stiffer laterally despite the inclusion of more connections on the larger model due to the allocation of less mass out away from the primary structure. Because these frequencies are closer to 1.0 Hz initially, it is observed that the structure gets pushed out of

26

the natural frequency range sooner (if not there initially) with a lower substructure stiffness required to drop the amplifications into reasonable values. In conclusion, because there is such variability in the response of the deck system depending on the deck board-to-joist connection, further exploration into the true rotational stiffness of the connection was necessary.

3.3 – Parameter Sensitivity Analysis | Structural Damping

3.3.1 - Methods

A model that predicts the dynamic behavior of a structural system must include damping. For an single degree of freedom (SDOF) system, the load amplification increases asymptotically as the natural frequency is approach with a relationship of $\left(\sqrt{(1-\beta^2)^2 + (2\zeta\beta)^2}\right)^{-1}$ where β is the ratio of the forcing function frequency to the natural frequency and ζ is the damping ratio. (Filiatrault et. Al, 2013 Eq. 4.85). This demonstrates that without damping, a steady state load amplification increases to infinity as the denominator goes to zero when $\beta = 1$ and $\zeta = 0$. Additionally, if $\beta = 1$, the equation reduces to $(2\zeta)^{-1}$ displaying that when excited at its natural frequency, a SDOF system is highly sensitive to changes in the damping coefficient, especially as it reaches small values (See Figure 13 below).
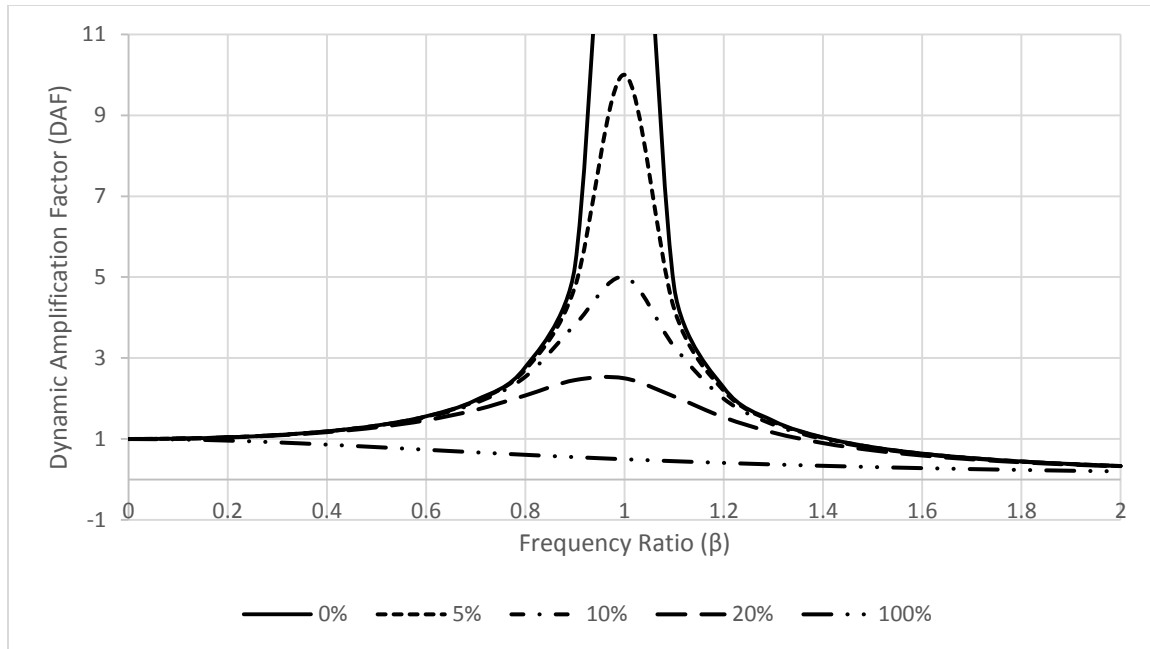
Figure 13: Frequency response of a damped SDOF system subjected to sinusoidal load (Recreated from Filiatrault et. Al., 2013, Figure 4.25).

Multiple degree of freedom systems (MDOF) systems will act differently due to the complexity that is added when accounting for various mode shapes and their relative contribution to the overall response of the system. This is defined as the modal participation factor (Filiatrault et Al, 2013). Because there are many mode shapes associated with the response of this model, a second parameter sensitivity analysis, similar to that conducted for the deck board-to-rotational stiffness was performed to determine the effect of structural damping on the system. Values for structural damping were selected based on several methods that were being explored for calculation of damping. The values chosen included 5%, 7% and 10% of critical damping. The lowest value was the current value chosen by the previous author of the model. Damping values of 7% and 10% were arbitrarily chosen to reflect an upper boundary and a value that forced the model to match experimental results. The model was run for several deck board-to-joist rotational stiffness values

to see how sensitive the model was to damping given different rotational stiffness. Results were collected for peak load amplifications considering the entire range of substructure stiffness in order to observe the total effect of the deck board-to-joist rotational stiffness given many substructure set-ups.

3.3.2 – Results and Discussion

As illustrated Table 4 and Figure 14, the initial total shear amplification (with zero substructure stiffness) is greatly affected by the amount of damping chosen. It was observed that small changes in damping have a large effect on the results produced by the model. 5% damping produced an initial value of 4.1 times the static load and more variation as substructure stiffness changed. 10% damping lowered the initial response to 2.3 times the static load and greatly reduced the variation as substructure stiffness changed. When damping varied from 5% to 7%, the initial total shear amplification changed from 4.1 times the static case to 3.1 times the static case, a 25% difference. With lower damping values, the load amplification tends to increase more than with higher damping values before moving out of the frequency range of interest. This is suspected to be due to a greater effect of the mass participating in the first dynamic mode with little damping. Results from previous testing show that for various static loading conditions, the load amplification averaged to 3.0 times the static load with minimal substructure stiffness (Parsons et al, 2014a). This value agrees most closely with the results obtained when structural damping was set to 7% for this study. Although structural damping could be used as a method of tuning the model because it exhibited a high sensitivity, a damping value that corresponds to physical testing was determined for use in the improved FEA model.

Table 4: Total Shear Amplification, Structural damping from 5% to 10%

Substructure Stiffness	ζ = 5%	ζ = 7%	ζ = 10%
0	4.094	3.066	2.310
200	4.270	3.184	2.386
600	2.549	2.425	2.199
1000	1.892	1.857	1.785
1500	1.655	1.636	1.596
2000	1.553	1.539	1.510
2500	1.497	1.485	1.460
3000	1.460	1.450	1.428
4000	1.417	1.408	1.390
6000	1.376	1.368	1.352

Figure 14: Total shear amplification for 12 ft. x 12 ft. deck varying structural damping.

3.4 - Physical Testing | Deck Board-to-Joist Monotonic Rotational Stiffness

Several data points were collected from the physical testing. Moment and rotation diagrams were created and fit to power curves. From those power curves, the rotational stiffness and subsequent damping were also determined. Additionally, moisture content and specific gravity values were obtained for each test specimen and general trends were determined. Finally, the rotational stiffness and damping values were input into the FEA models for lateral load amplifications by occupant use and amplifications for various aspect ratios and substructure stiffness values were generated and tabulated.

3.4.1 – Methods for Physical Testing

The rotational stiffness of a deck board attached to a joist needed to be more accurately determined in order to confirm the validity of the FEM model used to predict exterior deck amplifications under lateral, cyclic loads. Table 5 outlines three connection types that would conservatively represent the majority of decks constructed.

Table 5: Experimental Matrix

Test #	Fastener Type	Joist Type	Deck Board Type
1	10d Threaded Deck Nails	No. 2 Hem-Fir (2x)	No. 2 Hem-Fir (2x)
2	#10x3" Decking Screw	No. 2 Hem-Fir (2x)	No. 2 Hem-Fir (2x)
3	#10x2.75"Trex® Composite Decking Screw	No. 2 Hem-Fir (2x)	Trex® Composite Deck Board (1"x5.4")

The materials of choice are Hem-Fir for joists and deck boards as well as Trex® composite deck boards. These materials were selected due to common availability for exterior applications and likelihood of use in the Northwestern United States. Hem-Fir wood products will also provide conservative values for areas where Southern pine is used as the primary dimensional lumber for exterior uses. Hem-Fir is less dense and will to provide lower rotational stiffness values than Southern Pine; lower rotational stiffness will translate into conservative amplifications. For future testing, Douglas-Fir could be used to represent similar values in place of Southern Pine as its specific gravity is similar, and Douglas-Fir is much more available in the American Northwest. Cedar is also a common decking material due to its durability and aesthetic nature. Cedar would also provide a low, conservative density value in order to maintain a "lower boundary" type of exploration.

The fasteners chosen for the experimental connections are those that would likely to be used in common deck construction. The 10d threaded nails are beyond what is required by DCA6-12, but are more appropriate for the 1 ½ in. thickness of nominal 2 in. Hem-Fir decking. For similar reasons, the #10 x 3 in. screw was chosen over #8 screws of similar length that are required by DCA6-12. For the composite decking, a #10 x 2.75 in. Trex® decking screws designed for composite decking were chosen.

Before the fabrication of or testing of any specimens, materials were cut to length, and conditioned to the appropriate equilibrium moisture content (EMC). In order to achieve a desired EMC of 12%, the specimens conditioned in a room maintained at 65% relative humidity (+/- 2%) and a temperature of 70 degrees Fahrenheit (+/- 4 degrees Fahrenheit) as outlined in ASTM D4933-99.

The specimens remained in the room with sufficient airflow for a total of 14 days while the weight of several samples were measured periodically. As per Figure 14 below, the specimens' percent-initial-mass leveled out and equilibrated by the time they were tested on day 15 after being placed in the conditioning chamber. EMC measurements that were taken after the testing revealed that the actual moisture content of the specimens on test day was an average of about 17% for the wood specimens and 8% for wood composites. The higher value is suspected to be due to the preservative treatment in the board capturing moisture.
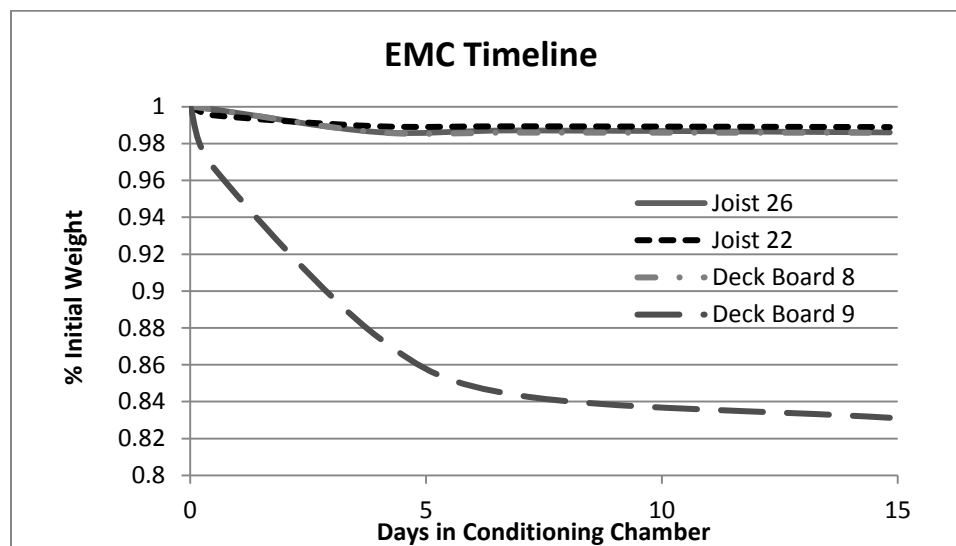
Figure 15: EMC Timeline

Ten specimens of each configuration were manufactured and tested (Nailed, Screwed, and Composite). To manufacture each test specimen, a nominal 2x6 PPT Hem-Fir deck board graded as No. 2 was placed perpendicular to a nominal 2 in. PPT Hem-Fir joist graded as No. 2 with the flat edge of the deck board resting on the narrow edge of the joist, representing actual installation. Nail and screw fasteners were placed at 3.5min. on center (1.75 in. away from the connection center), leaving approximately 1 in. edge distance the board. The deck board extended 14 in. on

one side of the joist and 12 in. on the other. The 12 in. on the leeward side of the joist provides splitting resistance as well as allows for placement of the string-potentiometer fixture. The joists were secured to a steel base with four ¼ in. diameter bolts to ensure it stayed rigid in the fixture while a load will be applied 12 in. away from the end of the joist. The application of the load was displacement controlled at a rate so that failure was achieved between 1 and 10 minutes. A displacement rate of 1 in. per minute provided approximately 0.08 radians of rotation every minute. Rotation was measured using two linear string-potentiometer displacement sensors placed at a 5 in. eccentricity about the centerline of the connection. Because each string-potentiometer has a precision of 0.001 in. over a 2 in. displacement gauge length. Therefore, this configuration will yield rotation measurements with a preciseness of $9 * 10^{-5}$ rad through the following conversion: $\theta\ (rad) = \tan^{-1}((\Delta_1 + \Delta_2)/e)$. Δ_1 and Δ_2 are the absolute displacements of the string potentiometers while e represents distance between the measuring points. The calibration of the string-potentiometers was checked prior to testing. String-potentiometers measured distance directly to the joist as they moved with the deck board, and therefore produced some error as the true values of Δ_i would be $Cos(\Delta)$. However, at the rotations considered in this study, this only resulted in a 0.2% error in the final stiffness on the conservative side (a lower stiffness would be achieved without this correction). This error is not large enough to compromise the validity of the measurement.   Figures 13 and 14 illustrate the test set-up from an elevation and plan view respectively.
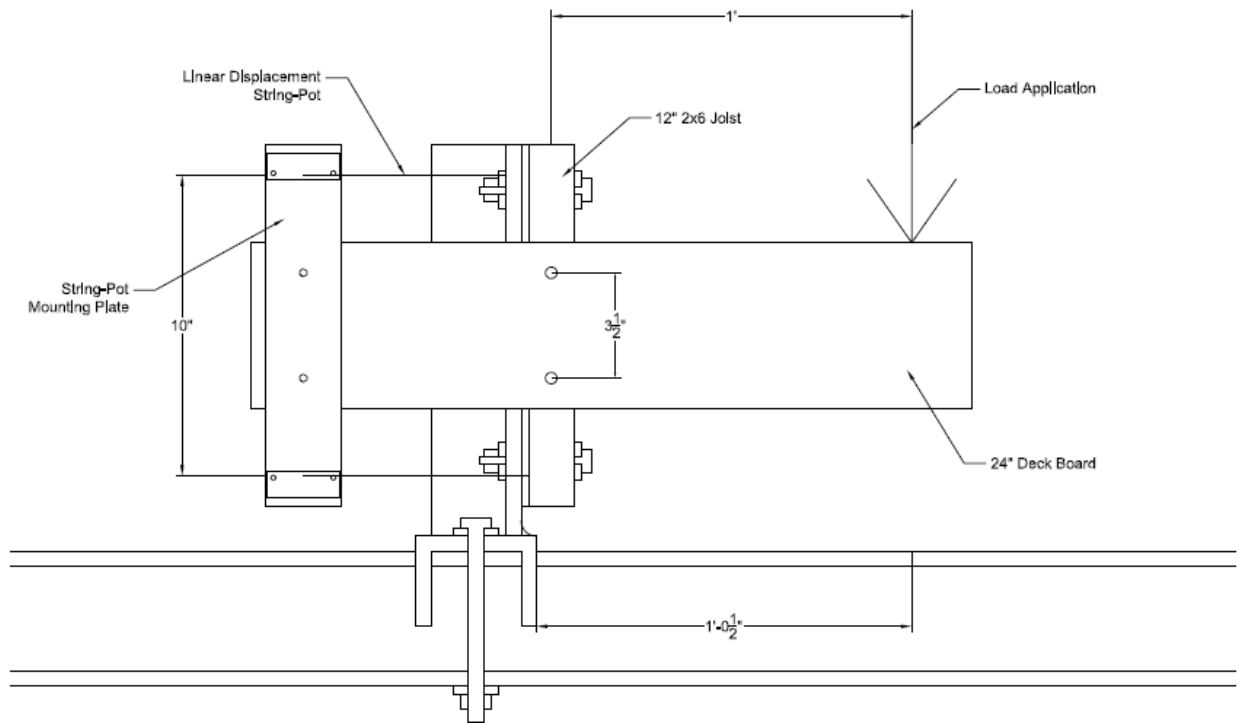
Figure 16: Elevation View of Test Set up.
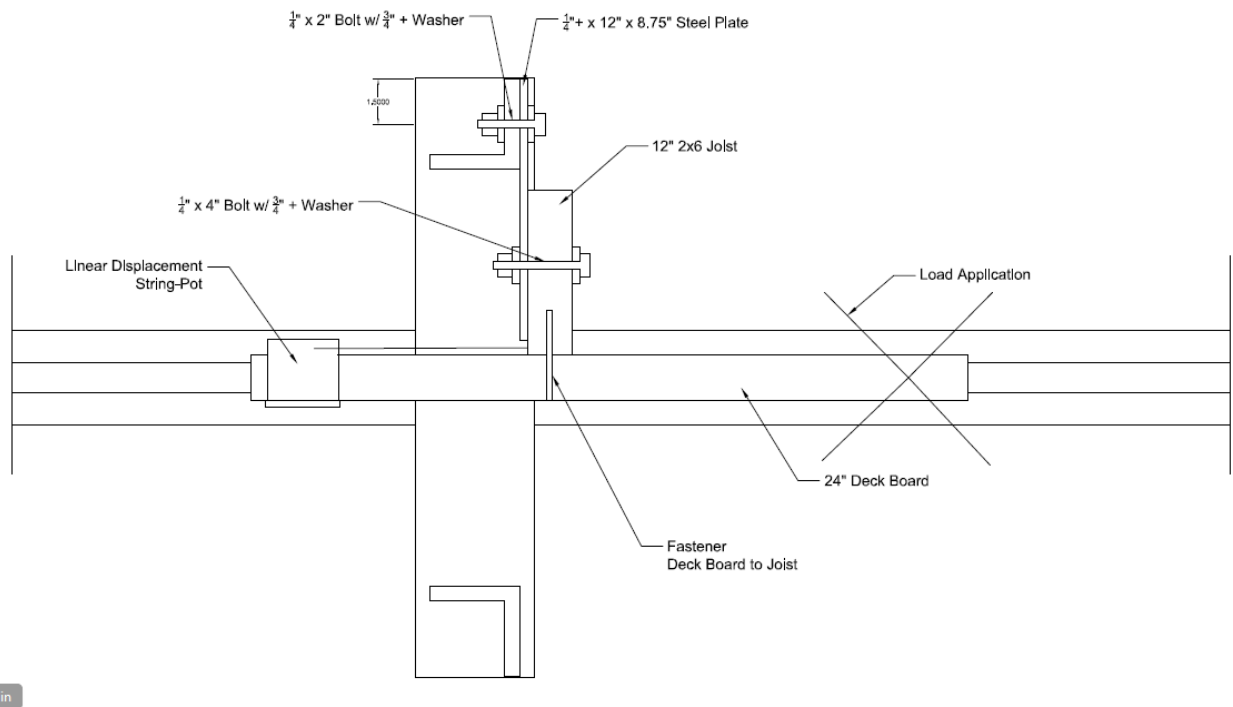
Figure 17: Plan view of test set-up

3.4.2–Methods for the Analysis of Experimental Data

Both load and displacement were recorded from initial values until either the ultimate failure of the specimen as observed, or the machine's maximum displacement of 3 in. from the original position was reached. A displacement of 3 in. was chosen due to physical restrictions of the testing machine. Very few specimens completely failed before reaching the maximum displacement. After completion of the test, the specimens were removed from the fixture and disassembled. After failure, 2 in. x 2in. blocks were cut, measured and weighed for specific gravity measurements and moisture content values. Each block was extracted near the site of failure to accurately estimate conditions at the failure site. These blocks were measured for density directly after testing as well as oven dried and measured for dry density as per ASTM D4442-15. Data from the testing included actuator displacement, load, and two displacements from the string-potentiometers located on the specimen. These data were converted to moment-rotation values by multiplying the load by the eccentricity between the load point and the center of the joint as well as applying the same transformation described above to the string-potentiometers measurement devices. An example of the data, as well as this calculation are found in Appendix B. This calculation produced graphical results similar to that depicted in Figure 18 for specimen N2 (Nail Fasteners, Specimen #2).
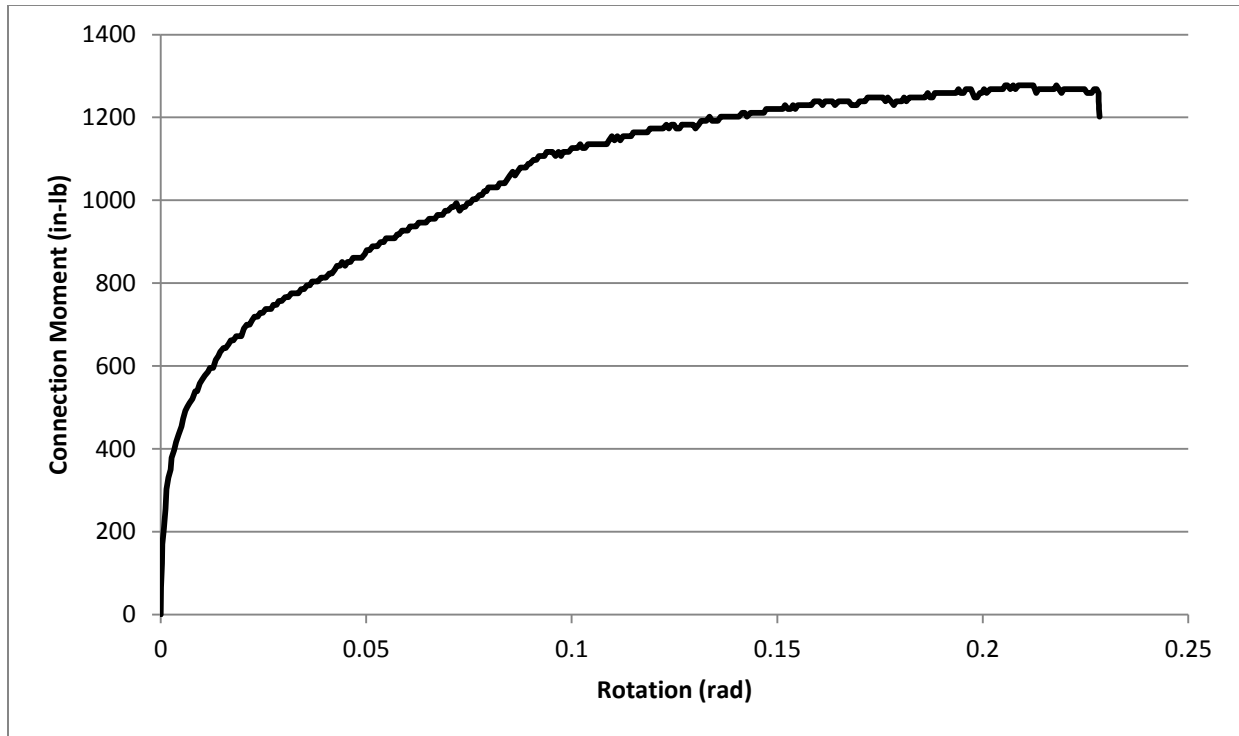
Figure 18: Connection moment vs rotation for test specimen N2.

A desired result of the testing was a single value for the load-slip modulus and associated damping coefficient of the connection representing an equivalent elastic response for the ABAQUS FEA model, for which non-linear connection properties were not feasible. When performing the steady state modal dynamic analysis discuss in section 2.3.5, the FEA model assumes materials stay within the elastic range and thus react linearly. However, when viewing the data provided by the testing, it is difficult to determine any given linear rotational stiffness value due to a constant non-linear trend in the data. For example, when enlarging the data for test specimen N2 (Figure 19) to a displacement range of 0-0.1 rad, a non-linear trend even with very small rotations is observed. As a result, a method of finding a single rotational stiffness was derived using hysteretic trends defined by past research (Dolan, 1994; Loss, 2012).
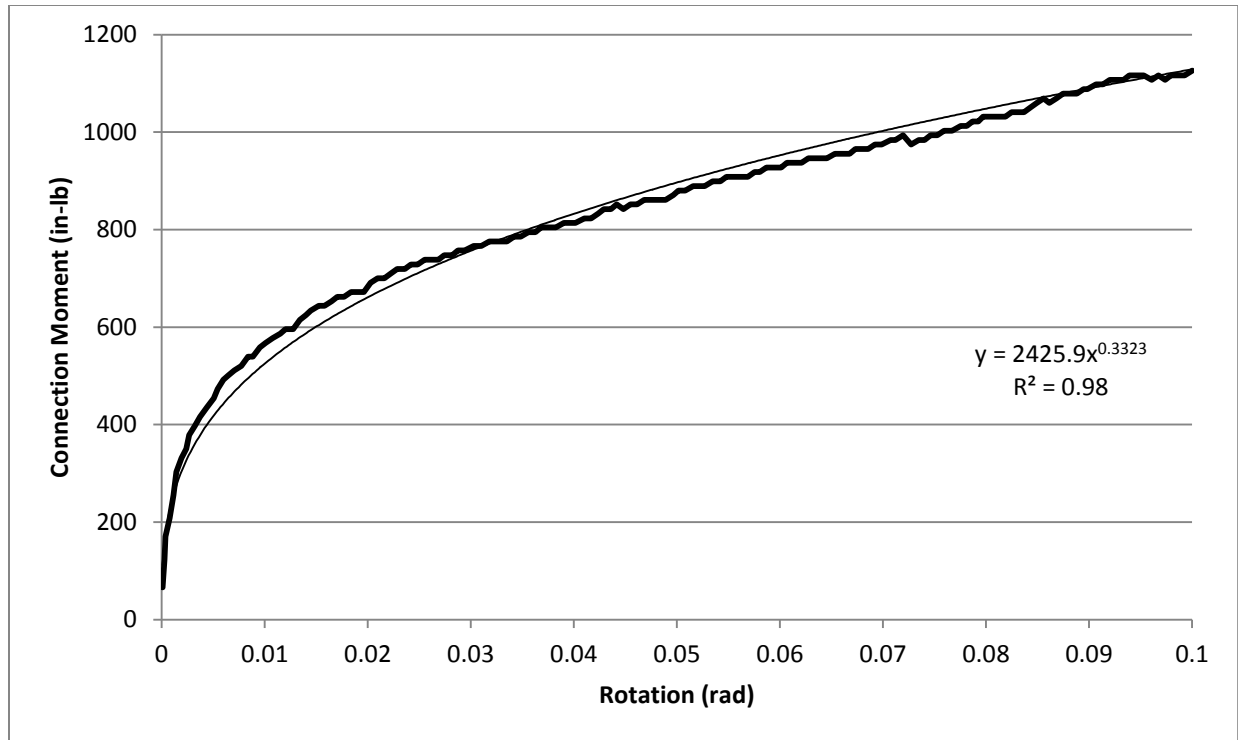
Figure 19 | Data for test Specimen N2 fitted with a power curve

Because the monotonic pushover curve for wood type structures and connections approximately matches that of the hysteretic envelope curve, a value for rotational stiffness and damping could be estimated directly from the data collected (Dolan, 1994). For this study, data was first fit to a power function of the form $M(x) = A x^n$. These curves fit with high coefficient of determination (R^2) values of greater than 0.9. The rotational stiffness of the specimen was estimated by taking the slope to the point on the power curve associated with 0.05 radians of rotation. This value represents the maximum cyclic displacement of 7 in. at the end of a 12 ft. deck (Parsons et. al, 2014a). The rotational stiffness calculated represents the recoverable strain energy when the system is loaded cyclically to the given displacement. The assumption that this is recoverable strain energy is important when considering that the model assumes a linear elastic response in the springs.

The softened stiffness can be assimilated to the rotational stiffness of the system after connection loosens and fatigues under cyclic loading conditions, but the response would be overestimated if it was assumed that all of this energy was put back into the system. Therefore, an associated damping must be estimated in order to account for the inevitable energy loss due to friction between members, slip from crushing of the wood, and fastener yielding.

Equivalent viscous damping (EVD) is an effective way of estimating the damping in a structural system for modeling. Although damping can come from many sources, the equation of motion used for dynamic analysis includes a critical damping ratio (ζ) next to the velocity component of the system. Therefore, it is sometimes mathematically convenient to lump all damping effects into a single EVD value for analyses purposes (Filiatrault 2013). EVD ratios from hysteretic behavior are determined through the following relationship (Dolan, 1994).

$$\zeta = \frac{D}{2\pi\ P} * 100$$

Where:

ζ = EVD ratio ((represented as percent of critical damping)

D = Energy dissipated during one full cycle of the system

P = Potential energy for one full cycle.

The potential energy (P) for one full cycle is defined as the rotational stiffness previously determined times the square of the max displacement. In Figure 20, this is the area underneath the

solid black line. The energy dissipated (D) is the area under the hysteretic curve. This curve is defined by the actual load-displacement of the specimen as it is put under cyclic loading. Because monotonic testing was only performed, this curve had to be estimated. There are several methods to determine this, including that developed by Chui (1998) using FEA methods. The method outlined by Chui (1998) takes into account fastener yielding, strain hardening, and wood embedment. Such a model is fairly accurate, but also labor intensive. To maintain simplicity for the scope of this project, a simplified method developed by Loss (2012) was adapted to suit this project. Loss (2012) defines a hysteretic curve via three portions, the initial rotational stiffness and the recharge rotational stiffness (to form the points of the curve), and the force required to return the connection to zero deflection (to represent the pinching effect of wood embedment).

For this project, the initial rotational stiffness was defined by the equations for load slip defined in Section 10.3.6 of the 2012 edition of the ANSI/AWC National Design Specification for Wood Construction. The recharge rotational stiffness was estimated at ½ the initial stiffness (Ceccotti, 1989). The force to return the connection to zero deflection was defined as 33% the yield force for the Mode IV failure of the Trex® screws and nails and calculated using a similar method to be about 25% for the Mode III yield of the regular screws (Loss, 2012). Failure modes are defined from TR-12, general dowel equations for yield modes in dowel type fasteners (AWC 2015 B). Calculations for the determination of the EVD parameters are found in Appendix B.
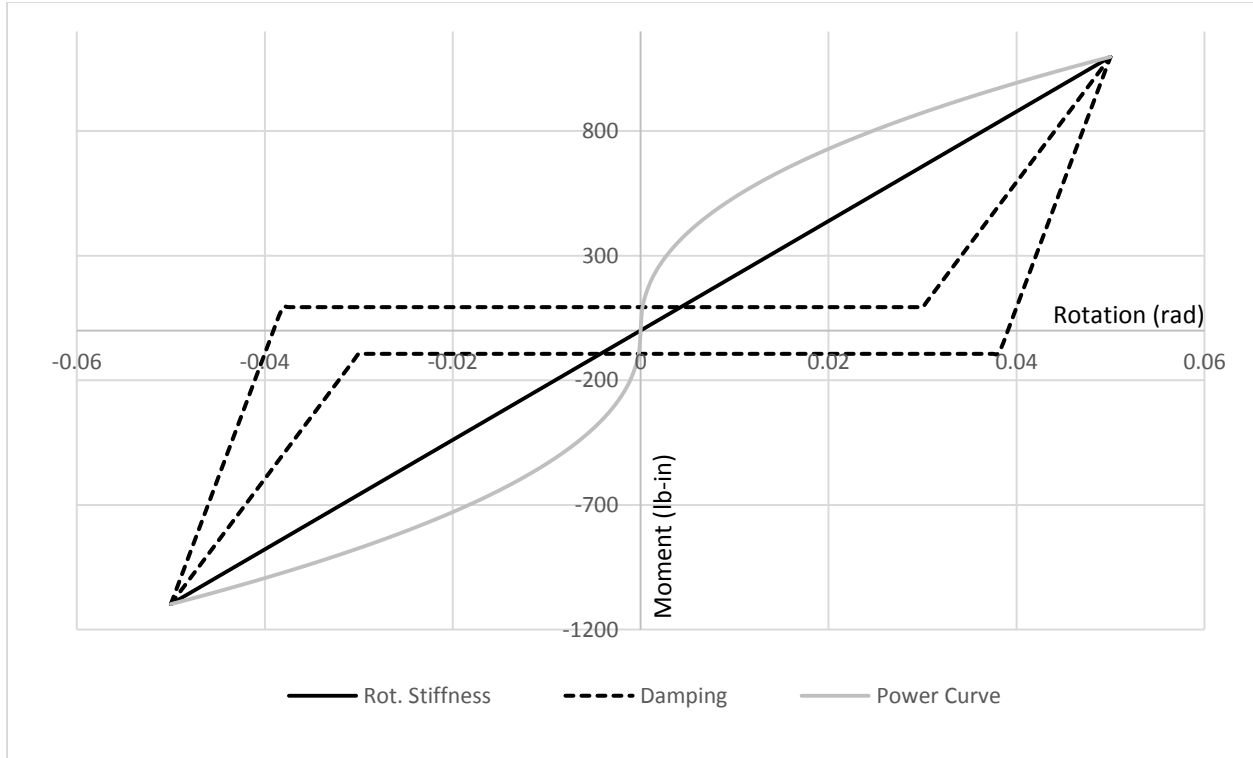
Figure 20: Data power curve, rotational stiffness and hysteretic damping used to determine the Equivalent Viscous Damping coefficient for the FEA model.

Values of rotational stiffness and damping were calculated for each test specimen then averaged linearly. The data sets were also averaged at a point-by-point basis and a single value for each test type was determined. These values agreed with the initial average value. These values were input for the FEA models for deck lateral load amplifications and the results for each aspect ratio and substructure stiffness were tabulated for each test type.

3.4.3 - Results and Discussion | Power Curves, Rotational Stiffness and Damping.

The results from the physical testing of the specimens containing Hem-Fir joists and deck boards

connected with #10 x 3 in. screws are presented in Figure 21. Data from the specimens containing

nailed fasteners and Trex® composite decking can be found in Appendix A. The moment-rotation

curves from the raw data for a rotation of 0-0.1 rad are presented in Figure 21. This range

corresponds to twice that of the maximum deflection seen in the physical trials performed in the

full-scale testing so as to provide a good fit for larger deflections if needed (Parsons et al, 2014

A). The data showed non-linear trends, but fit well with power curves. Therefore, each set of data

points were averaged on a point-to-point basis (displayed as the solid, bold line in Figure 21) and

a trend line was set to those points with an R^2 value greater than 0.9.
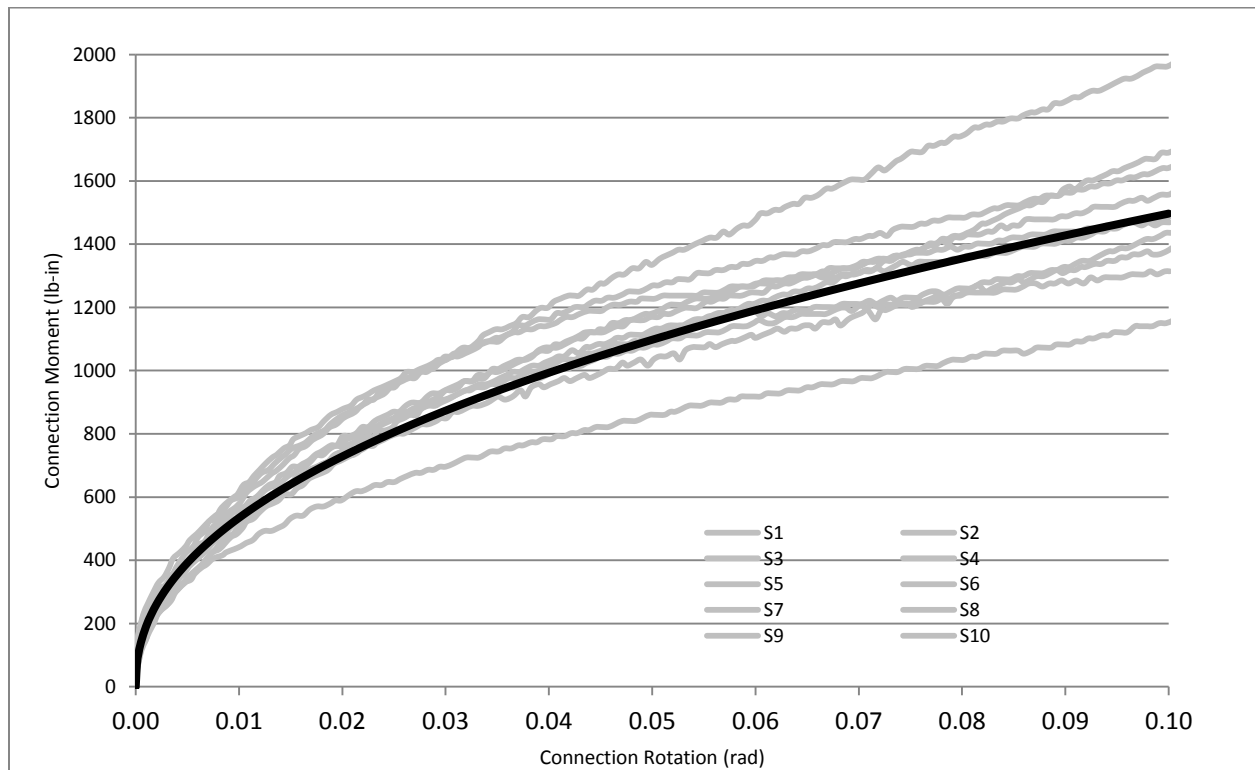
Figure 21: Moment vs. Rotation of the test specimens containing Hem-Fir Deck Boards and Joists

connected via #10 x 3 in. Decking Screws

Nailed and composite average power curves also matched well with high R^2 values. The variation in data curves was small except that, when testing the nailed specimens, one specimen was significantly stiffer than the others, pulling the trend line for the average to a higher value (see Figure 37, Appendix A). This is most likely attributed to the lesser amount of control over the connection strength when using nails, while a more consistently secure connection is possible when using screws and composite decking.

The power function viable values for each individual test specimen and can found in Appendix A. The power curve that represents the average of the data set is represented by the following equations for all three connection types, and are graphed in Figure 22 below.

$$\#10x\ 3\text{"} \text{ Decking Screws:} \quad M(\theta) = 4193\ \theta^{0.45}$$

$$\text{10d Threaded Deck Nails:} \quad M(\theta) = 3367\ \theta^{0.41}$$

$$\text{Trex\textregistered\ Composite Boards:} \quad M(\theta) = 4215\ \theta^{0.38}$$

Where:

$$M(\theta) = \text{Moment Resistance in the Connection}$$

$$\theta = \text{Connection rotation (rad)}$$

When comparing the average power functions from the three connection types, the monotonic push-over curves are similar for both the screw and nail type fasteners when the deck board was made from Hem-Fir graded as No. 2, but the moment resistance increased by 43% at a rotation displacement of 0.05 rad when composite deck board and composite decking screws were used.

There are a few possibilities as to the reason for this trend including side member density, and the amount of main member penetration. These trends are discussed more in the following sections.
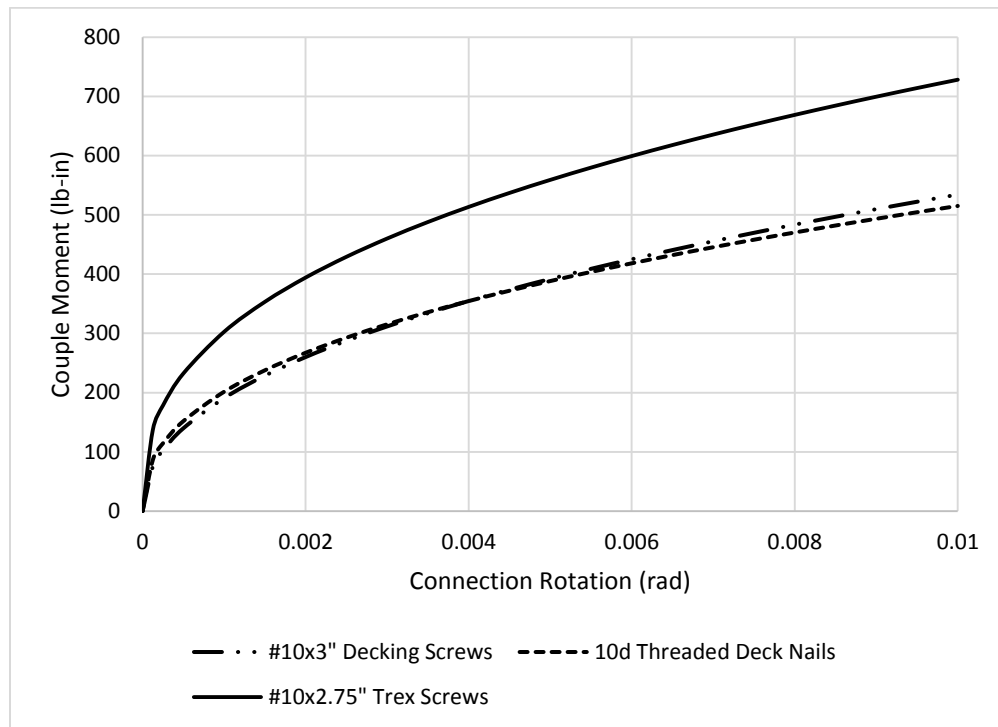
Figure 22: Averaged Power Functions of the Moment vs. Rotation data from the three test types

From the power functions produced for each connection type, the rotational stiffness and the damping was determined. Rotational stiffness values represent a secant stiffness to a deformation of 0.05rad, and the damping values represent the EVD associated with a hysteretic curve corresponding to the same point. The average values and their corresponding COV's are listed below in Table 6.

Table 6: Rotational stiffness and damping statistics from the physical test data

Statistic	#10x3" Screws		10d Threaded Nails		#10x2.75" Trex® Screws	
	K_{Rot} (lb.-in./rad)	Damping	K_{Rot} (lb.-in./rad)	Damping	K_{Rot} (lb.-in./rad)	Damping
Mean	22447	7.2%	20380	9.3%	26902	10.1%
COV	0.11	0.05	0.29	0.08	0.11	0.06

Values for rotational stiffness were rounded to 22000 lb.-in./rad, 20000 lb.-in./rad, and 27000 lb.-in./rad for the #10 x3 in. Deck Screws, 10d Threaded Nails, and Trex® Composite Board test types respectively. Respective values for damping were rounded to 7%, 9.5% and 10%. These calculations and their results are summarized in Appendix A. COV values for these statistics were fairly small, all approximately 0.10, with the exception of K_{Rot} for the 10d threaded nails at 0.29. COV values for modulus of elasticity of dimension lumber is 0.25 (AWC, 2012), so the values of this test are judged acceptable.

The damping values for the specimens containing 10d threaded nails and #10 x 2.75 in. Trex® Decking Screws were 2% to 3% higher than that of the #10 x 3 in. deck screws. This may be due to the yield mode of the fasteners, and it had a great effect on the dynamic response of the structure. The nails and composite deck screws were both observed as yielded in Mode IV as defined by AWC TR-12. This mode induces two plastic hinges in the fastener, increasing the amount of force required to return the connection to a point of zero rotation. This decreases the amount of pinching seen in the hysteretic damping curve, when compared to the #10 x 3 in. nails that exhibited a Mode III yield. Mode III is governed by only one plastic hinge in the fastener and only bearing in the main or side member. Pinching values for Mode IV type of failures are about 33% the yield moment on the return loop while Mode III yielding only provides about 25% of the yield moment. This greatly increases the amount of damped area for the nailed and composite test configurations.

It is interesting to note that the fasteners used in the physical testing performed by Parsons et al. (2014a) exhibited a Mode IV yield as defined by NDS equations when subjected to the installation described in his work (#8 x 3 in. wood screws). According to the damping calculations performed in this study, #8 x 3 in. wood screws would result in damping closer to 10%, and lower initial load amplifications in the FEA model. Physical test results most closely match the FEA test results where Mode III yield was observed using #10 x 3 in. screws (a 7% damping value). One explanation for this relationship is that this study assumes a tri-linear hysteretic damping curve (initial rotational stiffness, recharge rotational stiffness, and return strength to zero deflection, See Figure 57 Appendix B) where in reality, a composite of power functions based on wood embedment, fastener yielding, and friction in the connection is more accurate (Chui, 1998). Additionally, for this study, the recharge rotational stiffness was assumed to be ½ the initial rotational stiffness (Ceccotti, 1989).

3.4.4 - Results and Discussion | Rotational Stiffness and Damping vs. Specific Gravity, Moisture Content and Joist Fastener Penetration.

In addition to calculating the rotational stiffness and damping for each specimen, specific gravity values at the time of testing were calculated. The stiffness values and EVD with relation to side member (deck board) specific gravity, main member (joist) specific gravity, and average specific gravity are presented in Figure 23. The trends show that there is a positive correlation between rotational stiffness and side member specific gravity as well as average specific gravity. However, because there is little correlation to main member specific gravity, it can be assumed that the main member specific gravity has little effect on the result. Moisture content was also measured and compared to the rotational stiffness and EVD values.

46
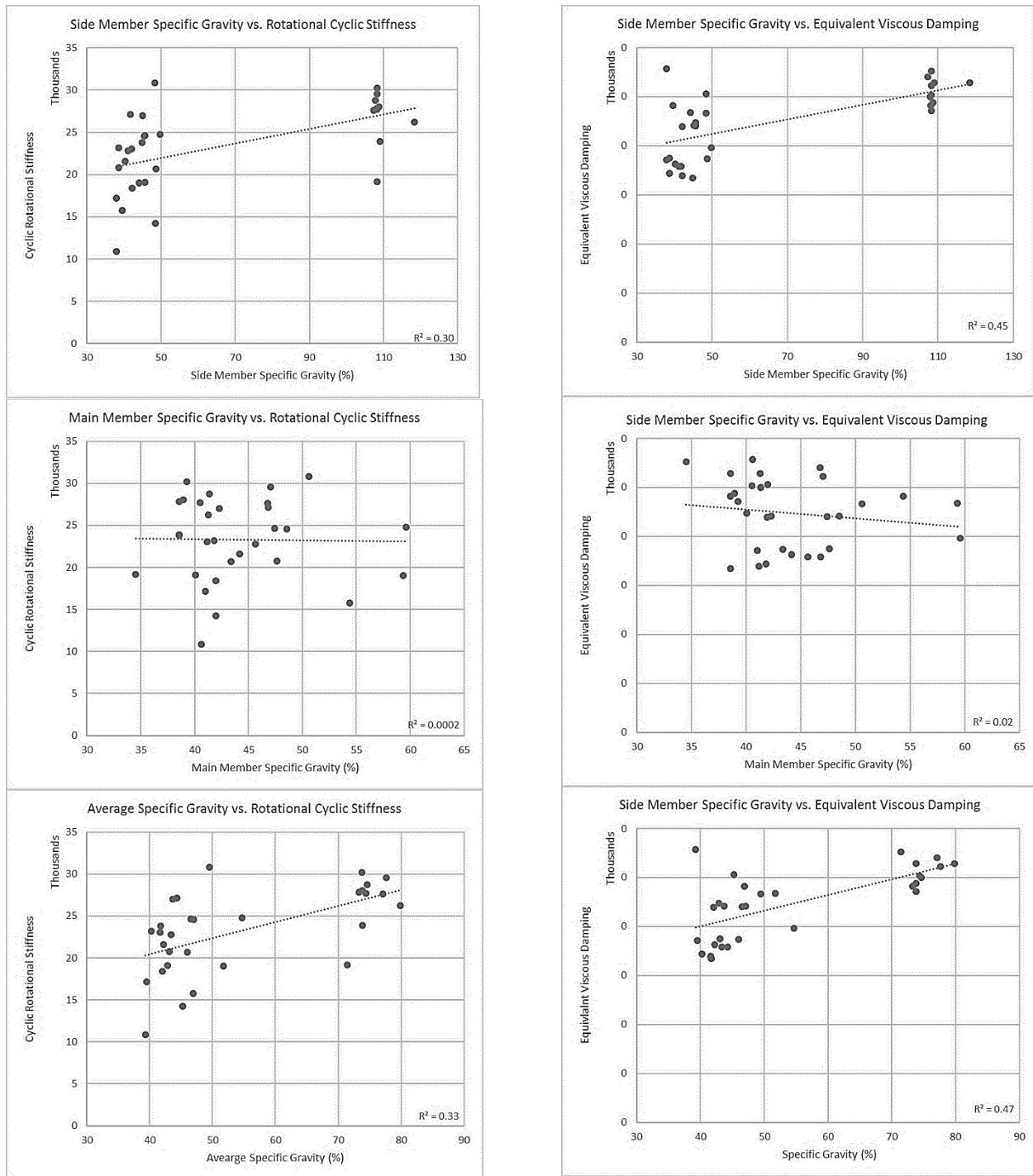
Figure 23: (Left Column) Specific Gravity vs. Rotational Stiffness. (Right Column) Specific Gravity vs. Equivalent Viscous Damping

The trends regarding moisture content are presented in Figure 24. Deck board and average moisture content had a negative correlation to the rotational stiffness. However, because main member moisture content shows little correlation, it can again be assumed that the side member has more effect on the results. Results for both specific gravity and moisture content showed little correlation to the calculated EVD values. It must be noted that the members with significantly lower moisture contents also have significantly higher densities. These members were Trex® composite deck boards where control over the quality of the board during manufacturing is much higher. Because the same specimens govern the trend for both analyses it is difficult to separate the cause for the increase in rotational stiffness although it can be concluded that the specimens that included the use of Trex® deck boards performed better than those with Hem-Fir deck boards graded as No. 2.
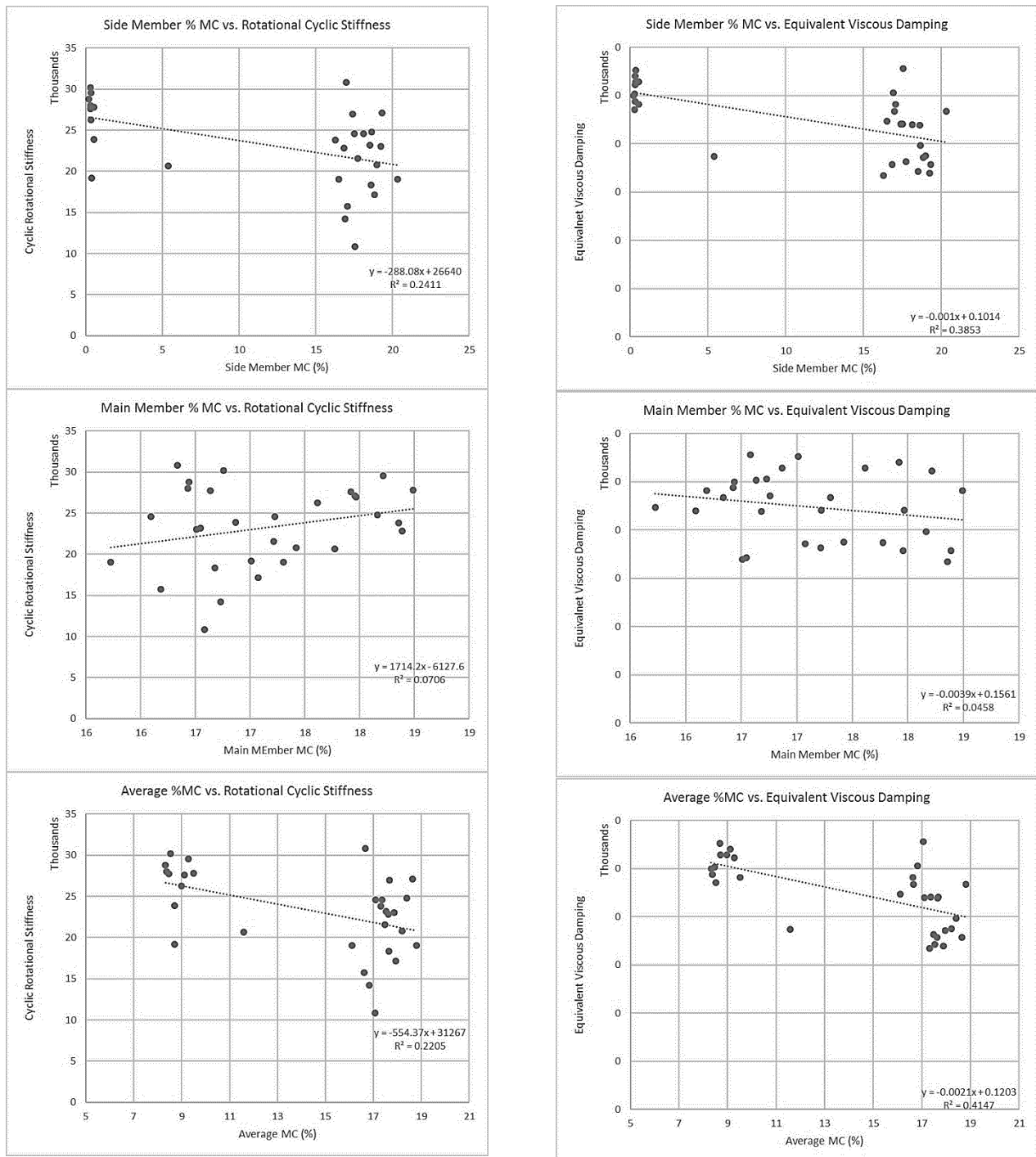
Figure 24: (Left Column) Moisture Content vs. Rotational Stiffness. (Right Column) Moisture

Content vs. Equivalent Viscous Damping

Additionally, because the side member thickness was not constant, the amount of main member penetration changed when different deck-boards were used and the rotational stiffness and EVD values were also compared to the percent-main member-penetration (PMP). PMP is defined by the amount of fastener penetration into the main member with respect to the total length of the fastener. As per Figure 25, there appears to be a positive correlation between PMP and the rotational stiffness, but little correlation to EVD values. However, the increased values are still associated with the Trex® composite boards, which also exhibit higher densities, and lower moisture contents, both of which could increase the performance, limiting the conclusion to that the Trex® deck boards performed better in general, and could be related to these parameters or others as well.
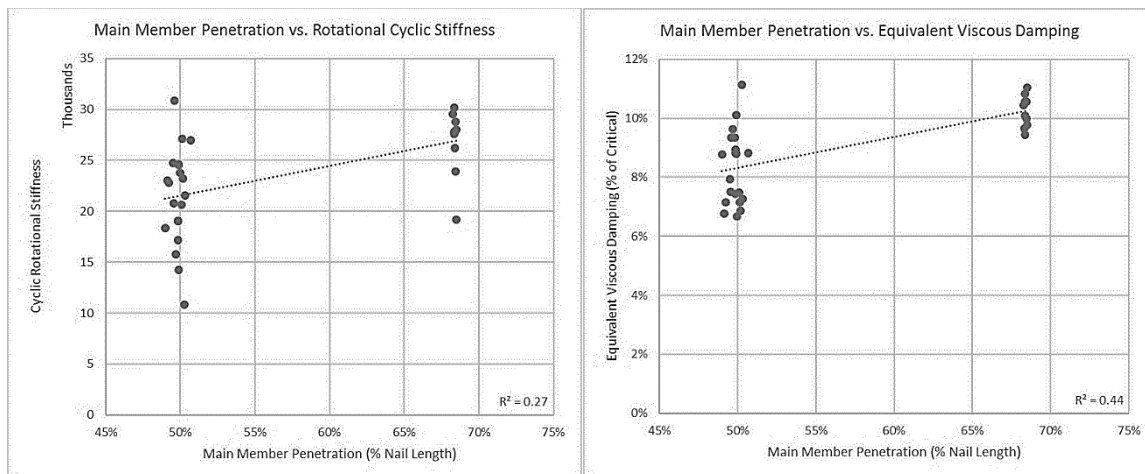
Figure 25: (Left) Percent-Main Member-Penetration vs. Rotational Stiffness. (Right) Percent-Main Member-Penetration vs. Equivalent Viscous Damping

None of the above analyses provided much insight into EVD values. This is thought to be due to the other assumptions made, and the model chosen when calculating damping values. The damping calculation was more dependent on yield moment, return strength and initial rotational stiffness, while yield moment incorporates material density and main member penetration, the initial

rotational stiffness is a function of only fastener diameter (NDS 2012 Section 10.3.6). In conclusion, for this study, damping is suspected to be more dependent upon fastener properties than material characteristics.

3.4.5 - Results and Discussion | FEA Lateral Load Amplifications

Once the rotational stiffness and damping values were calculated, they were used to tabulate the load amplification values for each FEA model, including all models ranging from 24 ft. x 12 ft. to 12 ft. x 24 ft. and considering substructure stiffness from 0 lb./in. to 10^9 lb./in. The models were run with the average values described above. The results for the 12 ft. x 12 ft. deck model comparing each test type with substructure stiffness ranging from 0 lb./in. to 2000 lb./in. are shown in Figure 26. Values for zero substructure stiffness show that the test configuration with #10 x 3 in. screws and Hem-Fir deck boards provides the highest load amplifications at around 3 times the static load. The configuration with 10d threaded deck nails and Hem-Fir deck boards showed an initial value of 2.4 times the static case and the configuration with Trex® deck boards and screws had an initial value of 2.3 times the static load. These values are much lower than the results obtained using the previous models. Initial values of 4.25 times the static from the previous version of the model indicates at least a 27% decrease in load amplifications given the updated rotational stiffness and damping values – a significant reduction.
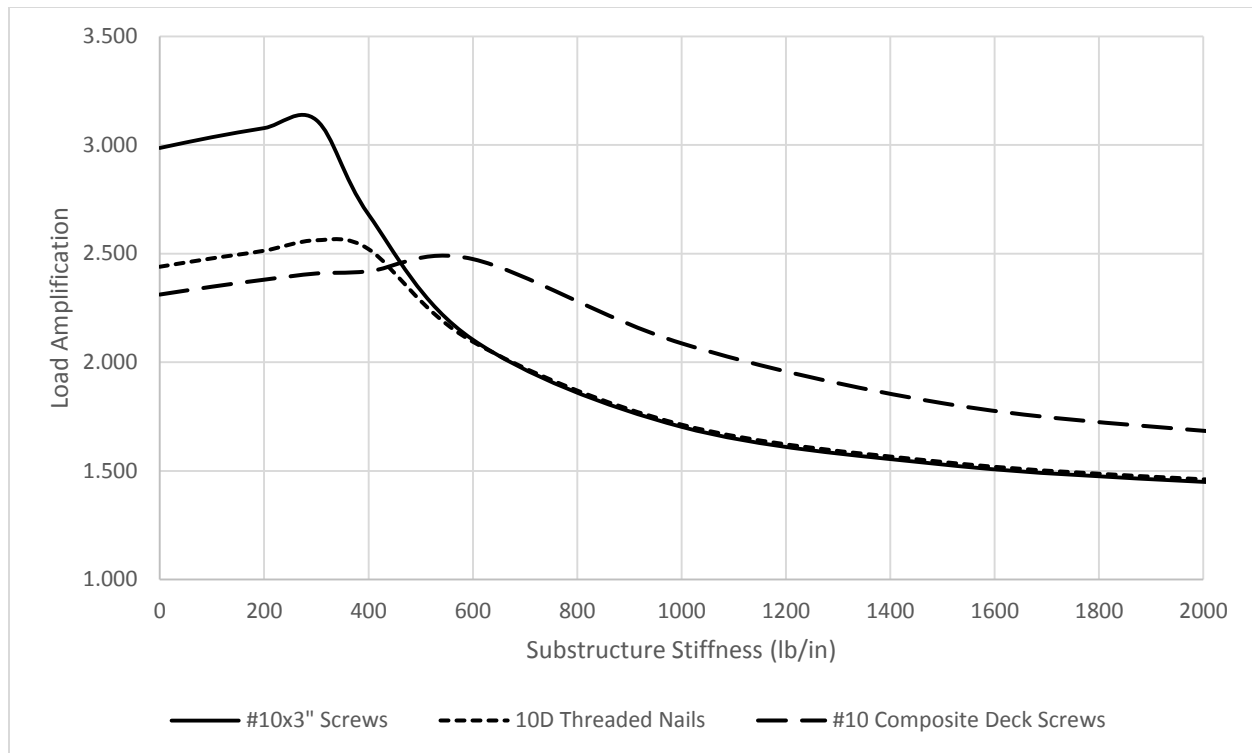
Figure 26:Total Shear Load Amplification of 12ft x12ft Deck Comparing 3 Test Types

It is intuitive that the configuration with Trex® products has the lower initial amplifications because it has the highest rotational stiffness and damping values. The larger amplifications associated with the #10 x 3 in. screws with respect to the 10d threaded nails is due to 22% smaller damping values associated with the #10 x 3 in. screws, despite a 10% increase in rotational stiffness values. The discrepancies between the test configuration with #10 x 3 in. screws and that with the 10d threaded nails dissolve at a substructure stiffness of around 600 lb./in. This could be due to that both structures are now reacting with natural frequencies well beyond the frequency range of 0-1Hz, and the effects from difference in rotational stiffness and damping becomes negligible (in comparison to the total stiffness including substructure stiffness).

It is important to note, however, that at a substructure stiffness of approximately 450 lb./in., the amplifications for the test configuration with Trex® deck boards and screws become larger than the other test types. The large increase in mass when using the Trex® deck boards in comparison with Hem-Fir deck boards could explain the difference; Trex® boards have a specific gravity of around 1.10 compared to 0.43 of Hem-Fir. When accounting for the difference in dimensions of the Trex® boards, this results in a 45% increase in mass. This significantly decreases the natural frequency for any given rotational or substructure stiffness, containing the response to within the range of 0-1.0 Hz for a larger range of substructure stiffness. These trends hold true for all of the aspect ratios. The results are found in Figures 48 through 52 in Appendix A.

4.0 – Design Aids

As a product of this research, several steps were taken to create tools for further research and aid in the design of deck structures for this type of loading. First, a simplified FEA model was created to provide an easier method of estimating lateral load amplifications for deck layouts different than those created in the full-scale model. Second, an excel spread sheet was developed to calculate the load amplification for some general cases so that FEA programs need not be run. Finally, using the excel spreadsheet, a list of tables was created so that lateral load amplifications could be selected using joist and ledger lengths as well as estimated substructure stiffness.

4.1 – Simplified FEA Model

The simplified FEA model consists of a single beam and spring supports that represent the behavior exhibited by the full-scale deck model. A visual representation of the simplified model is shown in Figure 27. The deck to ledger attachment was modeled as a spring connected to ground with high stiffness to simulate a fixed condition to the primary structure (K_{Ledger}). Connections to the substructure are modeled as linear springs to ground at the desired locations (K_{sub}), with any desired resistance. The deck super structure was modeled as a single 1in x1in member that exhibits the shear and bending characteristics of the full-scale model. The shear modulus was determined by extrapolating the rotational stiffness of the individual deck board-to-joist connections to the full-size of the deck, then reduced to a single, unit value. An example of this conversion can be found in Appendix B. The bending modulus for the simplified model was determined by applying a unit load to the end of the full-scale model and calculating an equivalent value to force a single beam to behave the same way. However, because the lateral behavior of the deck was governed by the shear characteristics of the system, the bending modulus of the beam in the simplified model

54

has little effect on the results. This was confirmed through a sensitivity analysis that showed marginal changes in model results with large changes in bending modulus, while large variations in results were observed with large changes in shear modulus.
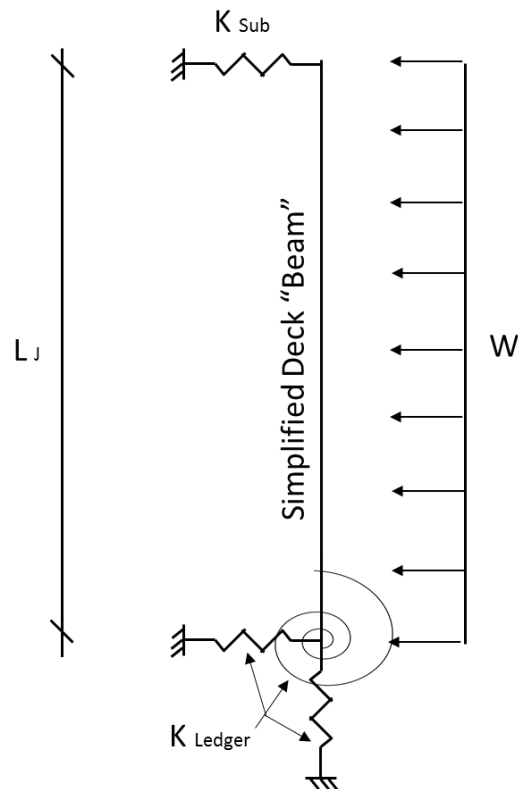
Figure 27: Illustration of simplified FEA analysis model with spring reactions and applied loads.

The simplicity of this model compared to the full-scale model allowed for much faster computation time and therefore the production of results in a more efficient manner. For example, the simplified model for the 12 ft. x 12 ft. deck consisted of 12 in. beam elements resulting in only 144 total elements in comparison to over 10,000 elements in the full-scale model. In addition, the lesser number of elements allowed for the use of quadratic elements in the simplified model to smooth out results instead of linear elements in the full-scale model.

To demonstrate the model's capability, the simplified FEA model results (shown in red) to the original full-scale model results (shown in black) are presented in Figure 28. The results of the simplified model match well with the full scale model. Where there are high amplifications (low substructure stiffness), the simplified model provides acceptable values. As the substructure stiffness increases relative to the diaphragm stiffness, the simplified model results deviate from the full-scale results. This may be attributed to the participation of additional modes considered in the full-scale 3-dimensional model. The full-scale model for a 12 ft. x 12 ft. deck considers over 2500 mode shapes, the simplified model considers only 125 mode shapes and is limited to the effects of only 2 dimensions. It is impossible for the simpler model to account for the interactions added through the increased number of DOF's and mode shapes of the full-scale model. However, the results are close enough for practical use if the simplified model is used to estimate lateral load amplifications where low substructure stiffness is a valid assumption.
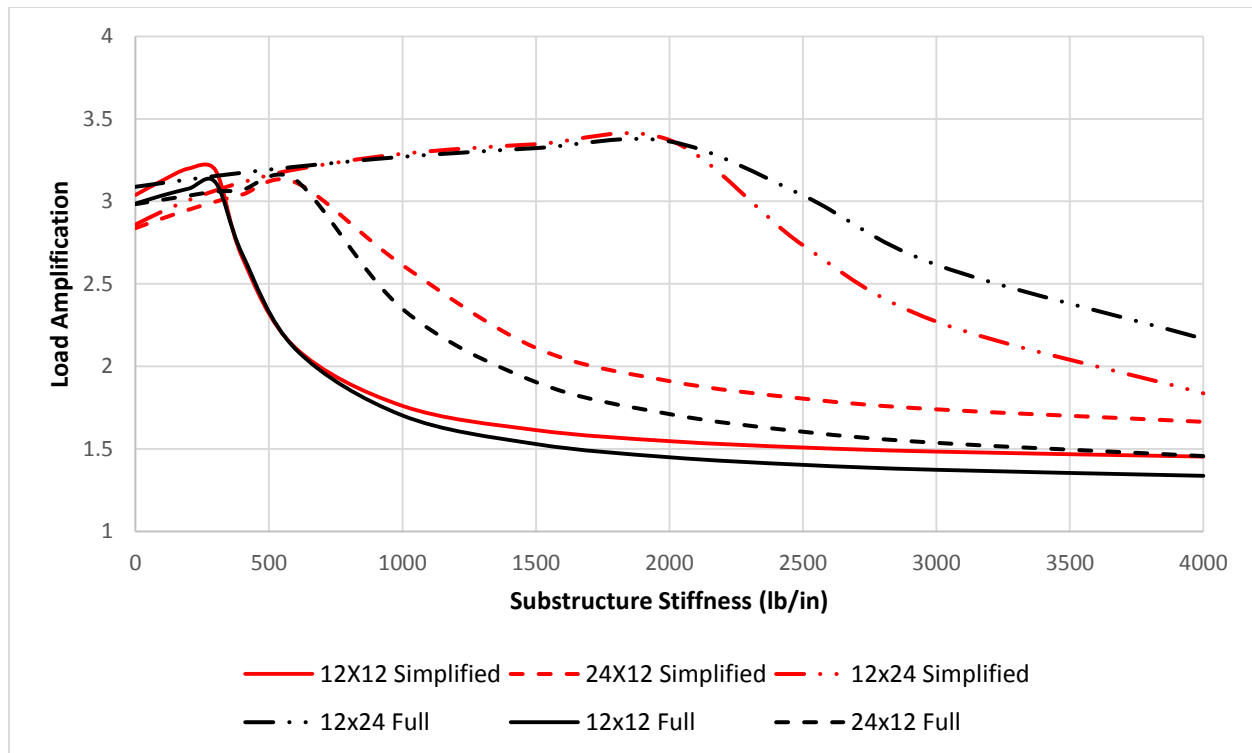
Figure 28: Comparison of the simplified FEA model results to the full-scale FEA model results

4.2 – Excel Spreadsheet

For those who may not have access to a FEA program, an excel spread sheet is of particular value. Thus for easier, faster computation of lateral load amplifications, an excel design aid was developed. A user friendly interface allows the engineer to input the following characteristics of the deck:

- Joist Length
- Ledger Length
- Joist Spacing
- Deck Board Spacing

- Deck Board Material
- Connector Type
- Substructure Stiffness
- Vertical Live Load

57

For this spreadsheet, the deck board material and connector type are limited to those that were tested during this study. Joist spacing and deck-board spacing are used to determine the total number of connections so that the shear modulus of the deck can be extrapolated to an equivalent SDOF system, a process that is similar to that of the simplified FEA model.

In order to easily calculate the dynamic amplification of a such a complex MDOF system, the MDOF system was converted to an equivalent SDOF, cantilevered pendulum with the mass lumped at the end of the deck. The stiffness of a single connection was extrapolated to the entire deck size, then reduced to a force per unit displacement at the end of the deck. Substructure stiffness was included and superimposed onto the deck stiffness via a single spring value at the end of the deck the represented the total substructure participation. Finally, the mass of the deck was estimated using a value of 6 psf over the deck area. With the mass and equivalent stiffness, the natural frequency of the SDOF system was calculated as $\sqrt{\frac{K_{total}}{Mass}}\left(\frac{1}{2\pi}\right)$. However, because this relationship describes the natural frequency of a SDOF system, it assumes there is 100% mass participation and only one mode. This is not the case, and the natural frequencies were corrected using an empirical correction factor of $1/[2.3+0.0002(K_{sub})]$. This correction factor was determined by comparing the calculated natural frequency to those calculated from the full scale FEA model. Finally, the dynamic amplification of the system was calculated via the following equation:

$$DAF = \frac{1}{\sqrt{(1-\beta^2)^2 + (2C_{DAF}\zeta\beta)^2}}$$

Where:

β = Ratio of the Forcing function to the natural frequency

ζ = % Critical Equivalent Viscous Damping Ratio

C_{DAF} = Correction Factor

The correction factor in this section was determined empirically and placed within the equation so that dynamic amplification values would match well with that from the full scale FEA model when comparing to values obtained for deck models ranging in size from 24 ft. x 12 ft. to 12 ft. x 24 ft., and considering substructure stiffness values ranging from 0 lb./in. to 4000 lb./in. As the substructure stiffness increases, the error increases (although conservative in most cases). The cap of 4000 lb./in. gives amplification values for a large array of substructure configurations. The equation used to determine the C_{DAF} factor is as follows:

$$C_{DAF} = 2.25 * \left(1 - \frac{K_{Sub}}{2 * 10^4 * \zeta}\right)$$

In addition to the estimated natural frequency and dynamic amplification, the spreadsheet provides the total amplified lateral load, and calculates the reactions at the ledger, substructure supports, and hold-down forces. Finally, the spreadsheet checks the diaphragm load against the allowable shear values for horizontally sheathed dimension lumber shear walls (NDS Table 4.3D).

To illustrate the capability of this design aid, the results from spreadsheet (shown in red) compared to the full-scale FEA results (shown in black) for a series of decks connected with #10 x 3 in. screws are presented in Figure 29. The results are acceptable. For the case of the decks that have

ledgers lengths greater than joist lengths, the amplifications are higher in the spreadsheet, but design based off such a value would be conservative.
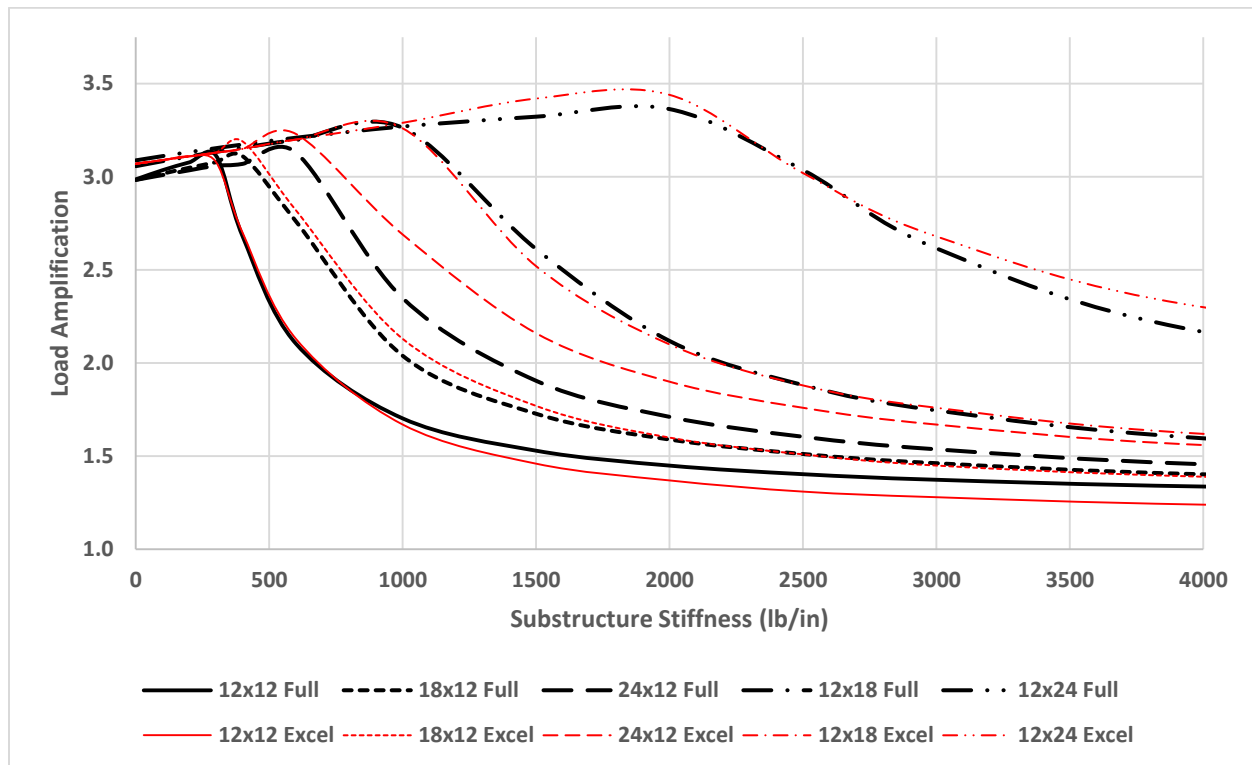
Figure 29: Comparison of Excel spreadsheet design aid to the full-scale FEA model results

It is important to note that this spreadsheet is a design aid only and is limited to the assumptions that derived it. Sound engineering judgement and care should be taken if the spreadsheet is used in the actual design of structures. The engineer of record should maintain the responsibility to design of safe, reliable structures holding paramount the safety health and welfare of the public. An example of the spreadsheet interface is also available in Appendix B.

4.3 – Load Amplification Tables

For even easier design, load amplification tables were constructed using the excel spreadsheet for general deck layouts and a variety of sizes and substructure stiffness. To use the table, (example in Table 7) determine the joist length, the ledger length and the estimated substructure stiffness of the deck. Then simply pick the amplified load from the table and apply it to the surface area of the deck to compare the design for occupant induced lateral loads along with earthquake and wind loads.

Table 7: Amplified Surface Tractions (psf)

Joist Length (ft)	Ledger Length (ft)	Sub Structure Stiffness (lb/in)										
		0	200	300	400	600	1000	1500	2000	2500	3000	4000
8	4	9.0	5.5	5.1	4.9	4.7	4.4	4.3	4.3	4.2	4.2	4.2
	6	9.0	6.0	5.6	5.3	5.0	4.6	4.5	4.4	4.4	4.3	4.3
	8	10.3	6.7	6.1	5.7	5.3	4.9	4.6	4.6	4.5	4.4	4.4
	12	10.8	7.6	6.9	6.4	5.9	5.3	5.0	4.8	4.7	4.6	4.6
	16	11.1	8.4	7.6	7.1	6.4	5.7	5.3	5.1	5.0	4.9	4.8
12	6	12.3	9.5	7.7	6.8	5.8	5.2	4.8	4.7	4.6	4.5	4.4
	9	12.3	12.3	10.3	8.7	7.1	5.9	5.3	5.0	4.9	4.8	4.7
	12	12.3	12.4	12.3	10.8	8.5	6.7	5.8	5.5	5.2	5.1	5.0
	18	12.3	12.4	12.5	12.8	11.3	8.5	7.1	6.4	6.0	5.8	5.6
	24	12.3	12.4	12.5	12.6	12.9	10.8	8.6	7.6	7.0	6.7	6.2
18	9	12.3	12.4	12.5	12.6	12.9	10.1	7.8	6.8	6.3	6.0	5.6
	12	12.3	12.4	12.5	12.6	12.8	13.0	10.1	8.4	7.5	7.0	6.5
	18	12.3	12.4	12.5	12.6	12.8	13.2	13.8	12.8	11.2	10.1	8.8
	24	12.3	12.4	12.5	12.6	12.8	13.2	13.7	14.2	14.9	14.4	12.7
	36	12.3	12.4	12.5	12.6	12.8	13.2	13.7	14.2	14.8	15.4	16.9
24	12	12.3	12.4	12.5	12.6	12.8	13.2	13.7	13.8	12.1	10.7	9.2
	18	12.3	12.4	12.5	12.6	12.8	13.2	13.7	14.2	14.8	15.4	16.0
	24	12.3	12.4	12.5	12.6	12.8	13.2	13.7	14.2	14.8	15.4	16.9
	36	12.3	12.4	12.5	12.6	12.8	13.2	13.7	14.2	14.8	15.4	16.9
	48	12.3	12.4	12.5	12.6	12.8	13.2	13.7	14.2	14.8	15.4	16.9

It should be noted that the table makes the same assumptions that the spreadsheet does, which includes a 4psf static lateral traction. If the surface traction is different from 4 psf, load values must be converted via the ratio of the desired static surface traction to the assumed 4 psf.

The values in Table 7 that appear in red correspond to those that do not check with respect to unit shear values in the deck diaphragm as per Table 4.3D in the SDPWS provided by AWC for horizontal lumber sheathed shear walls. Because a large percentage of the deck sizes considered do not check via this limit state, a second set off values is provided in Table 8 where the values are multiplied by a proposed ASD load reduction factor similar to wind of 0.6 to see the effect. Although this load case was performed in a laboratory and possible to achieve, the probability of the load actually occurring is fairly small. A reduction factor of 0.6 was chosen because the probability of exceedance is arbitrarily assumed to be similar to that of a wind scenario for illustration purposes. Before a true load factor can be chosen, the appropriate statistical analysis on the probability of exceedance should be performed. The number of deck sizes that do not pass unit shear values decreases as the effective total shear in the decks decrease.

Table 8: Amplified Surface Tractions with 0.6 Load Factor (psf)

Joist Length (ft)	Ledger Length (ft)	Sub Structure Stiffness (lb/in)										
		0	200	300	400	600	1000	1500	2000	2500	3000	4000
8	4	5.4	3.3	3.1	3.0	2.8	2.7	2.6	2.6	2.5	2.5	2.5
	6	5.4	3.6	3.3	3.2	3.0	2.8	2.7	2.6	2.6	2.6	2.6
	8	6.2	4.0	3.7	3.4	3.2	2.9	2.8	2.7	2.7	2.7	2.6
	12	6.5	4.6	4.2	3.9	3.5	3.2	3.0	2.9	2.8	2.8	2.7
	16	6.7	5.0	4.6	4.2	3.8	3.4	3.2	3.0	3.0	2.9	2.9
12	6	7.4	5.7	4.6	4.1	3.5	3.1	2.9	2.8	2.7	2.7	2.7
	9	7.4	7.4	6.2	5.2	4.2	3.5	3.2	3.0	2.9	2.9	2.8
	12	7.4	7.5	7.4	6.5	5.1	4.0	3.5	3.3	3.1	3.1	3.0
	18	7.4	7.5	7.5	7.7	6.8	5.1	4.2	3.8	3.6	3.5	3.3
	24	7.4	7.5	7.5	7.6	7.8	6.5	5.2	4.6	4.2	4.0	3.7
18	9	7.4	7.5	7.5	7.6	7.7	6.0	4.7	4.1	3.8	3.6	3.4
	12	7.4	7.5	7.5	7.6	7.7	7.8	6.0	5.0	4.5	4.2	3.9
	18	7.4	7.5	7.5	7.6	7.7	7.9	8.3	7.7	6.7	6.0	5.3
	24	7.4	7.5	7.5	7.6	7.7	7.9	8.2	8.5	8.9	8.6	7.6
	36	7.4	7.5	7.5	7.6	7.7	7.9	8.2	8.5	8.9	9.3	10.2
24	12	7.4	7.5	7.5	7.6	7.7	7.9	8.2	8.3	7.2	6.4	5.5
	18	7.4	7.5	7.5	7.6	7.7	7.9	8.2	8.5	8.9	9.3	9.6
	24	7.4	7.5	7.5	7.6	7.7	7.9	8.2	8.5	8.9	9.3	10.2
	36	7.4	7.5	7.5	7.6	7.7	7.9	8.2	8.5	8.9	9.3	10.2
	48	7.4	7.5	7.5	7.6	7.7	7.9	8.2	8.5	8.9	9.3	10.2

One could argue that these tables compare the limit state of a shear wall to that of a deck under lateral forces and therefore perhaps a higher load can be applied to the structure without complete failure. Under lateral load, the large deflections experienced are orthogonal to the forces of gravity. In this thesis, the effects of gravity are not included, and the P-Δ effects on both lateral response and failure are ignored. It could be argued that, even though the deck boards and joists may exhibit some splitting, as long as the supporting elements (joist hangers, ledger, hold-downs and substructure) are adequately designed to withstand those deflections, the deck should be allowed to pass the limit state having avoided a complete failure. However, it is highly suggested that further testing be done to confirm this theory before implementing a decrease in the design requirements for lateral loading from occupants.

5.0 – Avenues for Further Research

The physical experiments performed by Parsons et al. (2014b) and the initial FEM model by LaFave (2015) informed the investigation of dynamic sensitivity of the outdoor deck systems to lateral loads applied by occupants. However, there are several areas that still require study as follows

- Continued refinement of the analytical model

- Exploration of methods of deck stiffness restoration

- Exploration into ASD load factor for reasonable design practices

5.1 - Refinement of the Analytical Model

The FEA model is calibrated to reflect the results obtained in the physical experiments performed by Parsons et al (2014b). However, the laboratory test was an idealized structure and may not be representative of those built in the field. Therefore, refinement of the model developed to represent practical design and construction methods is warranted to validate the assumptions for the current model, or to determine governing parameters for future tabulation of load amplifications. In addition to the deck board-to-joist connection properties examined in this study, the inclusion of prescriptive design methods as outlined in DCA6-12 provided by AWC (2015) would allow the model to represent typical deck designs as follows.

- Application of overhanging joists/beams. Currently, outer edge support is given at the end of the joists. This could affect the ability of a substructure with a given stiffness to resist lateral load due to decreased eccentricity about the center of mass of the deck system.

- Non- Ledger Deck systems, with varying substructure stiffness for inner vs. outer posts. The anchors to the house would no longer be the main focus, but the distribution of forces to the substructure would be essential to design of supporting elements.

- The inclusion of a guard rail system as per Figure 24, DCA6-12 (AWC, 2015). This addition may not add stiffness, but will add mass allocated away from the primary structure, increasing the inertial affect and lowering the natural frequency.

- Incorporation of a stair system on a side, inside, or end of the deck. Because the stiffness of stair systems is difficult to determine, they could be estimated using a rigid element and the effect on the structure could be observed with various stair element locations.

- Including Reentrant corners or the case of a chimney or bay window disrupting the current rectangular geometry of the deck. This would create some discontinuity in the ledger and deck boards, but might also provide some rigidity by restricting lateral motion close to the structure.

5.2 - Exploration on Methods of Increasing Stiffness

Research should be applied to explore methods of increasing lateral stiffness and rigidity of deck and porch structures to values that will reduce the chance of high lateral load amplification by occupancy. This is especially important when hidden deck board fasteners are used. Due to the rotational flexibility of deck joist hangers, much of the deck's lateral stiffness is attributed to the interaction of the deck boards to the deck joists through the fasteners. In order to transmit lateral loads, some slip must occur before the fastener provides diaphragm stiffness in lateral shear (Parsons et al., 2014b). In contrast, hidden fasteners are not directly attached through the wood members, but rather clamp the members using plastic inserts. This allows for more slip before

transmitting load through screws to the framing below, greatly reducing lateral stiffness. Consequently, the natural frequency of the deck could remain below 1.0Hz for a larger range of substructure stiffness, allowing for occupancy loads to easily match the natural period of the structure, causing high lateral load amplification. Stiffening of the substructure and/or the deck diaphragm itself, lateral rigidity can be increased and loads can be reduced through decreased the amplification caused by dynamic effects. Preliminary proposed methods of increasing stability include:

Stiffening the substructure: This could include the formation of a sheathed arch system utilizing similar construction methods of a perforated shear wall. Another method could be developing a moment frame system that uses posts that extend through the deck surface and to the top railing. Then a truss system could be used to make the post-railing interaction into a wood truss moment frame. See Figure 58, in Appendix C for illustrations.

Stiffening of the deck diaphragm: Stiffening the deck diaphragm itself could include joist end-bracing or blocking to provide moment resistance to the ends of the joists. A second option would be to explore the effect of led-in bracing or a block and brace system between joists to increase the shear capacity of the deck diaphragm. See Figure 58, Appendix C for illustrations.

5.3 - Exploration into ASD Load Factor for Reasonable Design Practices

According to the models provided by James LaFave (2015), the loads at anchors and supports of the structure from occupant-induced lateral loads were in excess of 4 times the static case. In many cases this can be larger than the earthquake or wind loads for those structures. Implication of this

load as a maximum value to decks could render many existing decks theoretically unsafe despite the fact that very few, if any at all, deck failures have been caused by such a loading. A plausible response could be that the probability that existing structures will ever see this load is very low and highly dependent on the specific use of the structure. However, there are no data to back up such a claim. Consequently, exploration on evaluation of existing structures and load factors for new deck structures is necessary.

Load factors for existing wind and earthquake loads are currently based on structural reliability theory, and are derived using data from past seismic and wind events to estimate the probability that a structure would reach the design level event in its life. However, current load factors for wind and seismic are also "supported by extensive peer-reviewed data bases and the values [for mean and COV] are well established" (ASCE 7-10). No such data exists for lateral occupant loads. An extensive literature review and/or in-situ structural evaluations could be conducted in order to determine appropriate factors for new structures and to determine if existing structures have enough in-situ reserve strength to resist such loads while maintaining an appropriate level of reliability (Ellingwood, 1996).

6.0 - Conclusions

This study explored the effect of the deck board-to-joist connection characteristics on the response of exterior deck structures when subjected to occupant induced lateral loads. Physical testing performed provided data for moment and displacement for three types of connections; #10x3" screws with Hem-Fir deck boards, 10d threaded nails with Hem-Fir deck boards, and #10x2.75" Trex® composite deck screws with Trex® composite deck boards. This data was utilized to estimate a rotational stiffness and associated damping value for the connection that was input into FEA models to predict the behavior of various deck structures. It was discovered that a softened, rotational stiffness, and associated equivalent viscous damping was more appropriate when using linear methods to estimate the dynamic behavior of the deck system.

When comparing the results for the three test specimen types, the #10x3" wood screws had higher rotational stiffness values, but performed worse than the 10d threaded nails in the model due to a lower damping coefficient. The methods for calculating damping in this study relied heavily on the yield mode of the fastener to estimate the pinching effect in the hysteretic curve. The #10 woods screws exhibited a Mode III type yield rather than a Mode IV, which limits the yielding to only one plastic hinge in the fastener, reducing the strength required to return the connection to a point of zero displacement to about 25% the yield strength vs. 33% when Mode IV occurs. The Trex® composite boards and screws performed the best initially, with the highest stiffness and damping, but resulted in larger amplifications at higher substructure stiffness' due to the dramatic increase in mass associated with the dense wood-plastic composite board.

The previous version of the model assumed a higher rotational cyclic stiffness and a lower damping value than necessary. When these values modified to those determined by this study, the initial lateral load amplifications decreased by 27%, a significant reduction from the previous estimates. With this more accurate model, a simplified model, design aid, and amplified load tables were created to provide reasonable values for aiding in the design of new deck structures.

One area where this study could use refinement is with respect to the damping in deck structures. Therefore, in addition to those previously mentioned, a suggestion for continuing research relating to deck board-to-joist connections could include cyclic testing of the connection types in this study to validate the assumptions made during the calculation of the rotational stiffness and damping values. Incorporation of Chui's FEA model for dowel type fasteners under reversed cyclic loading could reduce the need for physical testing (1998). Results from such a study would lend insight to the assumptions made during this study regarding damping, which proved to be a key parameter in the response of the deck models.

In conclusion, the characteristics of the deck board-to joist connection play a large role in how exterior deck structures respond to occupant induced lateral loading. It is essential that sufficient diaphragm stiffness is achieved through appropriate deck board-to-joist connections to ensure the structure's fundamental frequency does not reside in the range of 0-1.0Hz. Additionally, connections that exhibit high damping capabilities are desirable so that if the structure does respond in the 0-1.0Hz range, amplifications are sufficiently damped resulting in lower demands at the connections.

References

American Society of Civil Engineers (ASCE). 2010. "Minimum Design Loads for Buildings and Other Structures*." ASCE/SEI 7-10*. Reston, VA.

American Wood Council (AWC). 2012. "National Design Specification for Wood Construction with Commentary." *ANSI/AWC NDS-2012*. Leesburg, VA.

American Wood Council (AWC). 2015 A. "Design for Code Acceptance 6: Prescriptive Residential Deck Construction Guide". *DCA6-12*. Leesburg, VA.

American Wood Council (AWC). 2015 B. "General Dowel Equations for Calculating Lateral Connection Values." Technical Report No. TR-12. Leesburg, VA

ASTM D4442-15 Standard Test Methods for Direct Moisture Content Measurement of Wood and Wood-Based Materials, ASTM International, West Conshohocken, PA, 2015,

ASTM D4933-99 (2010) Standard Guide for Moisture Conditioning of Wood and Wood Base Materials, ASTM International, West Conshohocken, PA, 2010

Ceccottie A., and Vignoli A. 1989. "A Hysteretic Behaviour Model for Semi-Rigid Joints." *European Earthquake Engineering Journal*. 3, 3-9

Chui B.Y.H., Ni C., Jiang L. 1998. "Finite-Element Model for Mailed Wood Joints under
Reversed Cyclic Load." *Journal of Structural Engineering.* 124(1), 96-103

Dolan, J.D. and Gutshall, S.T. 1994. "Monotonic and Cyclic Tests to Determine Short-Term
Duration-of-Load Performance of Nail and Bolt 102 Connections: Volume I: Summary
Report," Virginia Polytechnic Institute and State University Timber Engineering Report
No. TE-1994-001.

Ellingwood, Bruce R. 1996 "Reliability-based Condition Assessment and LRFD for Existing
Structures." S*tructural Safety* 18(2-3), 67-80.

Filiatrault A., Tremblay R., Christopoulos C., Folz B., Pettinga D. 2013. "Elements of
Earthquake Engineering and Structural Dynamics." 3rd Edition. Presses Internationales
Polytechnique

Homan, S.W., Boase, A.J., Raider C.J., Jensen H., Matthews H.W., Smith G.B., and Wetzel C.H.
1932. "Horizontal forces produced by movements of the occupants of a grandstand".
American Standards Association Bulletin 3(4).

International Code Council (ICC). 2011. A. "2012 International Building Code." *IBC 2012.*

International Code Council Inc. (ICC). 2011. A. "2012 International Residential Code." *IRC
2012.*

Irish, D. 2015. "Yarmouth, N.S., deck collapse picture-taker wants to set record Straight"
[Online Posting]. Retrieved July 7, 2016, from http://www.cbc.ca/news/canada/nova-scotia/yarmouth-n-s-deck-collapse-picture-taker-wants-to-set-record-straight-1.3124697

LaFave, J.M., Bender D.A., and Cofer W.F. 2014. "Investigation of Occupant-Induced Dynamic Lateral Loading on Exterior Decks." Thesis. *Washington State University, Department of Civil and Environmental Engineering*

Legacy Services. 2010. "Outdoor deck and porch injury study".
http://www.buildingonline.com/news/pdfs/Outdoor-Deck-and-Porch-Injury-Study.pdf

Loss C., Zonta D., Piazza M. 2012. "Analytical Model to Evaluate the Equivalent Viscous Damping of Timber Structures with Dowel-Type Fastener Connections." *Proc., World Conference on Timber Engineering.* Auckland, New Zealand

Lyman G.H., Bender D.A. 2013 A. "Wind Load Determination for Residential Decks." *A Journal of Contemporary Wood Engineering,* 23(2), 3–8.

Lyman G.H., Bender D.A, Dolan J.D. 2013 B. "Seismic Load Determination for Residential Decks." *A Journal of Contemporary Wood Engineering*, 23(2), 9–14.

Parsons B., Bender D.A., Dolan, J.D., and Woeste, F.E. 2014a. "Deck and Porch Floor Lateral Loading by Occupants." *Practice Periodical on Structural Design and Construction,* 19(3)

Parsons B, Bender D.A., Dolan J.D., Tichy R.J., Woeste F.E. 2014b. "Lateral Load Path and

Capacity of Exterior Decks." *Practice Periodical on Structural Design and Construction*

19(4)

Professional Deck Builder Magazine. Result for 'deck Collapse'. Web.

Schutt, C.A. (2011) "Improving Deck Safety." *LBM Journal,* 9(5), 26-28

Appendix A – Additional Results

Appendix A provides additional results for the concepts discussed in the preceding text. It includes tables and figures describing the sensitivity analyses for deck board-to-joist rotational stiffness and the sensitivity analyses with respect to damping in the deck model. This section includes additional results for physical testing that were not presented within the text including the data for the 10d threaded deck screws and #10x2.75" Trex ® composite screws with composite boards. This appendix displays the complete results package for the FEA modeling including load amplification graphs for each test specimen type as well as comparisons between each test specimen type with varying deck dimensions. Finally, an example of the user interface for the Excel design aid is presented.

- A1: Sensitivity Analyses – Deck Board-to-Joist Connection Stiffness
- A2: Sensitivity Analyses – Equivalent Viscous Damping
- A3: Physical Testing Data
- A4: FEA Modeling Results
- A5: Excel Spreadsheet User Interface

A1 - Sensitivity Analysis – Deck Board-to-Joist Rotational Stiffness

A1.1 – Deck Size 24 ft. x 12 ft.

Table 9: Total Shear Amplification of 24 ft. x 12 ft. Deck Structure with varying connection and substructure stiffness.

Substructure Stiffness	25%	100%	200%
0	4.251	4.287	4.308
200	4.378	4.333	4.337
600	4.558	4.420	4.396
1000	4.657	4.498	4.451
1500	4.709	4.580	3.959
2000	4.719	4.338	2.836
2500	4.759	3.216	2.341
3000	4.646	2.409	2.081
4000	3.344	2.167	1.813
6000	2.422	1.853	1.592
12000	1.868	1.571	1.409
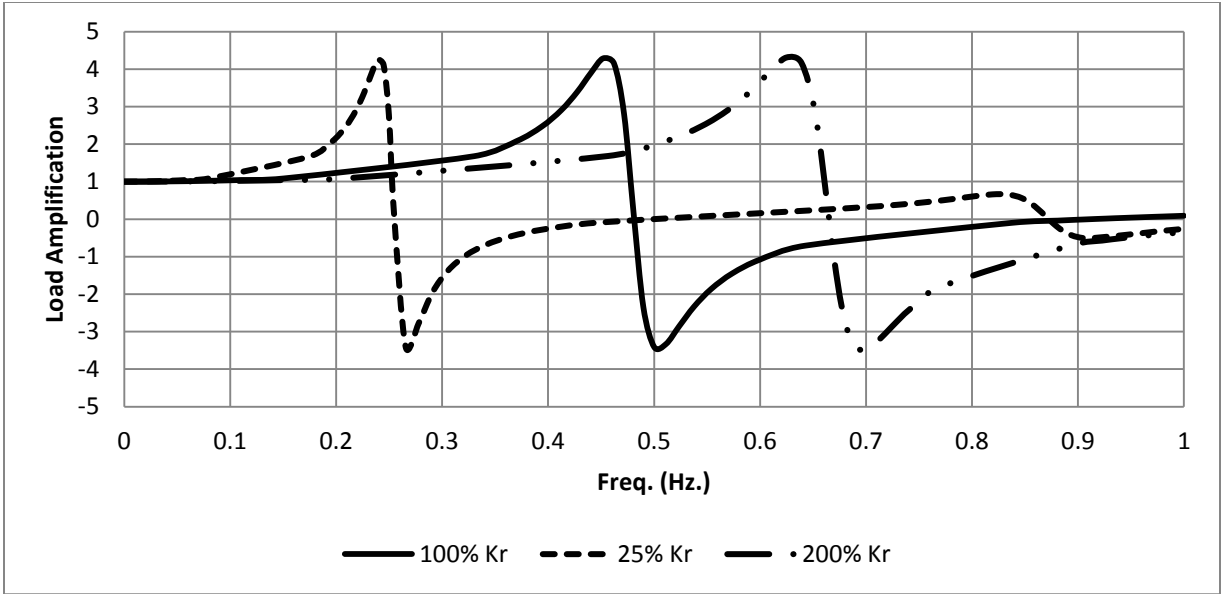
Figure 30: Total Shear Amplification of 24 ft. x 12 ft. deck structure with zero substructure stiffness while varying the deck board-to-joist stiffness (Kr) from 25% to 200% the original value.
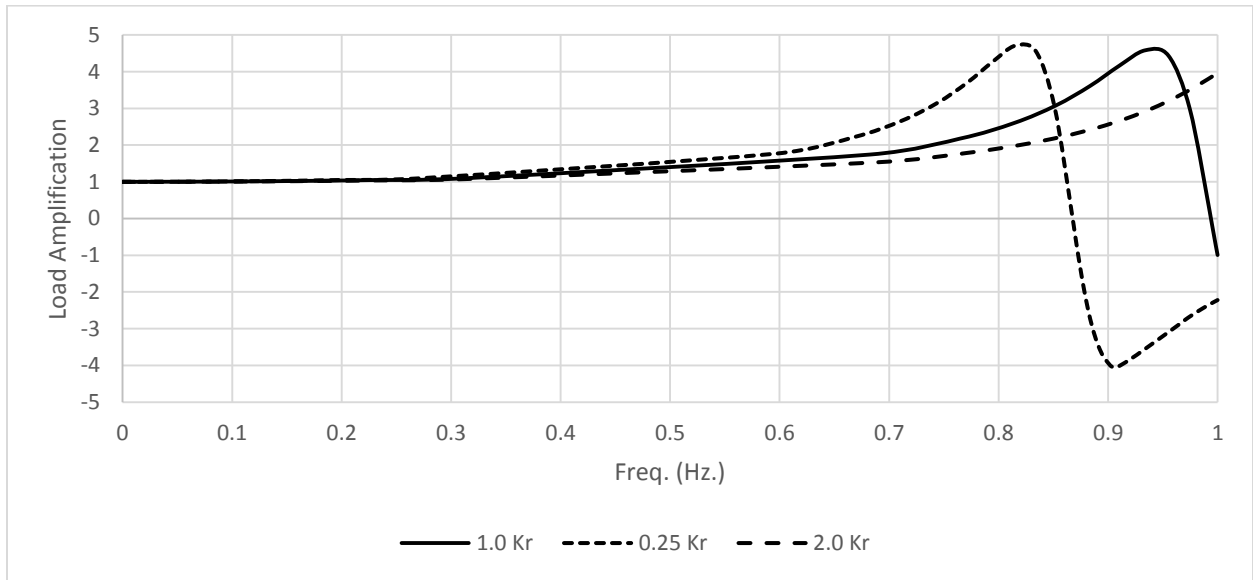
Figure 31: Total Shear Amplification of 24 ft. x 12 ft. deck structure with 1500 lb./in. substructure while varying deck board-to-joist stiffness (Kr) from 25% to 200% the original value.
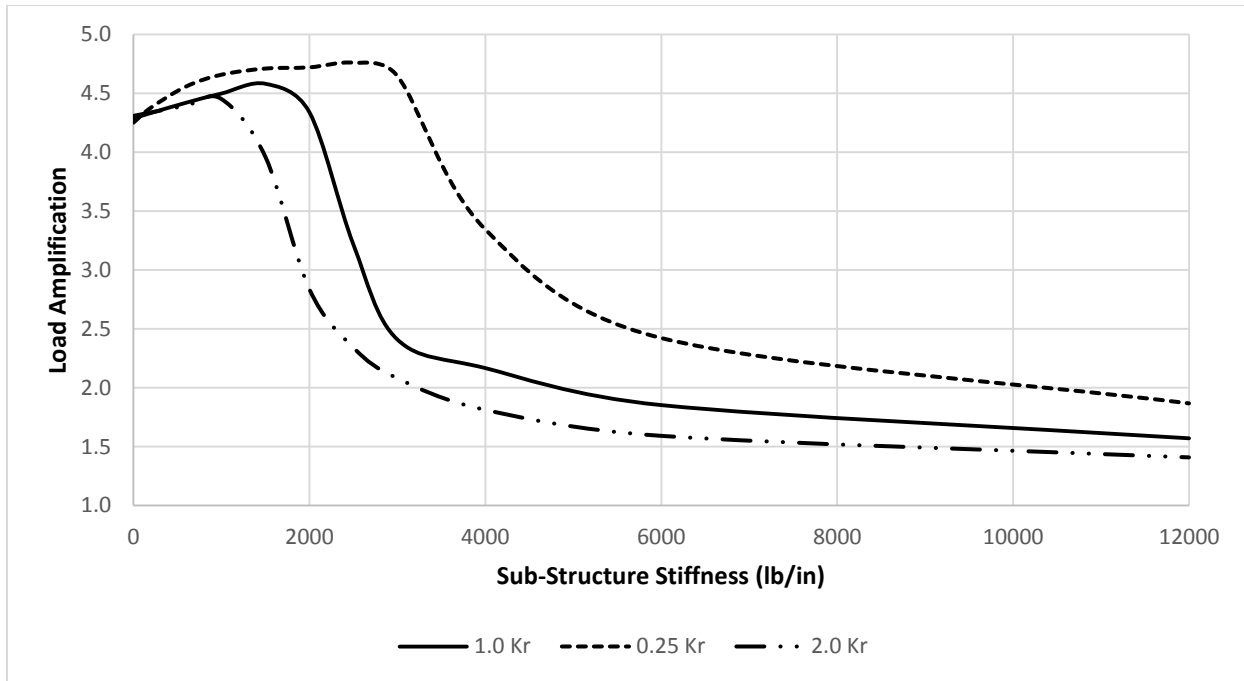
Figure 32: Maximum Total Shear Amplification of 24 ft. x12 ft. deck in response to a range of substructure stiffness values with varying deck board-to-joist connection stiffness (Kr).

A1.2 – Deck Size 12ft x12ft

Table 10: Total Shear Load Amplifications for the 12 ft. x 12 ft. aspect ratio FEA deck model |Deck Board-to-Joist Rotational Stiffness was varied from 25% the original value to 200% the original value.

Substructure Stiffness	25%	100%	200%
0	4.047	4.147	2.063
200	4.286	3.441	1.738
600	4.608	1.914	1.481
1000	2.766	1.611	1.372
1500	2.196	1.464	1.301
2000	1.987	1.392	1.260
2500	1.880	1.348	1.233
3000	1.815	1.320	1.214
4000	1.739	1.284	1.189
6000	1.669	1.249	1.162
12000	1.605	1.214	1.134
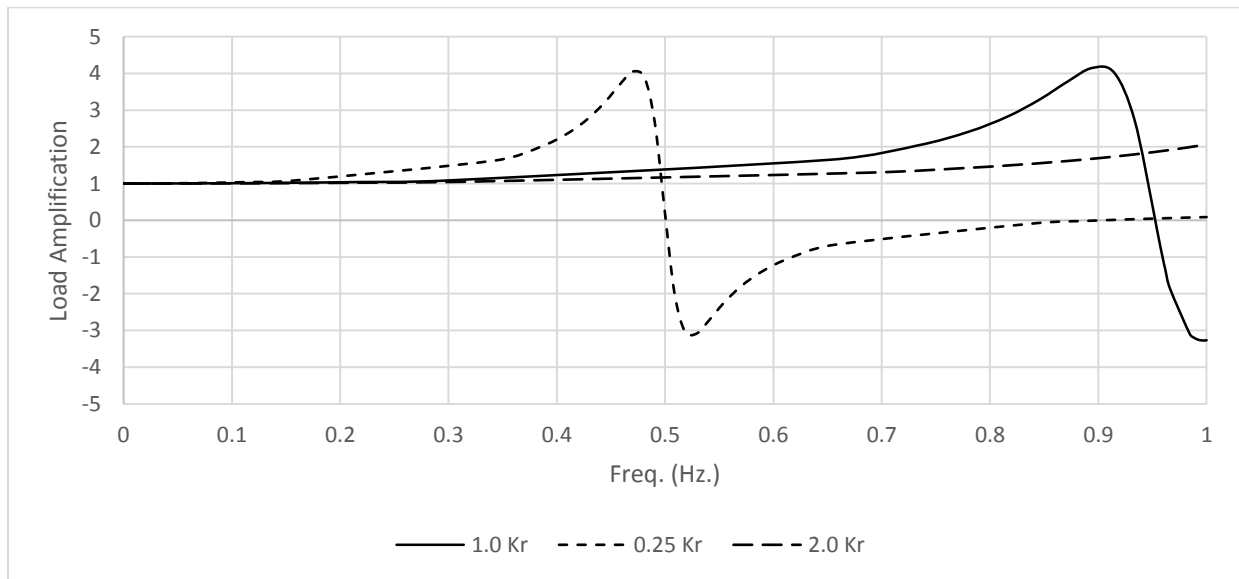
Figure 33: Total Shear Amplification of 12 ft. x 12 ft. deck structure under lateral load with zero substructure stiffness while the deck board-to-joist connection rotational stiffness (Kr) was varied from 25% the original value to 200% the original value
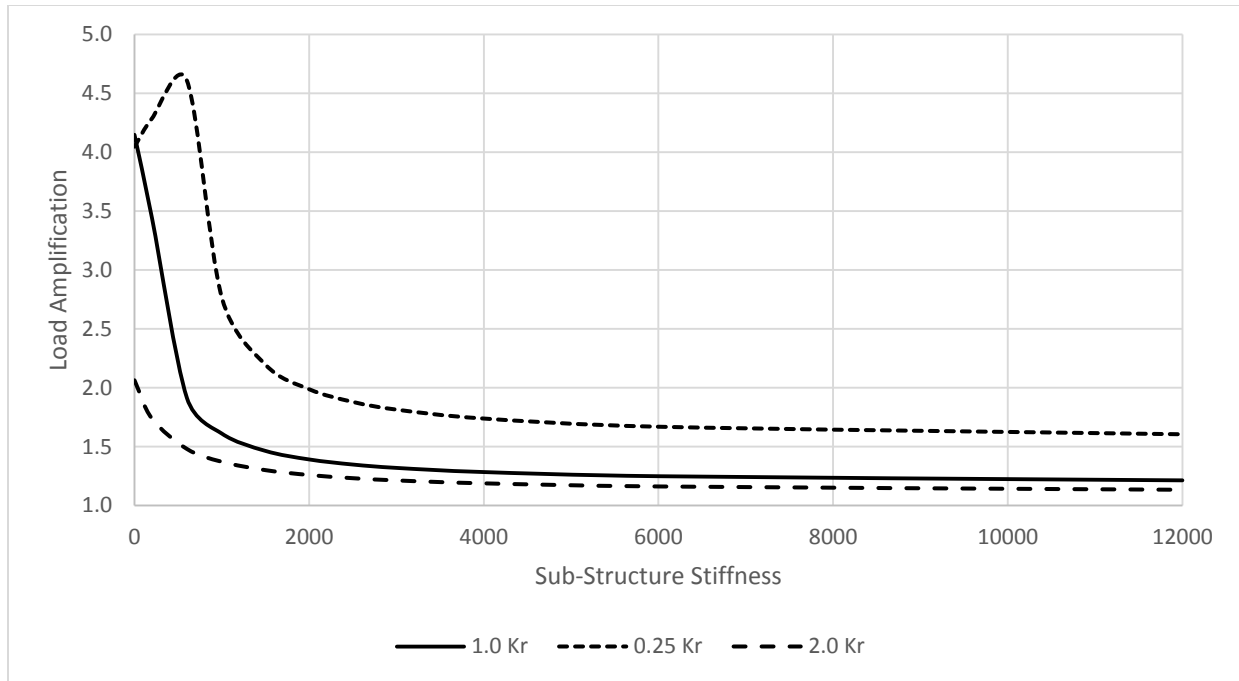
Figure 34: Total Shear Load Amplifications for the 12 ft. x 12 ft. deck structure while varying the deck board-to-joist connection stiffness (Kr) from 25% the original value to 200% the original value.

A.2 - Sensitivity Analysis – Damping Coefficient

Table 11: Total Shear Amplification for a 12 ft. x 12 ft. deck varying structural damping from 5% to 10%

Substructure Stiffness	ζ = 5%	ζ = 7%	ζ = 10%
0	4.094	3.066	2.310
200	4.270	3.184	2.386
600	2.549	2.425	2.199
1000	1.892	1.857	1.785
1500	1.655	1.636	1.596
2000	1.553	1.539	1.510
2500	1.497	1.485	1.460
3000	1.460	1.450	1.428
4000	1.417	1.408	1.390
6000	1.376	1.368	1.352

Figure 35: Total shear amplification vs. substructure stiffness for 12 ft. x 12 ft. deck while varying structural damping ζ.

A.3 - Physical Testing

A.3.1 – Physical Data with Average Power Curves
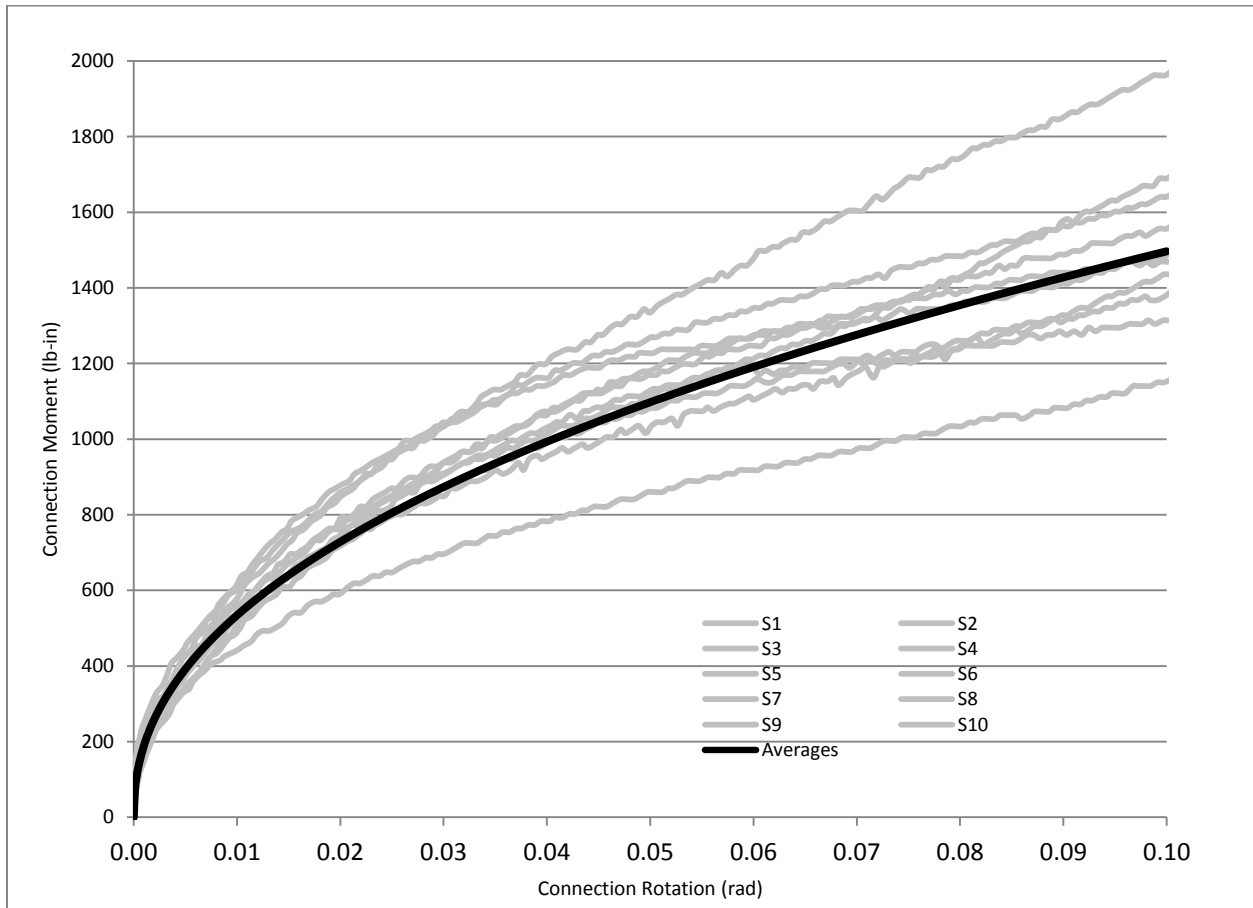
Figure 36: Moment vs. Rotation of the Test Specimens containing Hem-Fir Deck Boards and Joists

connected via #10 x 3 in. Decking Screws
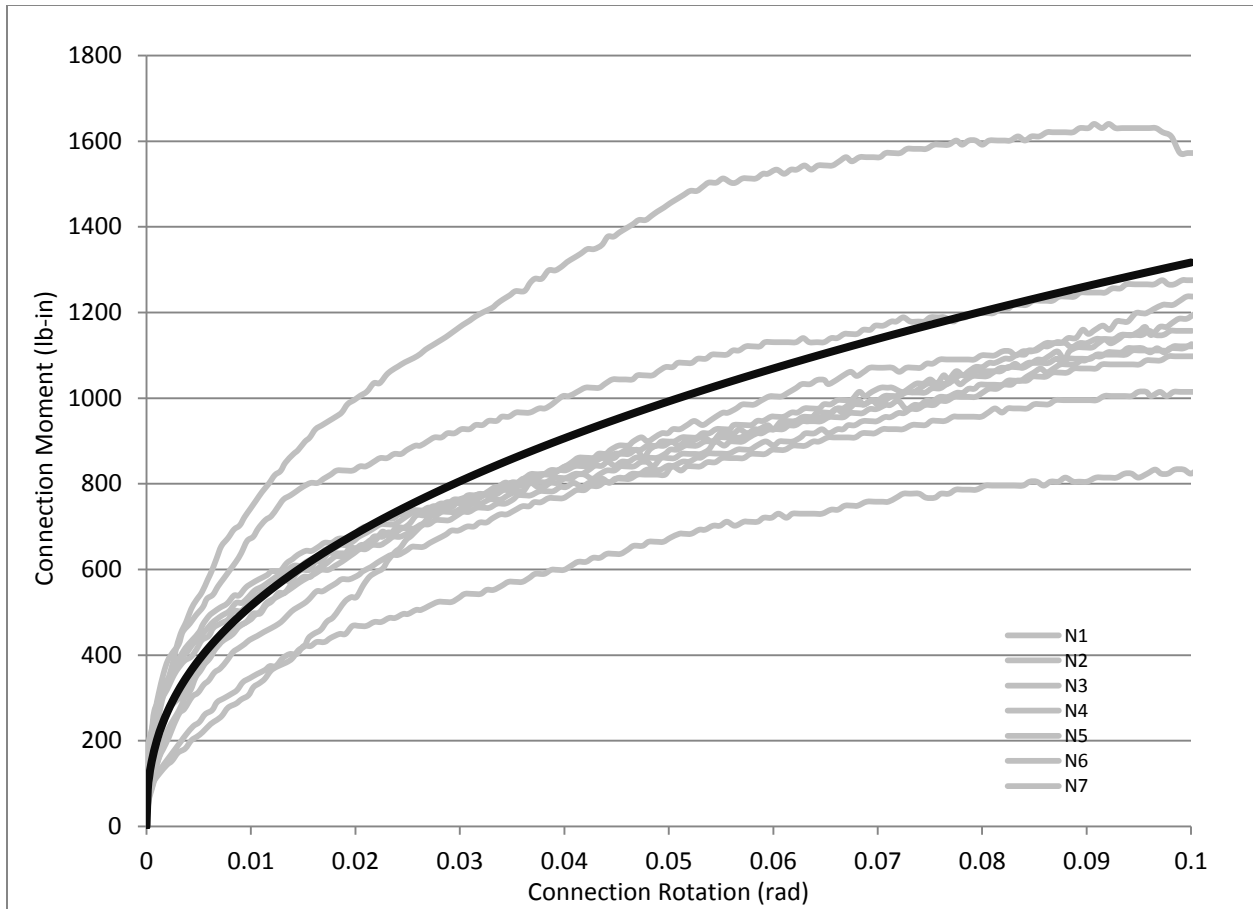
Figure 37: Moment vs. Rotation of the Test Specimens containing Hem-Fir Deck Boards and Joists connected via 10d Threaded Deck Nails
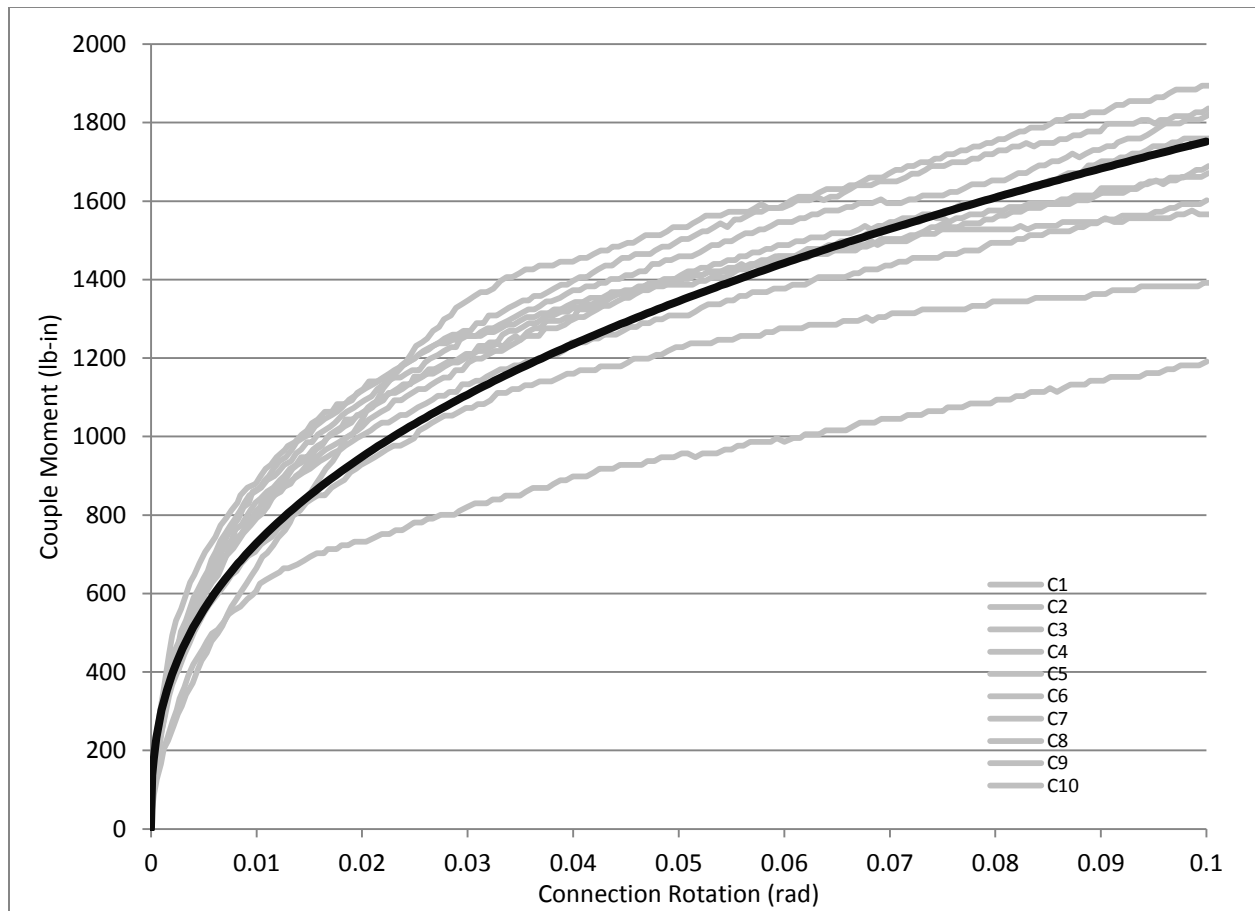
Figure 38:Moment vs. Rotation of the Test Specimens containing Trex® Deck Boards, Hem-Fir

Joists connected via #10 x 2.75 in. Trex® Deck Screws

Table 12: Power functions. $M(\theta) = A\,\theta^n$ for each specimen of all three test configurations.

Power Functions

Specimen	A'	n'	R^2
#10x3" Decking Screws - Hem-Fir Deck Board			
Screw 1	5275.9	0.4533	0.988
Screw 2	2934.5	0.4101	0.990
Screw 3	4643.5	0.4631	0.996
Screw 4	4410.1	0.4372	0.977
Screw 5	5010.8	0.4909	0.995
Screw 6	5080.4	0.4711	0.993
Screw 7	5128.1	0.5019	0.993
Screw 8	3931.6	0.4317	0.993
Screw 9	3976.6	0.4479	0.991
Screw 10	3289.1	0.3863	0.994
Screw Average	**4192.9**	**0.4474**	**0.999**
10d Threaded Decking Nails - Hem-Fir Deck Board			
Nailed 1	1738.5	0.3882	0.9824
Nailed 2	4485.3	0.4317	0.9779
Nailed 3	2821.7	0.4595	0.9976
Nailed 4	3701.1	0.4650	0.9901
Nailed 5	6257.7	0.5434	0.998
Nailed 6	4767.3	0.4216	0.9779
Nailed 7	6079.3	0.4579	0.9923
Nailed 8	2586.1	0.3331	0.9861
Nailed 9	1749.7	0.2665	0.9936
Nailed 10	3264.1	0.4117	0.9951
Nailed Average	**3366.8**	**0.4077**	**0.9999**
#10x2.75 Trex® Deck Screws - Trex® Decking			
Comp 1	4600.9	0.3882	0.9793
Comp 2	4651.2	0.4031	9817
Comp 3	3684.4	0.3264	0.9577
Comp 4	6388.8	0.4890	0.973
Comp 5	3985	0.3709	0.9720
Comp 6	2843.2	0.3629	0.9609
Comp 7	5075.8	0.4047	0.9903
Comp 8	4083.4	0.3570	0.9813
Comp 9	4172.8	0.3690	9819
Comp 10	3382	0.3473	0.977
Comp Average	**4215.4**	**0.3813**	**1**

Table 13: Rotational Stiffness and Damping for each test specimen

Specimen	Mmax	Krot	RSE	Ki	My	D.E.	Damping
#10x3" Decking Screws - Hem-Fir Deck Board							
Screw 1	1357	27137	67.8	100500	406	30.5	7.2%
Screw 2	859	17180	42.9	100500	340	20.1	7.4%
Screw 3	1160	23194	58.0	100500	354	25.0	6.9%
Screw 4	1190	23805	59.5	100500	336	25.0	6.7%
Screw 5	1151	23028	57.6	100500	343	24.5	6.8%
Screw 6	1239	24775	61.9	100500	490	30.9	7.9%
Screw 7	1140	22803	57.0	100500	382	25.6	7.2%
Screw 8	1079	21575	53.9	100500	382	24.6	7.3%
Screw 9	1039	20788	52.0	100500	396	24.5	7.5%
Screw 10	1034	20679	51.7	100500	392	24.3	7.5%
Screw Average	**1098**	**21951**	**55**	**100500**	**381**	**25.2**	**7.3%**
10d Threaded Decking Nails - Hem-Fir Deck Board							
Nailed 1	543	10868	27.2	60200	287	19.0	11.1%
Nailed 2	1231	24613	61.5	60200	336	34.0	8.8%
Nailed 3	712	14247	35.6	60200	326	22.6	10.1%
Nailed 4	919	18382	46.0	60200	308	25.3	8.8%
Nailed 5	1229	24573	61.4	60200	340	34.1	8.8%
Nailed 6	1348	26964	67.4	60200	319	37.4	8.8%
Nailed 7	1542	30842	77.1	60200	357	45.2	9.3%
Nailed 8	953	19068	47.7	60200	329	26.8	9.0%
Nailed 9	787	15750	39.4	60200	329	23.8	9.6%
Nailed 10	951	19018	47.5	60200	361	27.9	9.3%
Nailed Average	**993**	**19853**	**50**	**60200**	**329**	**27.7**	**8.9%**
#10x2.75 Trex® Composite Deck Screws - Trex® Composite Decking							
Comp 1	1438	28762	71.9	100500	634	45.1	10.0%
Comp 2	1390	27807	69.5	100500	578	42.1	9.6%
Comp 3	1386	27717	69.3	100500	623	43.9	10.1%
Comp 4	1476	29529	73.8	100500	704	48.5	10.5%
Comp 5	1312	26237	65.6	100500	641	43.6	10.6%
Comp 6	959	19173	47.9	100500	501	33.3	11.0%
Comp 7	1510	30200	75.5	100500	592	44.8	9.4%
Comp 8	1401	28027	70.1	100500	595	43.0	9.8%
Comp 9	1381	27630	69.1	100500	700	47.0	10.8%
Comp 10	1195	23898	59.7	100500	585	39.7	10.6%
Comp Average	**1345**	**26902**	**67**	**100500**	**615**	**38.2**	**9.0%**

A.4 - FEA Modeling

A.4.1 - #10 x 3 in. Screws | Hem-Fir Deck Boards | Hem-Fir Joists
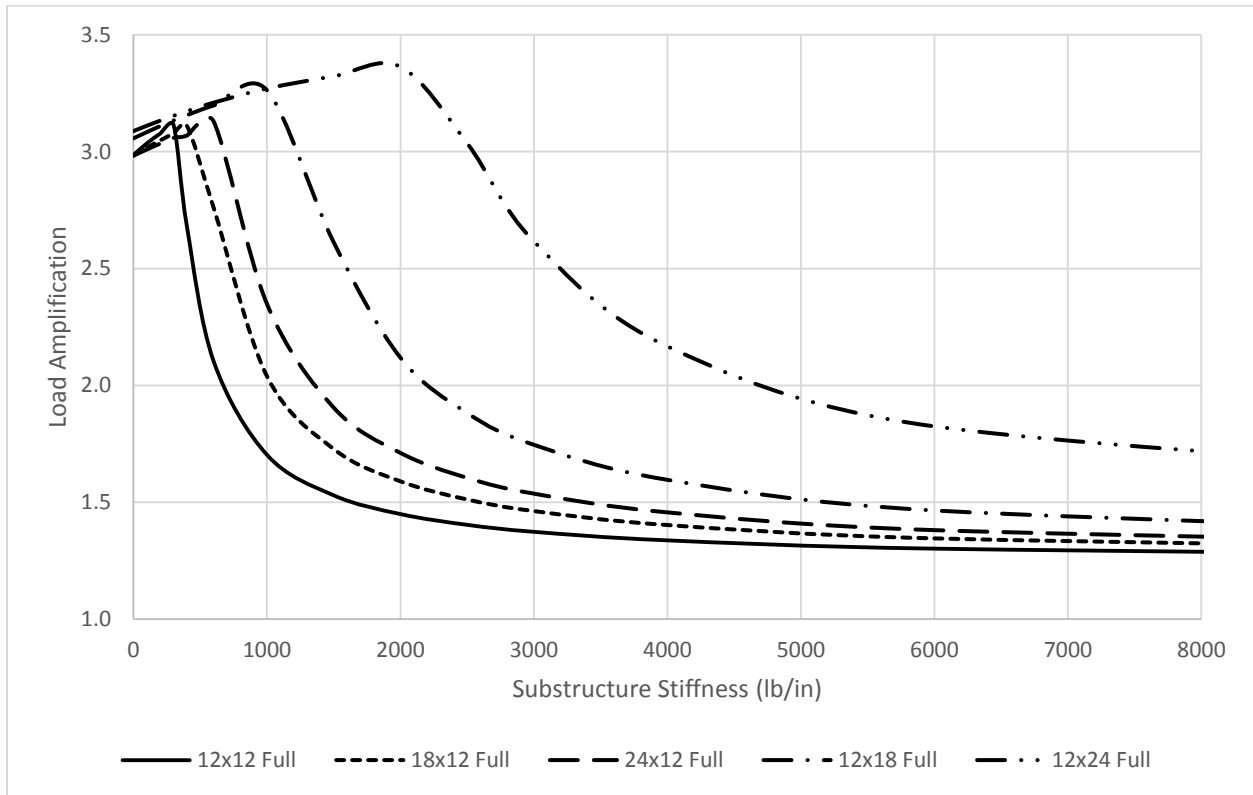
Figure 39: Lateral Load Amplification - #10 x 3in. Screw with Hem-Fir Deck Boards and Hem-Fir Joists

Figure 40: Lateral Load Amplification - #10 x 3 in. Screw with Hem-Fir Deck Boards and Hem-

Fir Joists | Substructure Stiffness' from 0-2000 lb./in.

Figure 41: Lateral Load Amplification - #10 x 3 in. Screw with Hem-Fir Deck Boards and Hem-

Fir Joists | Substructure Stiffness' from 2000-4000 lb./in.

87

Table 14: Lateral Load Amplifications, Total Shear and Dynamic Amplification Factor for deck structure with Hem-Fir deck boards, and #10 x 3 in. screws, Deck size 12 ft. x 12 ft.

Substructure Stiffness, K		Natural Frequency (Hz)	Total Resultant Shear Force (lb.)		Total Resultant Shear Force (N)		Dynamic Amplification Factor, Ck
(lb./in)	(N/mm)		Static	Dynamic	Static	Dynamic	
0	0	0.792	600	1792	2669	7970	2.986
100	18	0.911	600	1821	2669	8102	3.036
200	35	1.009	600	1847	2669	8214	3.078
300	53	1.094	600	1869	2669	8312	3.115
400	70	1.167	600	1608	2669	7153	2.680
600	105	1.288	600	1262	2669	5615	2.104
1000	175	1.463	600	1022	2669	4545	1.703
1500	263	1.605	600	918	2669	4083	1.530
2000	350	1.698	600	870	2669	3869	1.450
2500	438	1.762	600	842	2669	3746	1.404
3000	525	1.809	600	824	2669	3666	1.374
4000	701	1.871	600	802	2669	3569	1.337
6000	1051	1.936	600	781	2669	3474	1.302
12000	2102	2.004	600	760	2669	3382	1.267
1.0E+09	1.75E+08	2.073	600	740	2669	3292	1.233

Table 15: Lateral Load Amplifications, Total Shear and Dynamic Amplification Factor for deck structure with Hem-Fir deck boards, and #10 x 3 in. screws, Deck Size 18 ft. x 12 ft.

Substructure Stiffness, K		Natural Frequency (Hz)	Total Resultant Shear Force (lb.)		Total Resultant Shear Force (N)		Dynamic Amplification Factor, Ck
(lb./in)	(N/mm)		Static	Dynamic	Static	Dynamic	
0	0	0.785	933	2784	4150	12383	2.984
100	18	0.866	933	2815	4150	12521	3.017
200	35	0.936	933	2844	4150	12652	3.049
300	53	0.999	933	2872	4150	12776	3.078
400	70	1.056	933	2902	4150	12911	3.111
600	105	1.155	933	2576	4150	11457	2.761
1000	175	1.309	933	1902	4150	8463	2.039
1500	263	1.449	933	1612	4150	7171	1.728
2000	350	1.549	933	1483	4150	6597	1.590
2500	438	1.624	933	1411	4150	6275	1.512
3000	525	1.682	933	1364	4150	6070	1.462
4000	701	1.763	933	1309	4150	5822	1.403
6000	1051	1.854	933	1255	4150	5585	1.346
12000	2102	1.953	933	1204	4150	5357	1.291
1.0E+09	1.75E+08	2.056	933	1155	4150	5139	1.238

Table 16: Lateral Load Amplifications, Total Shear and Dynamic Amplification Factor for deck

structure with Hem-Fir deck boards, and #10 x 3 in. screws, Deck Size 24 ft. x 12 ft.

Substructure Stiffness, K		Natural Frequency (Hz)	Total Resultant Shear Force (lb.)		Total Resultant Shear Force (N)		Dynamic Amplification Factor, Ck
(lb./in)	(N/mm)		Static	Dynamic	Static	Dynamic	
0	0	0.782	1200	3580	5338	15924	2.983
100	18	0.846	1200	3612	5338	16065	3.010
200	35	0.903	1200	3642	5338	16200	3.035
300	53	0.956	1200	3671	5338	16330	3.059
400	70	1.004	1200	3683	5338	16384	3.069
600	105	1.089	1200	3756	5338	16706	3.130
1000	175	1.228	1200	2818	5338	12535	2.348
1500	263	1.360	1200	2286	5338	10168	1.905
2000	350	1.459	1200	2054	5338	9135	1.711
2500	438	1.537	1200	1925	5338	8565	1.604
3000	525	1.599	1200	1844	5338	8205	1.537
4000	701	1.689	1200	1748	5338	7776	1.457
6000	1051	1.796	1200	1657	5338	7371	1.381
12000	2102	1.917	1200	1571	5338	6988	1.309
1.0E+09	1.75E+08	2.007	1200	1489	5338	6625	1.241

Table 17: Lateral Load Amplifications, Total Shear and Dynamic Amplification Factor for deck structure with Hem-Fir deck boards, and #10 x 3 in. screws, Deck Size 12 ft. x 18 ft.

Substructure Stiffness, K		Natural Frequency (Hz)	Total Resultant Shear Force (lb.)		Total Resultant Shear Force (N)		Dynamic Amplification Factor, Ck
(lb./in)	(N/mm)		Static	Dynamic	Static	Dynamic	
0	0	0.526	912	2788	4057	12402	3.057
100	18	0.611	912	2813	4057	12511	3.084
200	35	0.683	912	2836	4057	12614	3.109
300	53	0.746	912	2858	4057	12712	3.134
400	70	0.803	912	2879	4057	12804	3.156
600	105	0.901	912	2916	4057	12973	3.198
1000	175	1.054	912	2976	4057	13236	3.263
1500	263	1.196	912	2382	4057	10597	2.612
2000	350	1.303	912	1932	4057	8595	2.119
2500	438	1.387	912	1716	4057	7635	1.882
3000	525	1.455	912	1592	4057	7083	1.746
4000	701	1.557	912	1456	4057	6475	1.596
6000	1051	1.684	912	1336	4057	5944	1.465
12000	2102	1.848	912	1230	4057	5472	1.349
1.0E+09	1.75E+08	2.068	912	1135	4057	5049	1.245

Table 18: Lateral Load Amplifications, Total Shear and Dynamic Amplification Factor for deck structure with Hem-Fir deck boards, and #10 x 3 in. screws, deck size 12 ft. x 24 ft.

Substructure Stiffness, K		Natural Frequency (Hz)	Total Resultant Shear Force (lb.)		Total Resultant Shear Force (N)		Dynamic Amplification Factor, Ck
(lb./in)	(N/mm)		Static	Dynamic	Static	Dynamic	
0	0	0.400	1200	3706	5338	16485	3.088
100	18	0.474	1200	3733	5338	16607	3.111
200	35	0.536	1200	3759	5338	16722	3.133
300	53	0.591	1200	3784	5338	16834	3.154
400	70	0.639	1200	3808	5338	16939	3.173
600	105	0.722	1200	3852	5338	17134	3.210
1000	175	0.853	1200	3924	5338	17456	3.270
1500	263	0.975	1200	3987	5338	17737	3.323
2000	350	1.068	1200	4036	5338	17954	3.364
2500	438	1.142	1200	3643	5338	16207	3.036
3000	525	1.201	1200	3139	5338	13964	2.616
4000	701	1.292	1200	2601	5338	11568	2.167
6000	1051	1.406	1200	2190	5338	9741	1.825
12000	2102	1.557	1200	1874	5338	8336	1.562
1.0E+09	1.75E+08	1.769	1200	1625	5338	7228	1.354
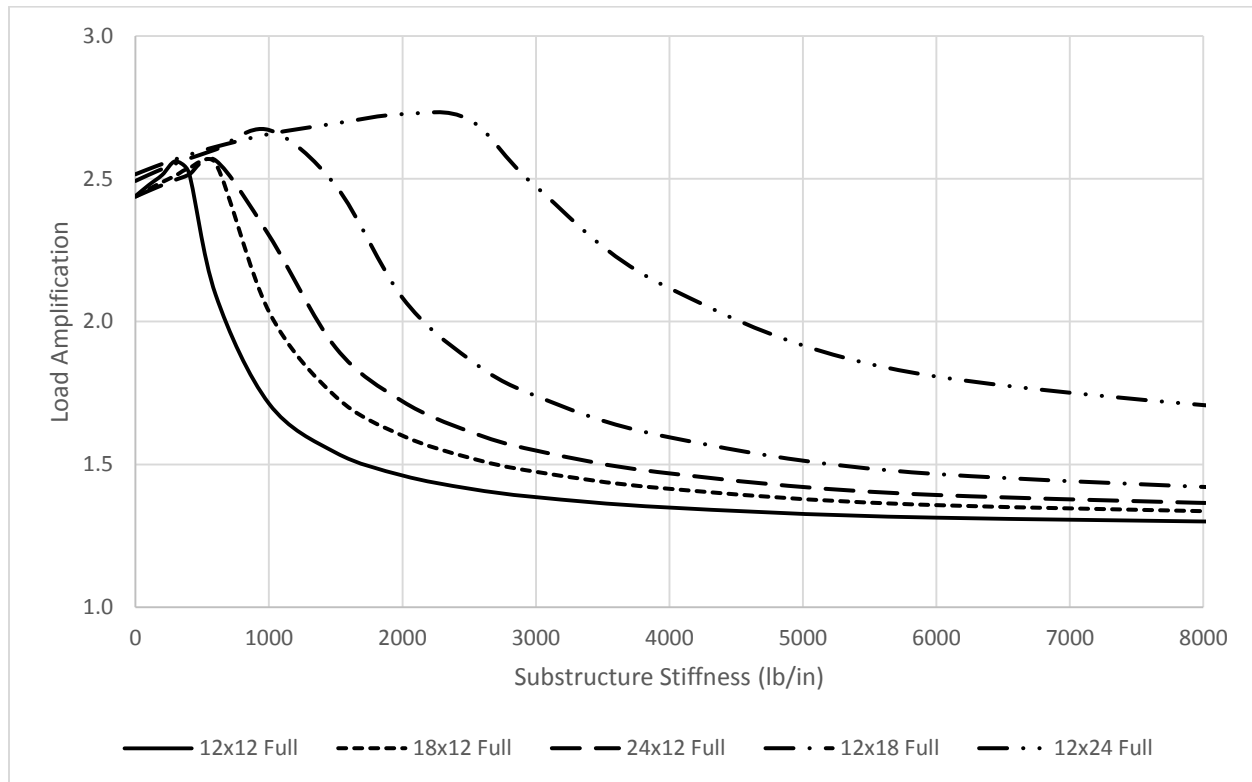
Figure 42: Lateral Load Amplification vs. Substructure Stiffness for 10dThreaded Deck Nails with
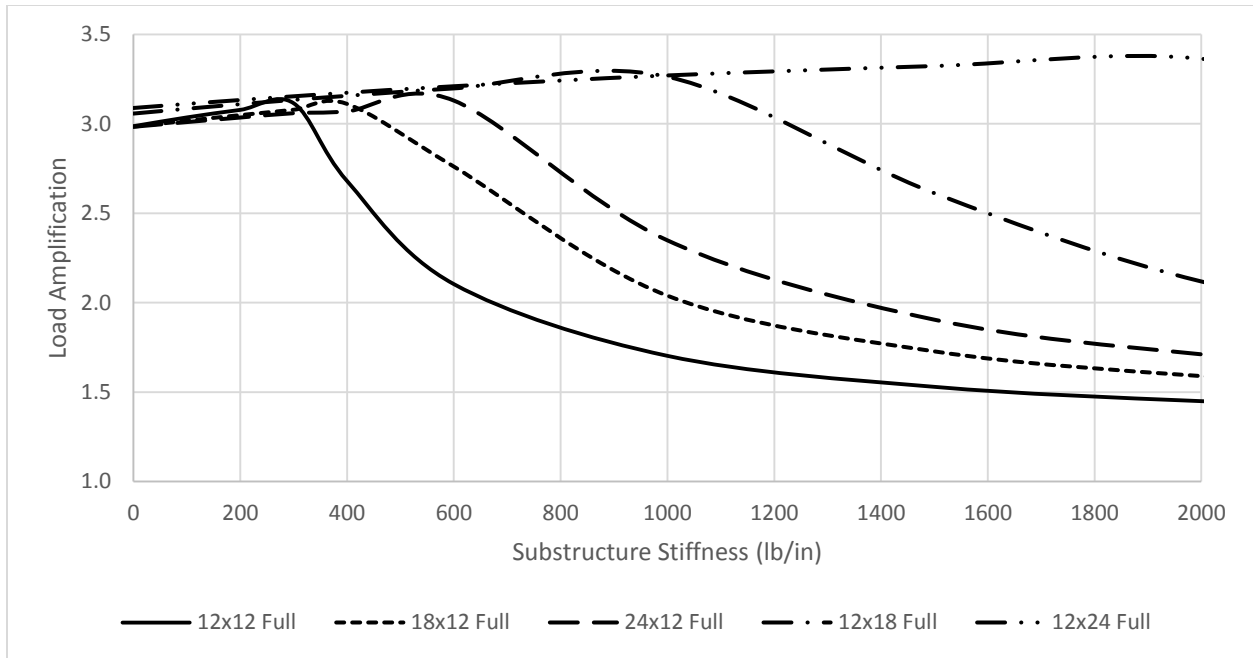
Hem-Fir Deck Boards and Hem-Fir Joists.
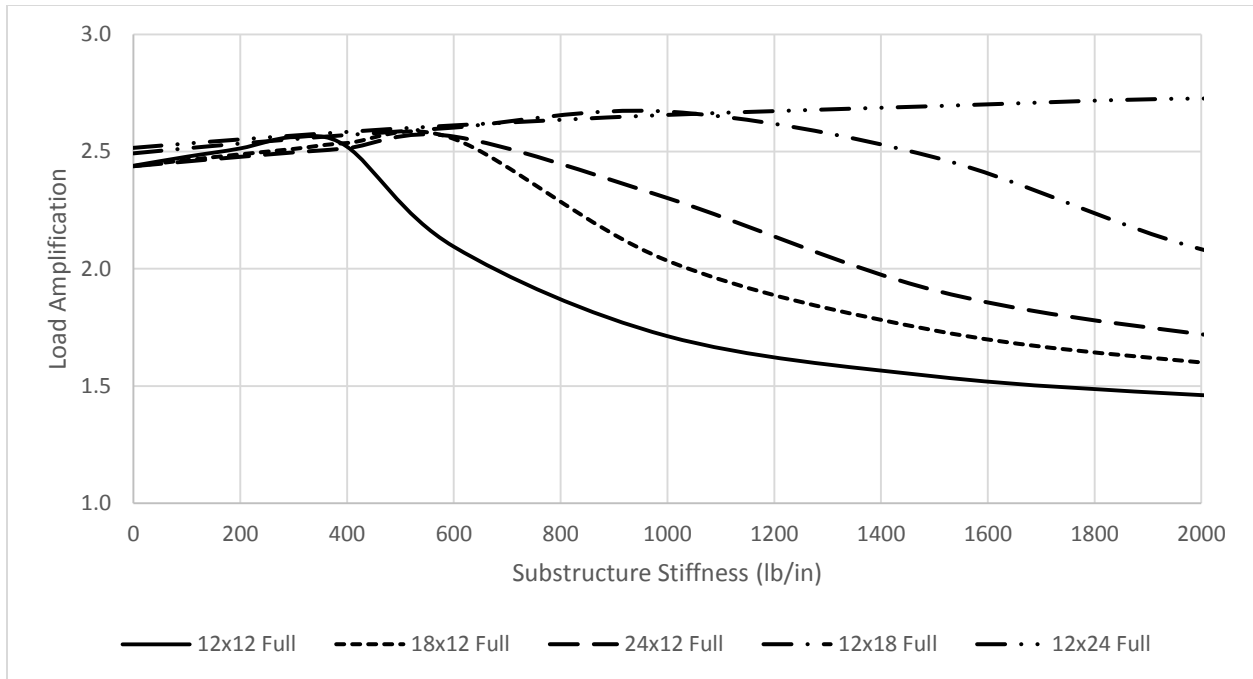
Figure 43:Lateral Load Amplification –10dThreaded Deck Nails with Hem-Fir Deck Boards and

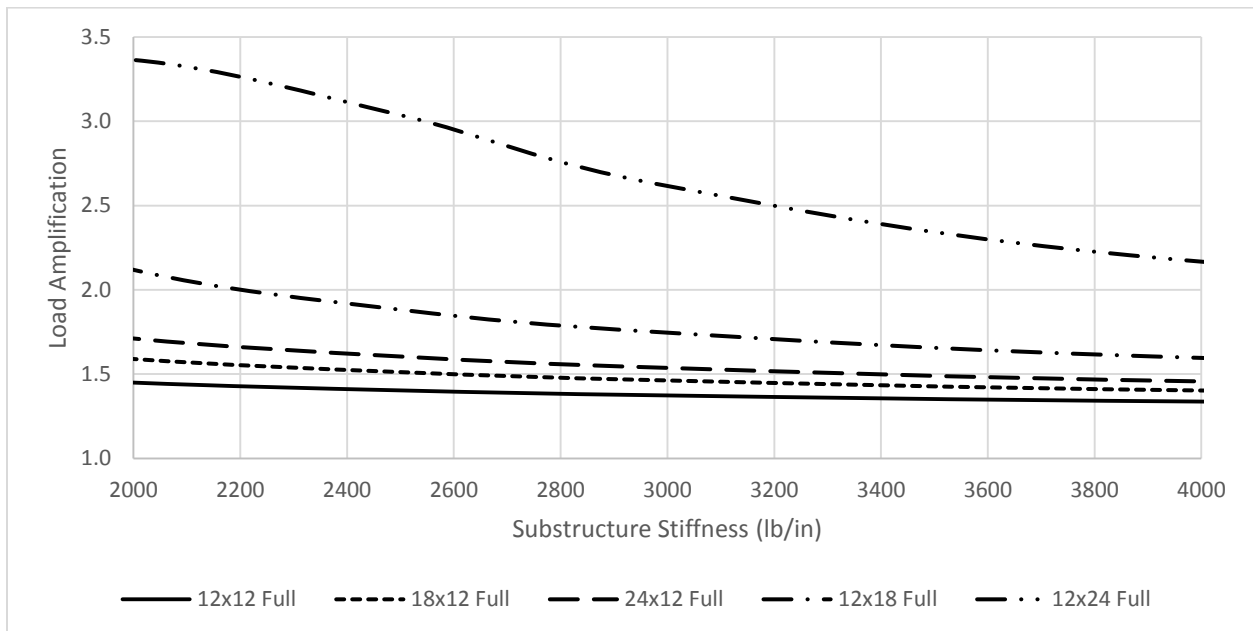Hem-Fir Joists | Substructure Stiffness' from 0-2000 lb./in.
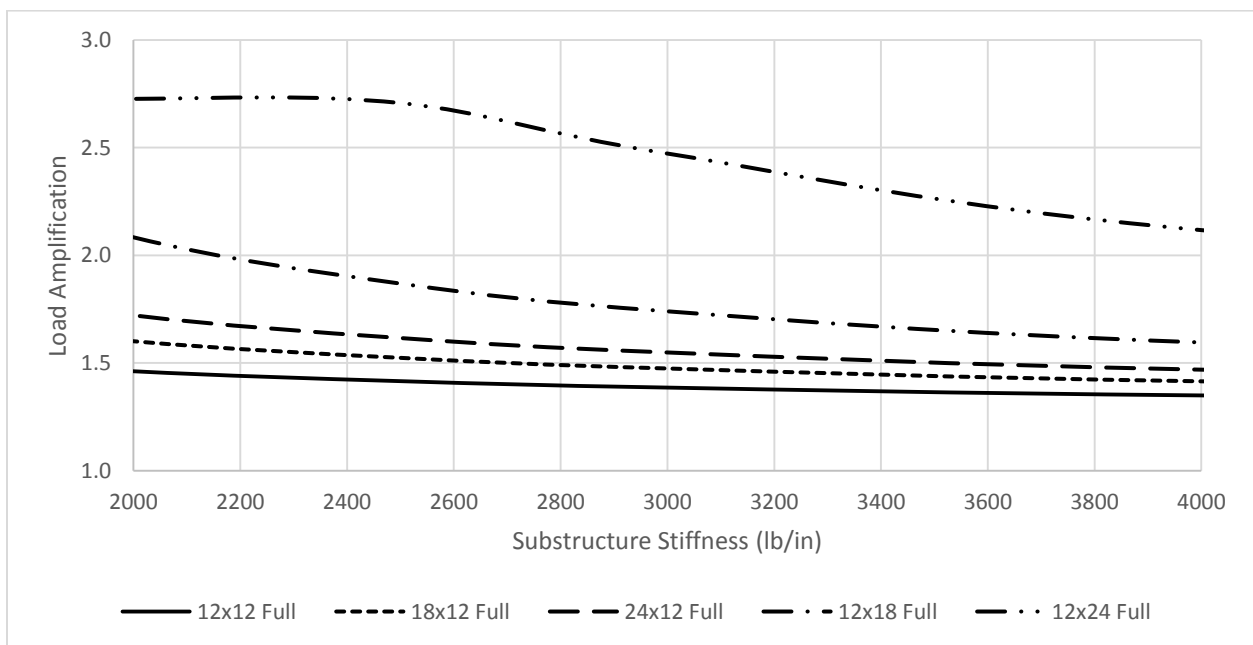
Figure 44: Lateral Load Amplification –10dThreaded Deck Nails with Hem-Fir Deck Boards and

Hem-Fir Joists | Substructure Stiffness' from 2000-4000 lb./in.

Table 19Lateral Load Amplifications, Total Shear and Dynamic Amplification Factor for deck structure with Hem-Fir deck boards, and 10d Threaded Deck Nails, deck size 12 ft. x 12 ft.

Substructure Stiffness, K		Natural Frequency (Hz)	Total Resultant Shear Force (lb.)		Total Resultant Shear Force (N)		Dynamic Amplification Factor, Ck
(lb./in)	(N/mm)		Static	Dynamic	Static	Dynamic	
0	0	0.758	600	1464	2669	6511	2.440
100	18	0.881	600	1487	2669	6614	2.478
200	35	0.983	600	1508	2669	6708	2.513
300	53	1.069	600	1537	2669	6837	2.562
400	70	1.143	600	1512	2669	6728	2.521
600	105	1.265	600	1257	2669	5590	2.094
1000	175	1.438	600	1028	2669	4572	1.713
1500	263	1.576	600	925	2669	4114	1.541
2000	350	1.664	600	877	2669	3900	1.461
2500	438	1.725	600	849	2669	3778	1.415
3000	525	1.769	600	831	2669	3698	1.386
4000	701	1.826	600	810	2669	3601	1.349
6000	1051	1.887	600	788	2669	3506	1.314
12000	2102	1.949	600	768	2669	3414	1.279
1.0E+09	1.75E+08	2.012	600	747	2669	3325	1.246

Table 20:Lateral Load Amplifications, Total Shear and Dynamic Amplification Factor for deck structure with Hem-Fir deck boards, and 10d Threaded Deck Nails, Deck Size 18 ft. x 12 ft.

Substructure Stiffness, K		Natural Frequency (Hz)	Total Resultant Shear Force (lb.)		Total Resultant Shear Force (N)		Dynamic Amplification Factor, Ck
(lb./in)	(N/mm)		Static	Dynamic	Static	Dynamic	
0	0	0.751	933	2275	4150	10118	2.438
100	18	0.835	933	2299	4150	10225	2.464
200	35	0.908	933	2322	4150	10327	2.488
300	53	0.973	933	2343	4150	10422	2.511
400	70	1.031	933	2367	4150	10527	2.536
600	105	1.131	933	2383	4150	10600	2.554
1000	175	1.286	933	1898	4150	8444	2.035
1500	263	1.424	933	1621	4150	7210	1.737
2000	350	1.522	933	1494	4150	6644	1.601
2500	438	1.594	933	1422	4150	6324	1.524
3000	525	1.649	933	1376	4150	6119	1.474
4000	701	1.725	933	1320	4150	5872	1.415
6000	1051	1.811	933	1267	4150	5635	1.358
12000	2102	1.902	933	1216	4150	5408	1.303
1.0E+09	1.75E+08	1.996	933	1167	4150	5190	1.251

Table 21:Lateral Load Amplifications, Total Shear and Dynamic Amplification Factor for deck structure with Hem-Fir deck boards, and 10d Threaded Deck Nails, Deck Size 24 ft. x 12 ft.

Substructure Stiffness, K		Natural Frequency (Hz)	Total Resultant Shear Force (lb.)		Total Resultant Shear Force (N)		Dynamic Amplification Factor, Ck
(lb./in)	(N/mm)		Static	Dynamic	Static	Dynamic	
0	0	0.748	1200	2925	5338	13011	2.437
100	18	0.815	1200	2950	5338	13121	2.458
200	35	0.875	1200	2973	5338	13226	2.478
300	53	0.929	1200	2996	5338	13326	2.497
400	70	0.978	1200	3017	5338	13421	2.514
600	105	1.065	1200	3077	5338	13687	2.564
1000	175	1.205	1200	2762	5338	12287	2.302
1500	263	1.336	1200	2290	5338	10188	1.909
2000	350	1.434	1200	2065	5338	9187	1.721
2500	438	1.510	1200	1939	5338	8624	1.616
3000	525	1.569	1200	1858	5338	8267	1.549
4000	701	1.655	1200	1763	5338	7840	1.469
6000	1051	1.756	1200	1672	5338	7436	1.393
12000	2102	1.868	1200	1586	5338	7054	1.322
1.0E+09	1.75E+08	1.987	1200	1505	5338	6693	1.254

Table 22: Lateral Load Amplifications, Total Shear and Dynamic Amplification Factor for deck

structure with Hem-Fir deck boards, and 10d Threaded Deck Nails, Deck Size 12 ft. x 18 ft.

Substructure Stiffness, K		Natural Frequency (Hz)	Total Resultant Shear Force (lb.)		Total Resultant Shear Force (N)		Dynamic Amplification Factor, Ck
(lb./in)	(N/mm)		Static	Dynamic	Static	Dynamic	
0	0	0.503	912	2273	4057	10111	2.492
100	18	0.591	912	2293	4057	10199	2.514
200	35	0.666	912	2311	4057	10281	2.534
300	53	0.731	912	2328	4057	10357	2.553
400	70	0.788	912	2344	4057	10429	2.571
600	105	0.887	912	2373	4057	10557	2.602
1000	175	1.041	912	2436	4057	10834	2.671
1500	263	1.182	912	2258	4057	10043	2.476
2000	350	1.289	912	1900	4057	8452	2.083
2500	438	1.372	912	1704	4057	7580	1.868
3000	525	1.438	912	1587	4057	7058	1.740
4000	701	1.538	912	1455	4057	6471	1.595
6000	1051	1.663	912	1337	4057	5949	1.467
12000	2102	1.824	912	1232	4057	5482	1.351
1.0E+09	1.75E+08	2.040	912	1137	4057	5060	1.247

Table 23: Lateral Load Amplifications, Total Shear and Dynamic Amplification Factor for deck structure with Hem-Fir deck boards, and 10d Threaded Deck Nails, Deck Size 12 ft. x 24 ft.

Substructure Stiffness, K		Natural Frequency (Hz)	Total Resultant Shear Force (lb.)		Total Resultant Shear Force (N)		Dynamic Amplification Factor, Ck
(lb./in)	(N/mm)		Static	Dynamic	Static	Dynamic	
0	0	0.383	1200	3019	5338	13429	2.516
100	18	0.460	1200	3041	5338	13528	2.534
200	35	0.524	1200	3062	5338	13621	2.552
300	53	0.579	1200	3082	5338	13709	2.568
400	70	0.628	1200	3101	5338	13792	2.584
600	105	0.712	1200	3134	5338	13941	2.612
1000	175	0.844	1200	3188	5338	14180	2.656
1500	263	0.967	1200	3233	5338	14379	2.694
2000	350	1.058	1200	3271	5338	14552	2.726
2500	438	1.131	1200	3248	5338	14448	2.707
3000	525	1.190	1200	2967	5338	13197	2.472
4000	701	1.279	1200	2540	5338	11299	2.117
6000	1051	1.392	1200	2169	5338	9649	1.808
12000	2102	1.541	1200	1868	5338	8309	1.557
1.0E+09	1.75E+08	1.752	1200	1624	5338	7224	1.353

A.4.3 - #10 x 2.75 in. Trex® Composite Deck Screws | Trex® Composite Deck Boards | Hem-Fir
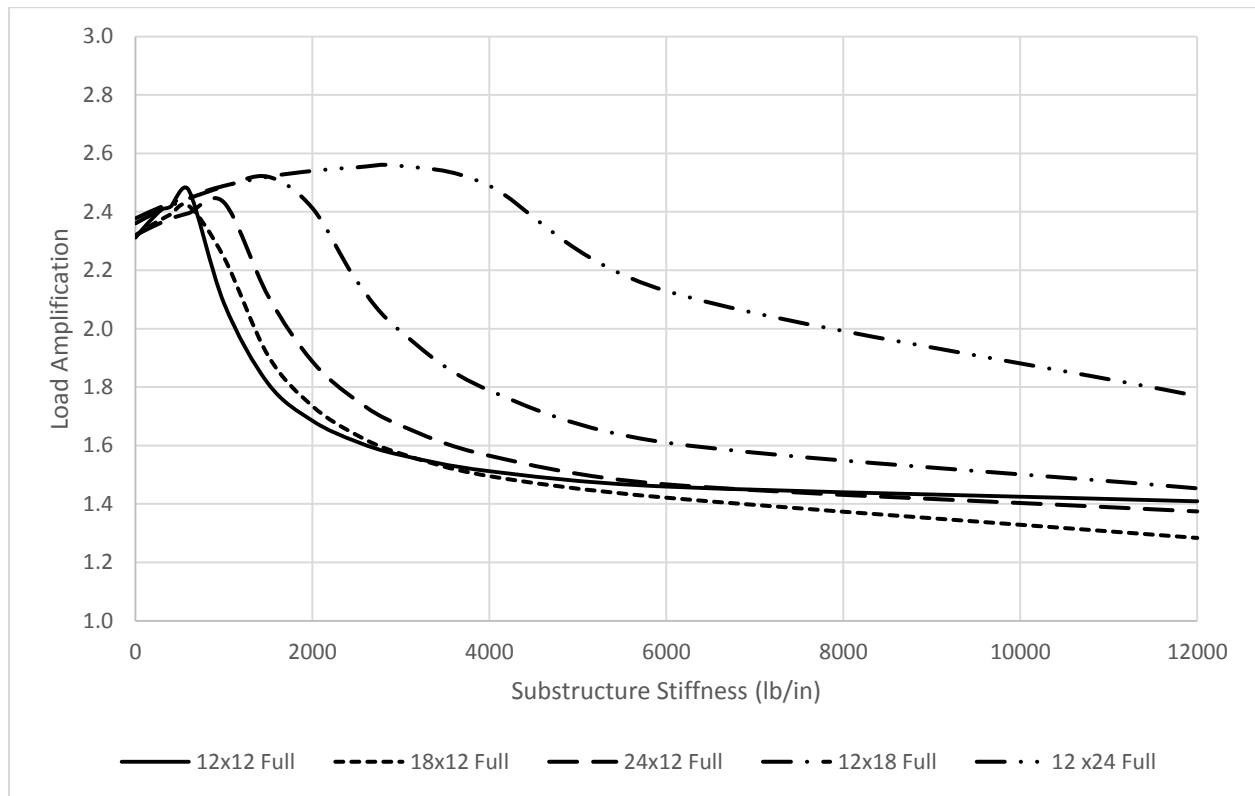
Joists

Figure 45:Lateral Load Amplification –#10 x 2.75 in. Trex® Composite Deck Screws with Trex®

Composite Deck Boards and Hem-Fir Joists
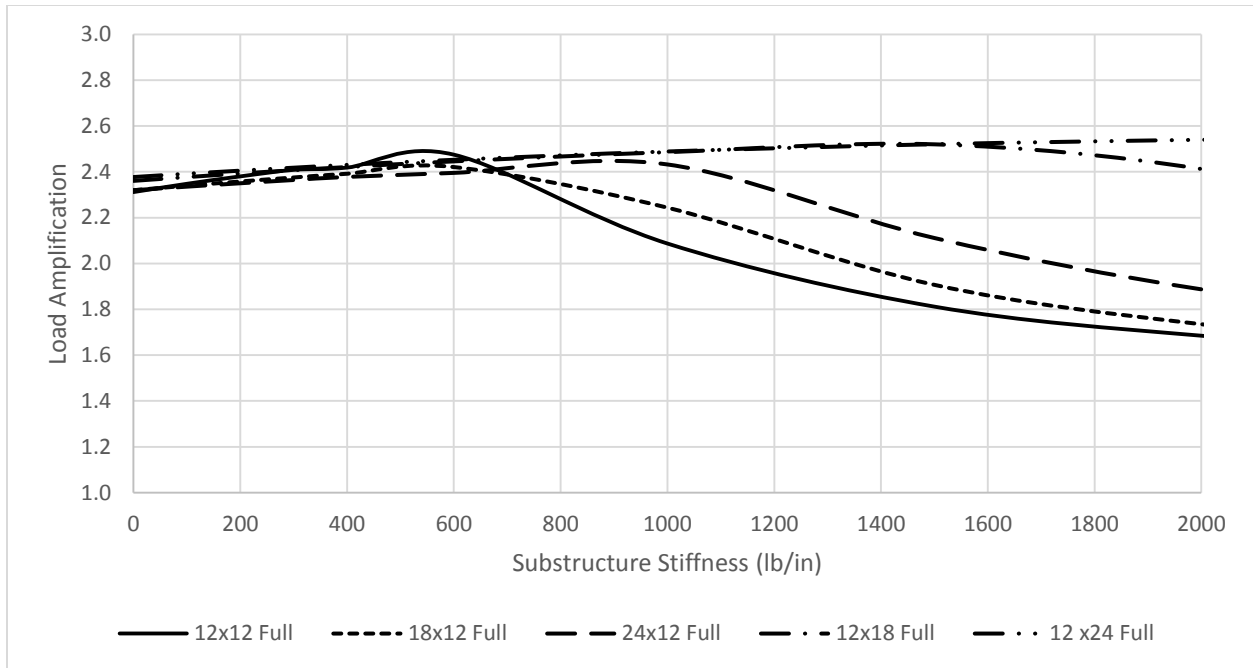
Figure 46: Lateral Load Amplification – #10 x 2.75 in. Trex® Composite Deck Screws with Trex® Composite Deck Boards and Hem-Fir Joists | Substructure Stiffness' from 0-2000 lb./in.
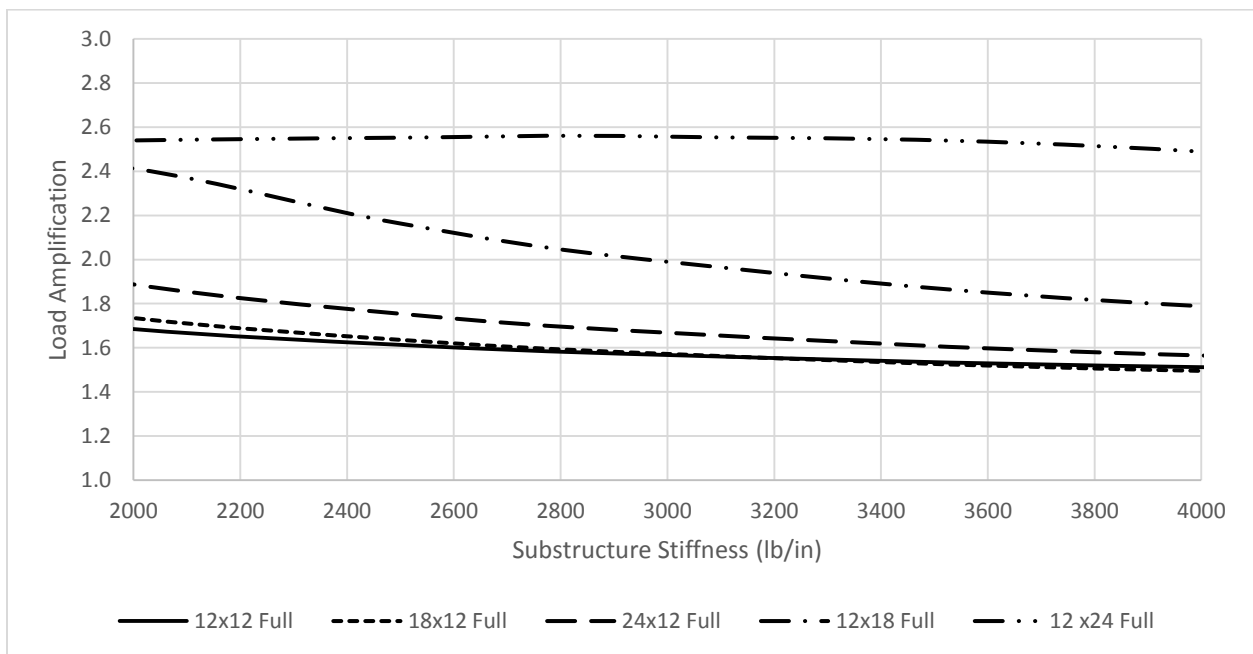
Figure 47: Lateral Load Amplification – #10 x 2.75 in. Trex® Composite Deck Screws with Trex® Composite Deck Boards and Hem-Fir Joists | Substructure Stiffness' from 2000-4000 lb./in.

Table 24: Lateral Load Amplifications, Total Shear and Dynamic Amplification Factor for deck structure with Trex® Composite deck boards, and #10 x 2.75 in. Trex® Deck Screws, Deck Size 12 ft. x 12 ft.

Substructure Stiffness, K		Natural Frequency (Hz)	Total Resultant Shear Force (lb.)		Total Resultant Shear Force (N)		Dynamic Amplification Factor, Ck
(lb./in)	(N/mm)		Static	Dynamic	Static	Dynamic	
0	0	0.662	600	1387	2669	6170	2.312
100	18	0.776	600	1409	2669	6266	2.348
200	35	0.868	600	1428	2669	6352	2.380
300	53	0.946	600	1445	2669	6428	2.409
400	70	1.012	600	1451	2669	6455	2.419
600	105	1.118	600	1485	2669	6605	2.475
1000	175	1.267	600	1252	2669	5570	2.087
1500	263	1.381	600	1087	2669	4836	1.812
2000	350	1.454	600	1011	2669	4497	1.685
2500	438	1.503	600	968	2669	4305	1.613
3000	525	1.538	600	940	2669	4183	1.567
4000	701	1.584	600	907	2669	4036	1.512
6000	1051	1.632	600	876	2669	3895	1.459
12000	2102	1.682	600	845	2669	3761	1.409
1.0E+09	1.75E+08	1.733	600	817	2669	3632	1.361

Table 25: Lateral Load Amplifications, Total Shear and Dynamic Amplification Factor for deck structure with Trex® Composite deck boards, and #10 x 2.75 in. Trex® Deck Screws, Deck Size 18 ft. x 12 ft.

Substructure Stiffness, K		Natural Frequency (Hz)	Total Resultant Shear Force (lb.)		Total Resultant Shear Force (N)		Dynamic Amplification Factor, Ck
(lb./in)	(N/mm)		Static	Dynamic	Static	Dynamic	
0	0	0.759	933	2164	4150	9627	2.320
100	18	0.826	933	2183	4150	9709	2.339
200	35	0.885	933	2200	4150	9786	2.358
300	53	0.939	933	2216	4150	9858	2.375
400	70	0.987	933	2231	4150	9926	2.392
600	105	1.072	933	2259	4150	10047	2.421
1000	175	1.206	933	2093	4150	9312	2.244
1500	263	1.329	933	1779	4150	7914	1.907
2000	350	1.418	933	1619	4150	7201	1.735
2500	438	1.486	933	1526	4150	6790	1.636
3000	525	1.538	933	1467	4150	6525	1.572
4000	701	1.613	933	1395	4150	6205	1.495
6000	1051	1.699	933	1326	4150	5899	1.421
12000	2102	1.895	933	1198	4150	5328	1.284
1.0E+09	1.75E+08	1.895	933	1198	4150	5328	1.284

Table 26: Lateral Load Amplifications, Total Shear and Dynamic Amplification Factor for deck structure with Trex® Composite deck boards, and #10 x 2.75 in. Trex® Deck Screws, Deck Size 24 ft. x 12 ft.

Substructure Stiffness, K		Natural Frequency (Hz)	Total Resultant Shear Force (lb.)		Total Resultant Shear Force (N)		Dynamic Amplification Factor, Ck
(lb./in)	(N/mm)		Static	Dynamic	Static	Dynamic	
0	0	0.756	1200	2784	5338	12382	2.320
100	18	0.809	1200	2802	5338	12465	2.335
200	35	0.858	1200	2820	5338	12545	2.350
300	53	0.902	1200	2837	5338	12620	2.364
400	70	0.943	1200	2853	5338	12692	2.378
600	105	1.016	1200	2874	5338	12786	2.395
1000	175	1.135	1200	2919	5338	12982	2.432
1500	263	1.250	1200	2533	5338	11270	2.111
2000	350	1.338	1200	2265	5338	10074	1.887
2500	438	1.407	1200	2105	5338	9364	1.754
3000	525	1.463	1200	2002	5338	8905	1.668
4000	701	1.545	1200	1878	5338	8354	1.565
6000	1051	1.644	1200	1760	5338	7831	1.467
12000	2102	1.759	1200	1649	5338	7337	1.374
1.0E+09	1.75E+08	1.779	1200	1545	5338	6872	1.287

Table 27: Lateral Load Amplifications, Total Shear and Dynamic Amplification Factor for deck structure with Trex® Composite deck boards, and #10 x 2.75 in. Trex® Deck Screws, aspect ratio 12 ft. x 18 ft.

Substructure Stiffness, K		Natural Frequency (Hz)	Total Resultant Shear Force (lb.)		Total Resultant Shear Force (N)		Dynamic Amplification Factor, Ck
(lb./in)	(N/mm)		Static	Dynamic	Static	Dynamic	
0	0	0.503	912	2153	4057	9576	2.361
100	18	0.575	912	2168	4057	9643	2.377
200	35	0.637	912	2182	4057	9706	2.393
300	53	0.691	912	2195	4057	9765	2.407
400	70	0.740	912	2208	4057	9821	2.421
600	105	0.825	912	2230	4057	9921	2.446
1000	175	0.959	912	2267	4057	10084	2.486
1500	263	1.083	912	2298	4057	10223	2.520
2000	350	1.177	912	2200	4057	9787	2.412
2500	438	1.251	912	1973	4057	8776	2.163
3000	525	1.311	912	1815	4057	8073	1.990
4000	701	1.401	912	1631	4057	7256	1.789
6000	1051	1.513	912	1468	4057	6531	1.610
12000	2102	1.658	912	1325	4057	5896	1.453
1.0E+09	1.75E+08	1.853	912	1200	4057	5337	1.315

Table 28: Lateral Load Amplifications, Total Shear and Dynamic Amplification Factor for deck structure with Trex® Composite deck boards, and #10 x 2.75 in Trex® Deck Screws, aspect ratio 12 ft. x 24 ft.

Substructure Stiffness, K		Natural Frequency (Hz)	Total Resultant Shear Force (lb.)		Total Resultant Shear Force (N)		Dynamic Amplification Factor, Ck
(lb./in)	(N/mm)		Static	Dynamic	Static	Dynamic	
0	0	0.382	1200	2853	5338	12689	2.377
100	18	0.445	1200	2870	5338	12766	2.392
200	35	0.498	1200	2886	5338	12838	2.405
300	53	0.544	1200	2902	5338	12907	2.418
400	70	0.586	1200	2916	5338	12972	2.430
600	105	0.658	1200	2943	5338	13091	2.452
1000	175	0.773	1200	2987	5338	13285	2.489
1500	263	0.879	1200	3024	5338	13453	2.520
2000	350	0.961	1200	3048	5338	13557	2.540
2500	438	1.026	1200	3063	5338	13623	2.552
3000	525	1.078	1200	3068	5338	13649	2.557
4000	701	1.157	1200	2987	5338	13286	2.489
6000	1051	1.257	1200	2555	5338	11365	2.129
12000	2102	1.389	1200	2123	5338	9445	1.769
1.0E+09	1.75E+08	1.524	1200	1776	5338	7899	1.480

Figure 48: Total Shear Load Amplification of Deck structure 12 ft. x 12 ft. model Comparing 3 Test Specimen Types

Nails, screws and composite test types were all simulated using the 12 ft. x12 ft. FEA model for deck load amplifications. Screws have a higher initial load amplification than nails and screws but equates to nails at about 600 lb./in. substructure stiffness. Trex® composite boards and screws had the lower initial amplifications, but higher amplifications with substructure stiffness higher than about 500 lb./in.

Figure 49:Total Shear Load Amplification of Deck structure with 18 ft. x 12 ft. FEA Model
Comparing 3 Test Specimen Types

Nails, screws and composite test types were all simulated using the 18 ft. x 12 ft. aspect ratio FEA
model for deck load amplifications. Screws have a higher initial load amplification than nails and
screws but equates to nails at about 1000 lb./in. substructure stiffness. Trex® composite boards
and screws had the lower initial amplifications, but higher amplifications with substructure
stiffness higher than about 750 lb./in.
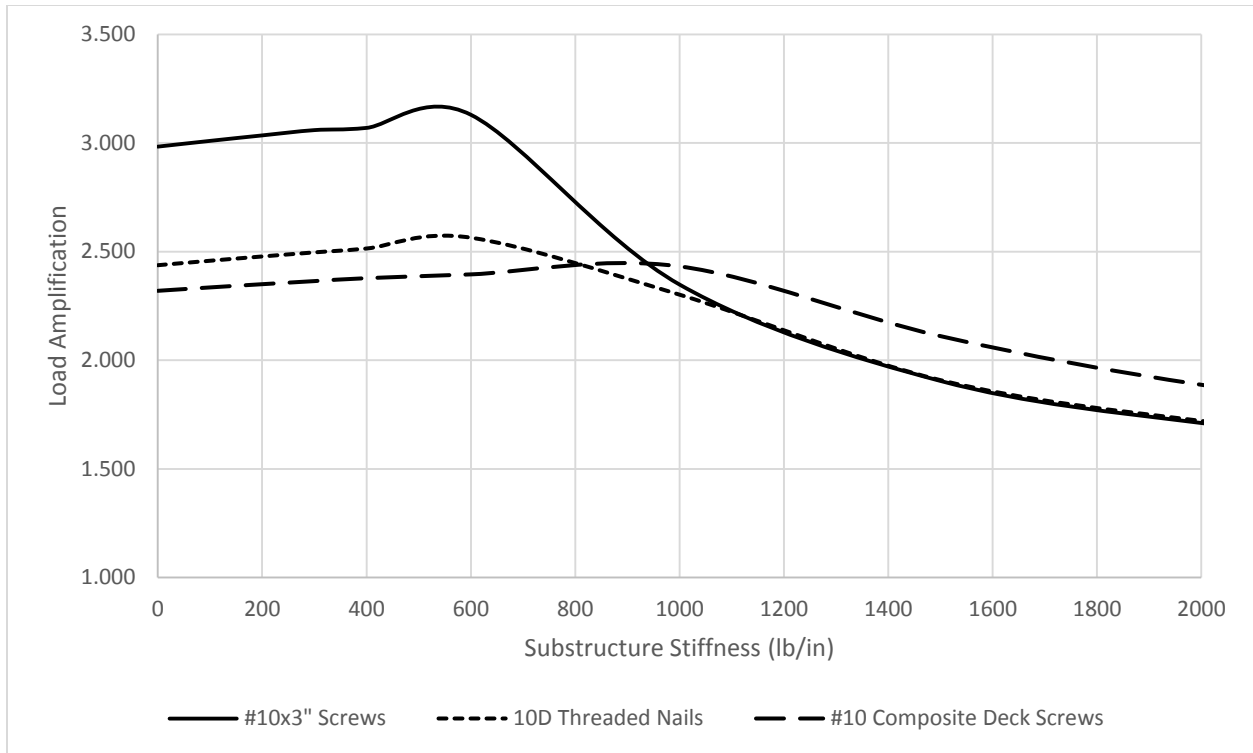
Figure 50: Total Shear Load Amplification of Deck structure with 24 ft. x 12 ft. FEA Model Comparing 3 Test Types

Nails, screws and composite test types were all simulated using the 24 ft. x 12 ft. FEA model for deck load amplifications. Screws have a higher initial load amplification than nails and screws but equates to nails at about 1500 lb./in. substructure stiffness. Trex® composite boards and screws had the lower initial amplifications, but higher amplifications with substructure stiffness higher than about 950 lb./in.
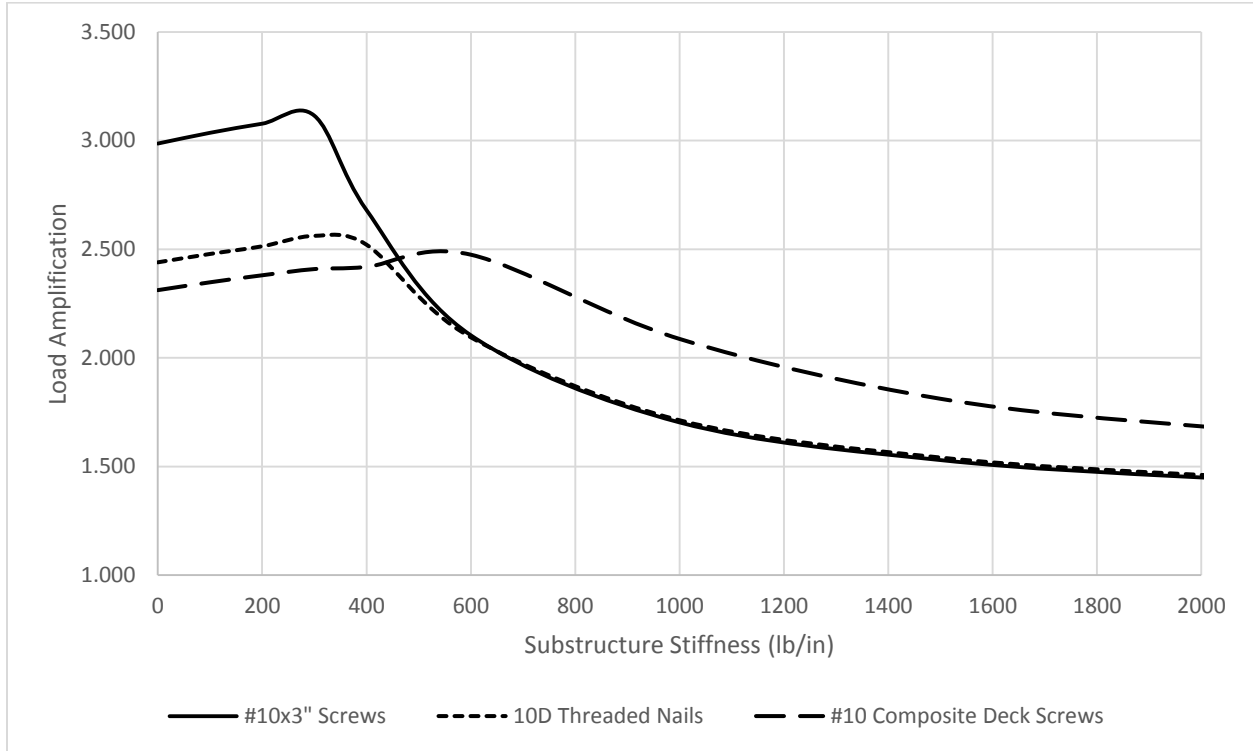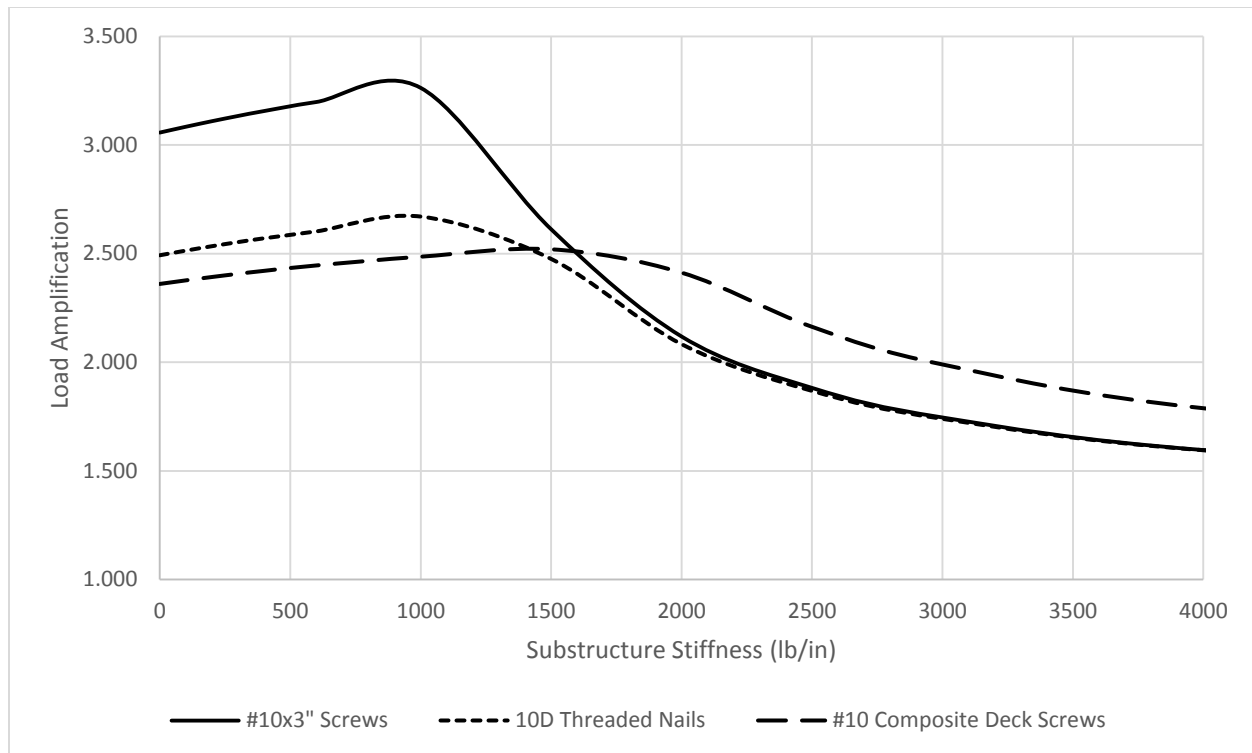
Figure 51:Total Shear Load Amplification of Deck structure with 12 ft. x 18 ft. FEA Model Comparing 3 Test Specimen Types

Nails, screws and composite test types were all simulated using the 12 ft. x 18 ft. FEA model for deck load amplifications. Screws have a higher initial load amplification than nails and screws but equates to nails at about 2000 lb./in. substructure stiffness. Trex® composite boards and screws had the lower initial amplifications, but higher amplifications with substructure stiffness higher than about 1600 lb./in.
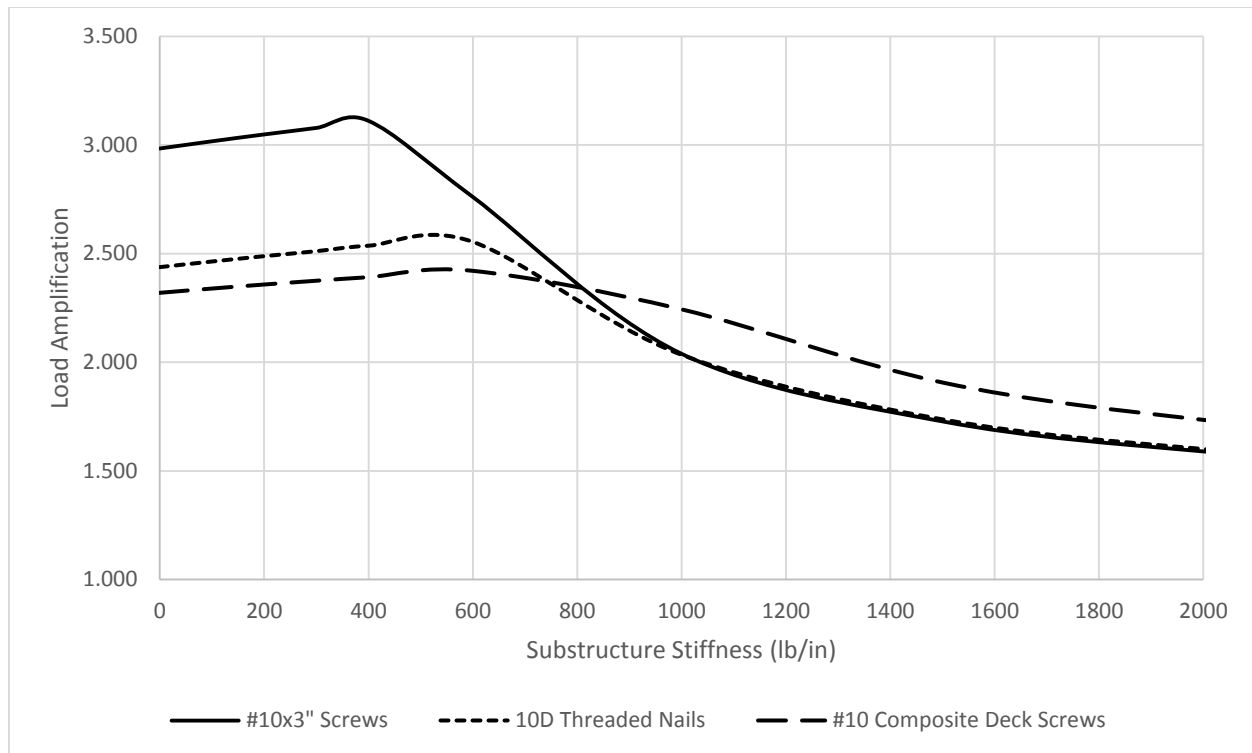
Figure 52:Total Shear Load Amplification of Deck structure with 12 ft. x 24 ft. FEA Model Comparing 3 Test Specimen Types

Nails, screws and composite test types were all simulated using the 12 ft. x 24 ft. FEA model for deck load amplifications. Screws have a higher initial load amplification than nails and screws but equates to nails at about 5000 lb./in. substructure stiffness. Trex® composite boards and screws had the lower initial amplifications, but higher amplifications with substructure stiffness higher than about 3100 lb./in.
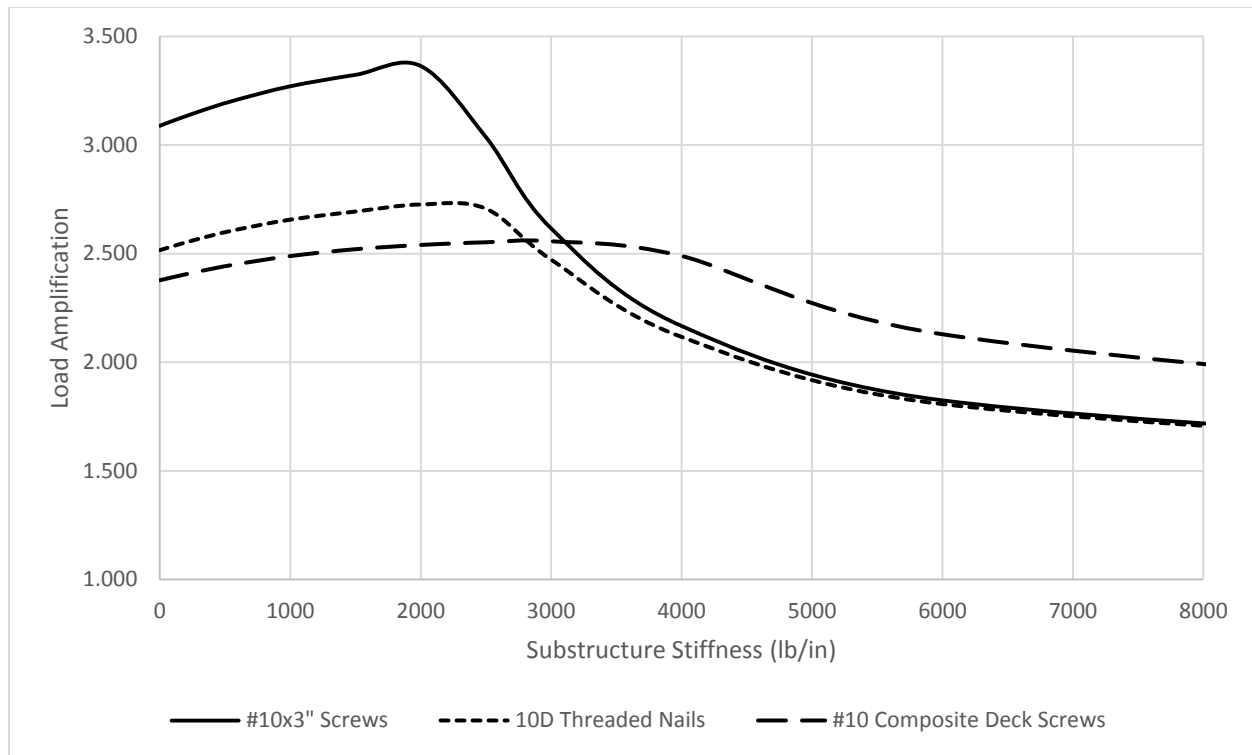
A.5 – Excel Spreadsheet design aid interface

Occupant Induced Deck Load Amplification Calculator

Inputs

Joist Length (L_{Joist}):	8 ft
Ledger Length (L_{Ledger}):	12 ft
Joist Spacing (S_J):	16 in
Deck Board Spacing (S_L):	5.75 in
Deck Board Material:	Wood
Deck Board Connection Method:	#10 x3" Wood Screw
Substructure Stiffness (K_S):	600 lb/in
Assumed Vertical Live Load (LL):	25.6 psf

Outputs

Natural Frequency (Fn):	1.71 Hz
Dynmamic Amplification Factor (Ck):	1.47 x Static Load

Design Assistance

Note: *This calculation assumes that all supporting framing lines in the lateral direction share an equal percentage of the total substructure stiffness and are equaly spaced.*

Diaphragm Stiffness (G):	405.8 lb/in	
Substructure Stiffness (Ks):	600 lb/in	
Amplified Total LateraL Load (q):	360.16 lb	$= (L_{joist} * L_{ledger})(10\% * LL)(Ck)$
Assumed # of Supporting Frame Lines:	1	

	Reaction	Unit Shear (+/-)
Ledger:	253 lb	21 lb/ft
Outer Post Line:	107 lb	9 lb/ft

Hold-Down Compression/Tension:	48 lb
Allowable Shear (SDPWS Table 4.3D):	140 lb/in
Safety Factor:	2
Adjusted Allowable Shear:	70 lb/in **PASS**

Appendix B – Calculations

This appendix serves to illustrate some of the calculations that were necessary to conduct the research. Included in this appendix are the conversions from raw data to moment-rotation curves, specific gravity and moisture content measurements, and the calculation of the yield modes for each test specimen type. It also includes the process for calculating EVD values, the required moment to return the connection to zero rotation, and how the simplified FEA model shear modulus was determined.

- B1: Raw Data Conversion to Moment vs. Rotation

- B2: Specific Gravity and Moisture Content

- B3: TR-12 Yield Mode for Fasteners

- B4: Equivalent Viscous Damping Coefficient

- B5: Moment Required to Return to Zero Rotation

- B6: Shear Modulus Conversion to Simplified Model

B.1 - Raw Data Conversion

Raw data needed to be converted to Moment-Rotation graphs. Below is an example data and

calculation for specimen N2 (Nailed Connecter, Specimen 2) at a load of 40 lb.

String-Pot1 (in)	Sting-Pot2 (in)	Load (lb)	Rotation (rad)	Moment (lb-in)
0	0	4.84	0	0
-0.001	0	10.47	9.52381E-05	66.1525
-0.002	0.001	15.31	0.000285714	123.0225
-0.002	0.002	19.33	0.000380952	170.2575
-0.003	0.005	22.55	0.000761905	208.0925
-0.005	0.007	26.58	0.001142857	255.445
-0.006	0.009	30.61	0.00142857	302.7975
-0.008	0.012	33.02	0.00190476	331.115
-0.011	0.014	34.64	0.002380948	350.15
-0.012	0.016	37.05	0.00266666	378.4675
-0.015	0.019	38.66	0.003238084	397.385
-0.017	0.022	40.27	0.003714269	416.3025

Notes: - String-Pot1, String-Pot2, and Load are recorded values from testing
- Measured distance to Load Cell from connection center = 11.75"
- Measured distance between string-pots = 10.5"

Calculate Rotation

$d1$:	-0.017 *in*	- String-Pot1 Value
$d2$:	0.022 *in*	- String-Pot2 Value
e_r:	10.5 *in*	- Dist. Between String-Pots
Rotation:	0.003714269 *rad*	$= Tan^{-1}\left(\dfrac{|d1| + |d2|}{e_r}\right)$

Calculate Moment

Load:	40.27 *lb*	- Load Cell Value
e_m:	11.75 *in*	- Dist. To Load Cell
c:	4.84 *lb*	- Initial Point Correction Factor
Moment:	473.1725 *lb-in*	$= Load * e_m$

Graph Results

114
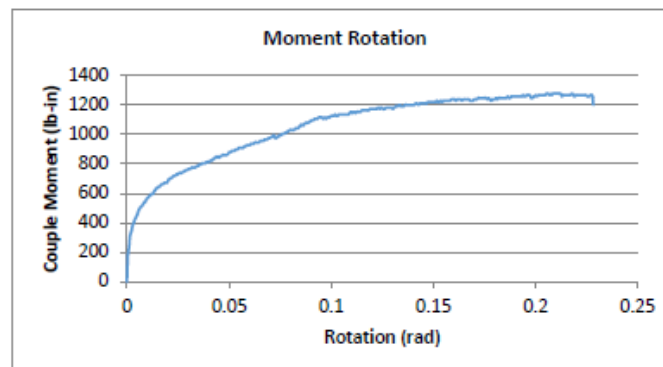
B.2 - Specific Gravity /Moisture Content

Table 29: Specific Gravity Measurements and Calculations of Nailed Specimens

Specimen	Description	Wet Volume (ci)	Wet Mass (g)	Wet Specific Gravity	Dry Volume (ci)	Dry Mass (g)	Dry Specific Gravity	Test MC
				Specific Gravity Calculation - Nailed Fasteners - Specimens #1-#10				
Nailed 1	Deck Board	6.113	40.6	40.54	5.558	34.5	37.94	17.5
	Joist	6.355	45.7	43.90	5.895	39.2	40.60	16.6
Nailed 2	Deck Board	5.885	48.3	50.10	5.469	40.9	45.65	18.1
	Joist	5.969	48.7	49.81	5.401	42.0	47.42	16.1
Nailed 3	Deck Board	6.191	52.7	51.97	5.679	45.1	48.45	16.9
	Joist	6.107	47.1	47.08	5.868	40.4	41.98	16.7
Nailed 4	Deck Board	5.985	45.8	46.72	5.596	38.6	42.12	18.6
	Joist	6.087	44.7	44.83	5.576	38.3	41.95	16.7
Nailed 5	Deck Board	6.222	50.6	49.65	5.772	43.1	45.55	17.5
	Joist	6.598	58.4	54.04	6.267	49.8	48.53	17.2
Nailed 6	Deck Board	6.213	48.2	47.36	5.560	41.1	45.08	17.4
	Joist	6.186	48	47.37	5.876	40.7	42.27	18.0
Nailed 7	Deck Board	6.935	60.8	53.53	6.565	52.0	48.33	17.0
	Joist	5.407	47.5	53.64	4.927	40.8	50.59	16.3
Nailed 8	Deck Board	6.161	50.4	49.94	5.791	43.3	45.61	16.5
	Joist	6.413	45.7	43.51	6.019	39.5	40.05	15.7
Nailed 9	Deck Board	6.128	43.5	43.34	5.743	37.2	39.50	17.1
	Joist	6.368	60.3	57.81	5.829	51.9	54.36	16.2
Nailed 10	Deck Board	5.657	47.29	51.03	5.434	39.3	44.16	20.3
	Joist	5.494	58.78	65.32	5.156	50.1	59.33	17.3

Note – Wet mass values were adjusted to account for miss-calibration of scale during wet mass measurements. This did not affect dry S.G. values.

Table 30: Specific Gravity Measurements and Calculations of Nailed Specimens |

Specimen	Description	Wet Volume (ci)	Wet Mass (g)	Wet Specific Gravity	Dry Volume (ci)	Dry Mass (g)	Dry Specific Gravity	Test MC
Specific Gravity Calculation - Screw Fasteners - Specimens #1-#10								
Screw 1	Deck Board	6.113	48.6	40.54	5.558	34.5	37.94	40.7
	Joist	6.355	53.7	43.90	5.895	39.2	40.60	37.0
Screw 2	Deck Board	5.885	56.3	50.10	5.469	40.9	45.65	37.7
	Joist	5.969	56.7	49.81	5.401	42.0	47.42	35.2
Screw 3	Deck Board	6.191	60.7	51.97	5.679	45.1	48.45	34.7
	Joist	6.107	55.1	47.08	5.868	40.4	41.98	36.6
Screw 4	Deck Board	5.985	53.8	46.72	5.596	38.6	42.12	39.3
	Joist	6.087	52.7	44.83	5.576	38.3	41.95	37.6
Screw 5	Deck Board	6.222	58.6	49.65	5.772	43.1	45.55	36.1
	Joist	6.598	66.4	54.04	6.267	49.8	48.53	33.3
Screw 6	Deck Board	6.213	56.2	47.36	5.560	41.1	45.08	36.9
	Joist	6.186	56	47.37	5.876	40.7	42.27	37.6
Screw 7	Deck Board	6.935	68.8	53.53	6.565	52.0	48.33	32.4
	Joist	5.407	55.5	53.64	4.927	40.8	50.59	35.9
Screw 8	Deck Board	6.161	58.4	49.94	5.791	43.3	45.61	35.0
	Joist	6.413	53.7	43.51	6.019	39.5	40.05	36.0
Screw 9	Deck Board	6.128	51.5	43.34	5.743	37.2	39.50	38.6
	Joist	6.368	68.3	57.81	5.829	51.9	54.36	31.6
Screw 10	Deck Board	5.657	55.29	51.03	5.434	39.3	44.16	40.7
	Joist	5.494	66.78	65.32	5.156	50.1	59.33	33.3

Table 31: Specific Gravity Measurements and Calculations of Nailed Specimens.

Specimen	Description	Wet Volume (ci)	Wet Mass (g)	Wet Specific Gravity	Dry Volume (ci)	Dry Mass (g)	Dry Specific Gravity	Test MC
Specific Gravity Calculation - Composite Deck Boards - Specimens #1-#10								
Comp 1	Deck Board	6.113	40.6	40.54	5.558	34.5	37.94	17.5
	Joist	6.355	45.7	43.90	5.895	39.2	40.60	16.6
Comp 2	Deck Board	5.885	48.3	50.10	5.469	40.9	45.65	18.1
	Joist	5.969	48.7	49.81	5.401	42.0	47.42	16.1
Comp 3	Deck Board	6.191	52.7	51.97	5.679	45.1	48.45	16.9
	Joist	6.107	47.1	47.08	5.868	40.4	41.98	16.7
Comp 4	Deck Board	5.985	45.8	46.72	5.596	38.6	42.12	18.6
	Joist	6.087	44.7	44.83	5.576	38.3	41.95	16.7
Comp 5	Deck Board	6.222	50.6	49.65	5.772	43.1	45.55	17.5
	Joist	6.598	58.4	54.04	6.267	49.8	48.53	17.2
Comp 6	Deck Board	6.213	48.2	47.36	5.560	41.1	45.08	17.4
	Joist	6.186	48	47.37	5.876	40.7	42.27	18.0
Comp 7	Deck Board	6.935	60.8	53.53	6.565	52.0	48.33	17.0
	Joist	5.407	47.5	53.64	4.927	40.8	50.59	16.3
Comp 8	Deck Board	6.161	50.4	49.94	5.791	43.3	45.61	16.5
	Joist	6.413	45.7	43.51	6.019	39.5	40.05	15.7
Comp 9	Deck Board	6.128	43.5	43.34	5.743	37.2	39.50	17.1
	Joist	6.368	60.3	57.81	5.829	51.9	54.36	16.2
Comp 10	Deck Board	5.657	47.29	51.03	5.434	39.3	44.16	20.3
	Joist	5.494	58.78	65.32	5.156	50.1	59.33	17.3

B.3 - TR-12 Yield Strength/Mode

Fastener Lateral Rerence Design Values (Including gap)

Inputs

Main Member Characteristics

Wood Type:	Hem-Fir	
Thickness (T_m):	5.5 *in*	
Specific Gravity:	0.43	- *NDS Table 11.3.3A*
Angle of Connection (Θ):	90 *degrees*	- *Angle from Load Direction to Grain*

Side Member Characteristics

Wood Type:	Hem-Fir	
Thickness (T_s):	1.5 *in*	
Specific Gravity:	0.43	- *NDS Table 11.3.3A*
Angle of Connection (Θ):	0 *degrees*	- *Angle from Load Direction to Grain*

Connector Characteristics

Connector Type:	Wood Screw	
Bending Strenght (F_b):	80000 *psi*	- *NDS App. I - Table I1*
Connector Diameter (D):	0.19 *in*	
Fastener Length	3 *in*	*Main Member Penetration < 10D*
		Final Values Adjusted by p/10D

Other

Connection Gap (g):	0 *in*	- *Gap Between Connnecting Members*

Outputs

Dowel Bearing Strengths

Main Member (F_m):	3500 *psi*	*As per NDS Table 11.3.3 - Footnote 2 and*
Side Member(F_s):	3500 *psi*	*NDS Section 11.3.4 - Eq. 11.3-11*

Reference Design Values (lbs/fastener)			Yield Modes	
Yield Mode	Single Shear	Double Shear	Mode	Yield Type
I_m	310	310	I_m	
I_s	416	831	I_s	
II	153	NA	II	
III_m	135		III_m	
III_s	163	326		
IV	145	291	III_s	
Minimum	**107**	**229**	IV	

Nails and Wood Screws Should NOT Be Loaded in Double Shear

NDS Reference Design Strength (Z):	
Single Shear:	**107 lbs**
Double Shear:	**229 lbs**

*Illustration retrieved from AWC TR - 12, 2014

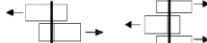Figure 53: Calculation for Yield Strength and NDS Yield Mode for #10 x 3 in. Screw**s.**
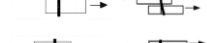
Fastener Lateral Rerence Design Values (Including gap)

Inputs	

Main Member Characteristics

Wood Type:	Hem-Fir	
Thickness (T_m):	5.5 *in*	
Specific Gravity:	0.43	- *NDS Table 11.3.3A*
Angle of Connection (Θ):	90 *degrees*	- *Angle from Load Direction to Grain*

Side Member Characteristics

Wood Type:	Hem-Fir	
Thickness (T_s):	1.5 *in*	
Specific Gravity:	0.43	- *NDS Table 11.3.3A*
Angle of Connection (Θ):	0 *degrees*	- *Angle from Load Direction to Grain*

Connector Characteristics

Connector Type:	Nail	
Bending Strenght (F_b):	90000 *psi*	- *NDS App. I - Table I1*
Connector Diameter (D):	0.148 *in*	
Fastener Length	3 *in*	

Other

Connection Gap (g):	0 *in*	- *Gap Between Connnecting Members*

Outputs	

Dowel Bearing Strengths

Main Member (F_m):	3500 *psi*	*As per NDS Table 11.3.3 - Footnote 2 and*
Side Member(F_s):	3500 *psi*	*NDS Section 11.3.4 - Eq. 11.3-11*

Reference Design Values (lbs/fastener)			Yield Modes	
Yield Mode	Single Shear	Double Shear	Mode	Yield Type
I_m	283	283	I_m	
I_s	353	706	I_s	
II	133	NA	II	
III_m	112		III_m	
III_s	132	264		
IV	102	204	III_s	
Minimum	**102**	**204**	IV	

Nails and Wood Screws Should NOT Be Loaded in Double Shear

NDS Reference Design Strength (Z):	
Single Shear:	***102 lbs***
Double Shear:	***204 lbs***

Illustration retrieved from AWC TR - 12, 2014

Figure 54: Calculation for Yield Strength and NDS Yield Mode for 10d Threaded Deck Nails.

Fastener Lateral Rerence Design Values (Including gap)

Inputs

Main Member Characteristics

Wood Type:	Hem-Fir	
Thickness (T_m):	5.5 *in*	
Specific Gravity:	0.43	*- NDS Table 11.3.3A*
Angle of Connection (Θ):	90 *degrees*	*- Angle from Load Direction to Grain*

Side Member Characteristics

Wood Type:	Hem-Fir	
Thickness (T_s):	0.89 *in*	
Specific Gravity:	1.10	*- NDS Table 11.3.3A*
Angle of Connection (Θ):	0 *degrees*	*- Angle from Load Direction to Grain*

Connector Characteristics

Connector Type:	Wood Screw	
Bending Strenght (F_b):	80000 *psi*	*- NDS App. I - Table I1*
Connector Diameter (D):	0.19 *in*	
Fastener Length	2.75 *in*	*Main Member Penetration < 10D*
		Final Values Adjusted by p/10D

Other

Connection Gap (g):	0 *in*	*- Gap Between Connnecting Members*

Outputs

Dowel Bearing Strengths

Main Member (F_m):	3500 *psi*	*As per NDS Table 11.3.3 - Footnote 2 and*
Side Member(F_s):	19800 *psi*	*NDS Section 11.3.4 - Eq. 11.3-11*

Reference Design Values (lbs/fastener)		
Yield Mode	Single Shear	Double Shear
I_m	410	410
I_s	1395	2790
II	306	NA
III_m	194	
III_s	323	646
IV	189	379
Minimum	185	371

Nails and Wood Screws Should NOT Be Loaded in Double Shear

NDS Reference Design Strength (Z):	
Single Shear:	***185 lbs***
Double Shear:	***371 lbs***

Yield Modes	
Mode	Yield Type
I_m	
I_s	
II	
III_m	
III_s	
IV	

Illustration retrieved from AWC TR - 12, 2014

Figure 55: Calculation for Yield Strength and NDS Yield Mode for #10 x 2.75 in. Trex® Composite Deck Screws and Trex® Composite Deck Boards.

119

B.4 - Calculation of Damping Coefficient from Physical Test Data

$$Recoverable\ Strain\ Energy = \frac{2(M_{Max})(0.05rad)}{2}$$

$$Damped\ Energy = 2\ A_1 + A_2$$

$$A_1 = \frac{d_1(M_{Max}-M_r)}{2}$$

$$d_1 = \frac{M_{Max}-M_r}{K_r} - \frac{M_{Max}-M_r}{K_i}$$

$$K_r = \frac{1}{2}K_i$$

$$d_1 = \frac{M_{Max}-Mr}{K_i}$$

$$M_r = \frac{M_y}{4}$$

$$A_1 = \frac{(M_{Max}-M_y/4)^2}{2\ K_i}$$

$$A_2 = \frac{2\ M_y}{4}\left(0.1 - \frac{2\ M_{Max}}{Ki}\right)$$

$$Damped\ Energy = \frac{2\left(M_{Max}-M_y/4\right)^2}{K_I} + \frac{2\ M_y}{4}\left(0.1 - \frac{2\ M_y}{K_i}\right)$$

$$Critical\ Damping\ Ratio = \frac{Damped\ Energy}{2\ \pi\ (Recoverable\ Strain\ Energy)} * 100\%$$

Notes: See figure __ on the following page for illustrations

$M_{Max} = M_{0.05}$ from physical test data

M_y = Yield Moment Defined from yield values from NDS yield limit equations

K_i = Initial Stiffness values from stiffness values defined from NDS 2012, Section 10.3.6

$\frac{M_y}{4}$ Changes to $\frac{M_y}{3}$ for Trex® screws and nails due to Mode III changing to Mode IV yielding
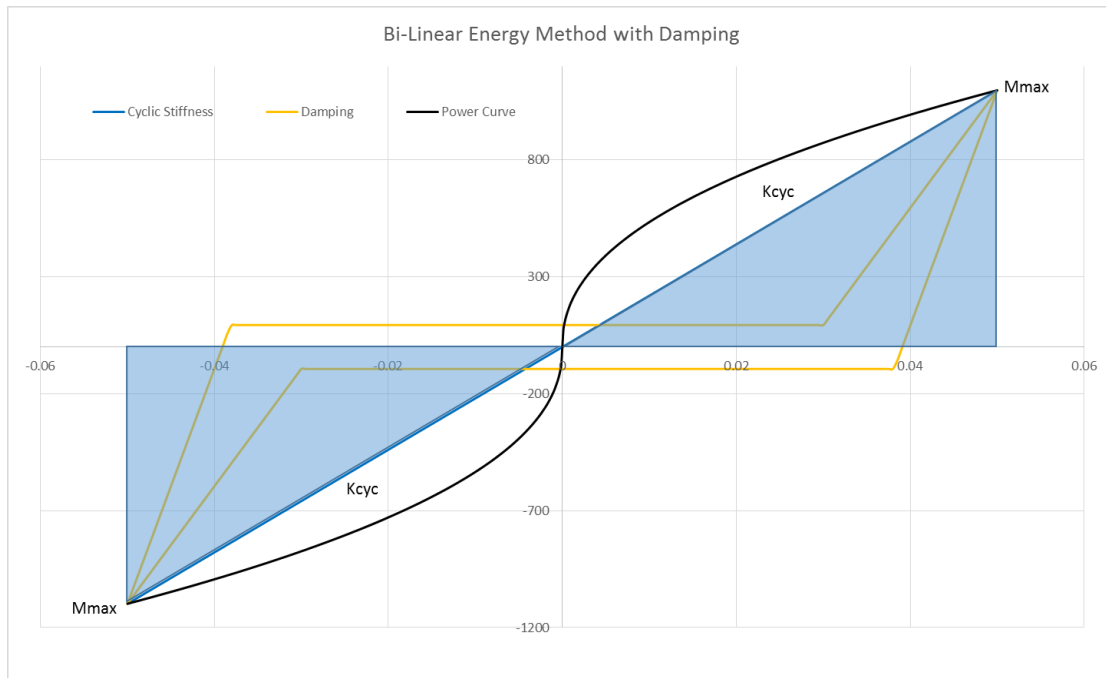
120
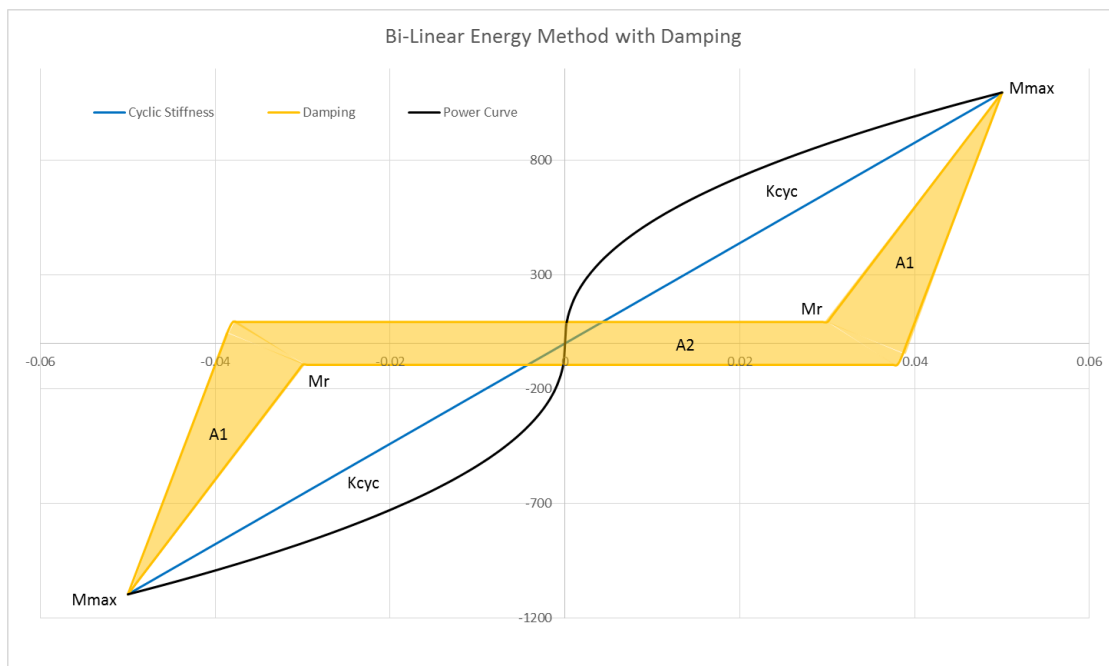
Figure 56: Illustration of Recoverable Strain Energy

Figure 57: Illustration of Damped Energy

B.5 - Calculation of Return Moment

#10 x 3 in Wood Screw

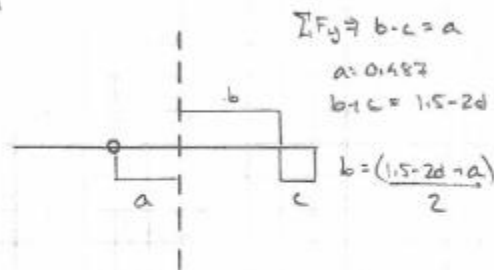1½ in Side member - No.2 Hem Fir

10 in Main Member - No.2 Hem Fir

TR 12 Pvalue = 324# (Mode III main)

Bearing Length in main Member

$$\frac{P}{F_e d} = \frac{324\#}{3500 psi (0.19 in)} = 0.487 in$$

$\Sigma F_y \rightarrow b - c = a$

$a = 0.487$

$b + c = 1.5 - 2d$

$b = \frac{(1.5 - 2d - a)}{2}$

Bearing Length in Side Member

$$\frac{(1.5 - 2(0.19) + 0.487)}{2} = 0.803$$

Total moment arm to plastic hinge location

$$0.487 + 0.803 = 1.29 in$$

Moment Demand M_d

$$\frac{F_{by}(d)^3}{6} = \frac{80,000 psi (0.19 in)^3}{6} = 91.5 in-\#$$

Force Required to Return Hinge to $\emptyset$ deflection F_r

$$\frac{91.5 in-\#}{1.29 in} = 70.93\#$$
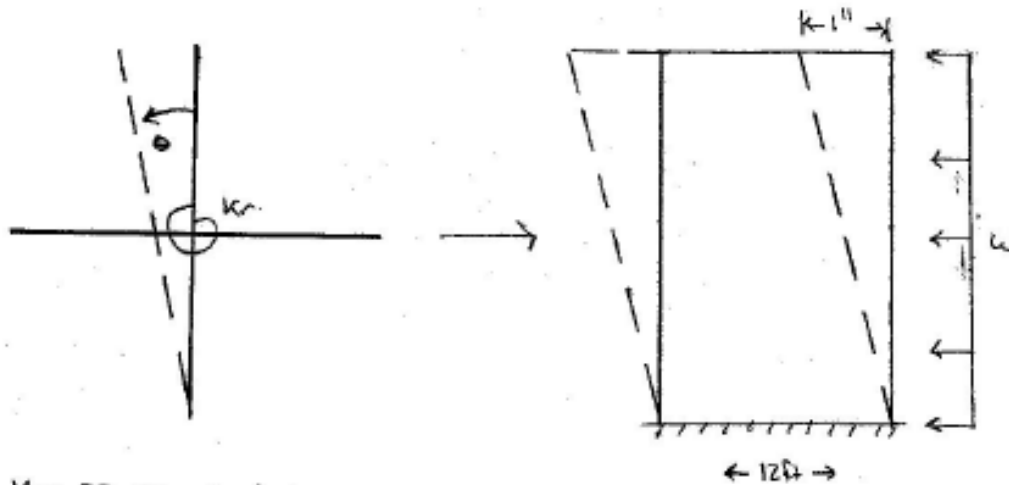
% Original Force

$$\frac{70.93\#}{324\#} = 22\% \Rightarrow \underline{Round\ to\ 25\%\ or\ ¼\ M_{max}}$$
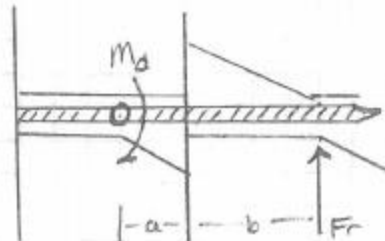
→ Mode III Returned to $\emptyset$ Deflection.

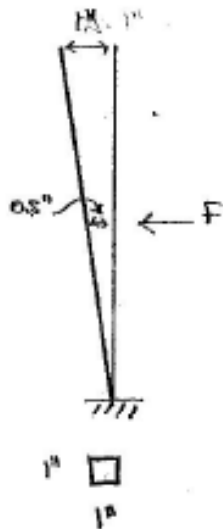## B.6 - Calculation of Shear Modulus for Simplified FEA Model

$K_r = 22,000$ lb-in/rad

$\Delta_\theta = \tan^{-1}\left(\frac{1''}{144}\right) = 0.00694$ rad/in

$K_r \Delta_\theta = 152.775$ lb-in/rad   For 1 connection

$n_{connection} = (10_{joists})(25_{DECK\,BOARDS}) = 250$

$(K_r \Delta_\theta)(n_{connection}) = 38193 \frac{lb\text{-}in}{in}$

$G = \frac{FL}{A\,\Delta x}$

$F = 38193 \frac{lb\text{-}in}{in}\left(\frac{1}{72in}\right) =$

$L = 72 in$

$\Delta x = 0.5 in$

$\underline{G = 76,386 \, psi}$

Note: F = Resultant From Distributed Surface Traction

123

Appendix C – Additional Figures and Tables

This Appendix serves as a place holder for additional figures and tables that did not belong in other sections. The figures outlined in this section are suggestions for increasing the stiffness in new and existing deck structures.

- Suggestions for Increasing Stiffness in New and Existing Deck Structures

C.1 – Suggestions Increasing Stiffness to New and Existing Deck Structures

Sheathed Arch

Railing-Truss

Truss Below Deck

Joist End-Bracing
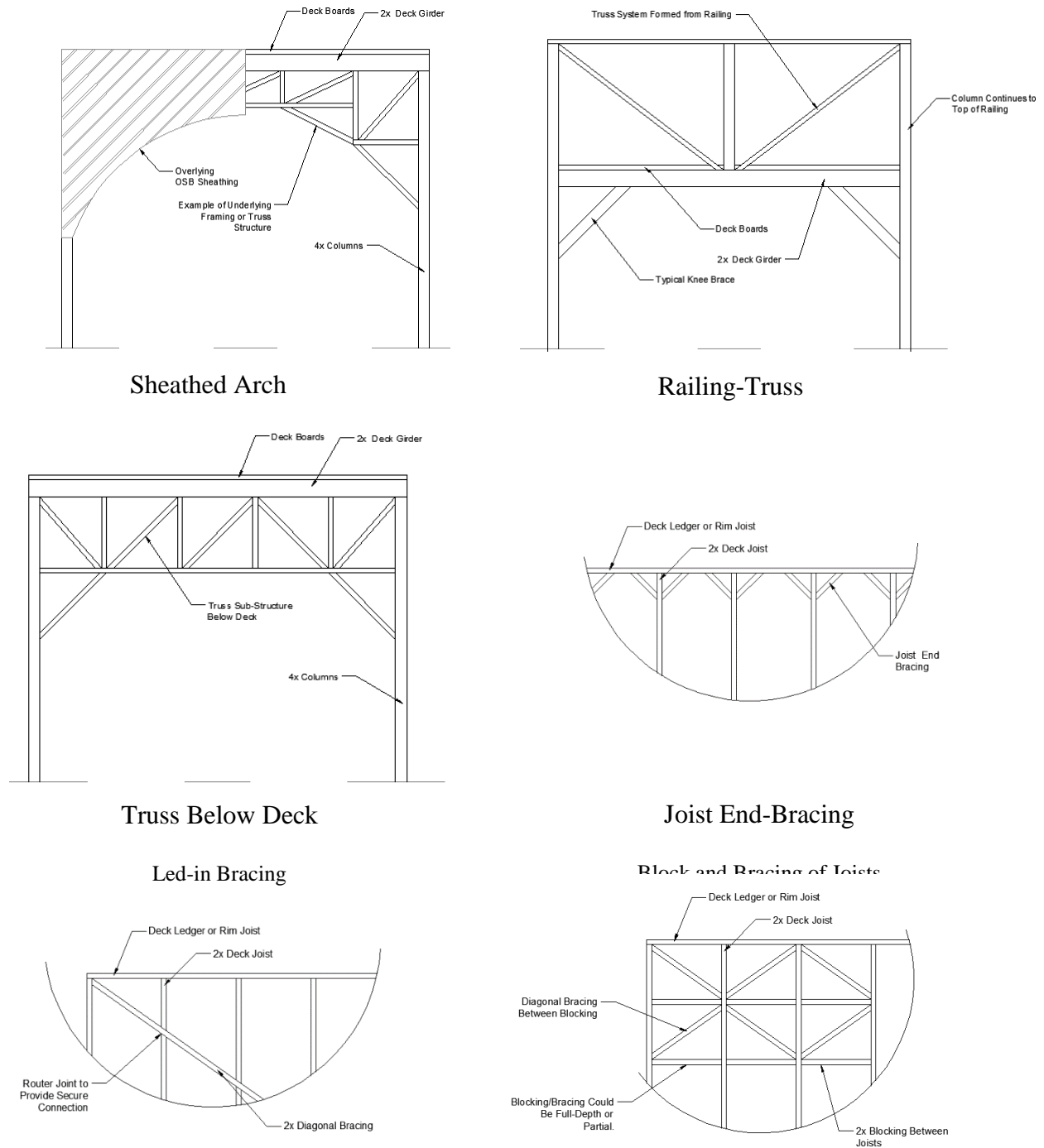
Led-in Bracing

Block and Bracing of Joists

Figure 58: Examples of Stiffness Restoration Systems | These will be essential for maintaining sufficient stiffness on structures that have lower diaphragm stiffness.